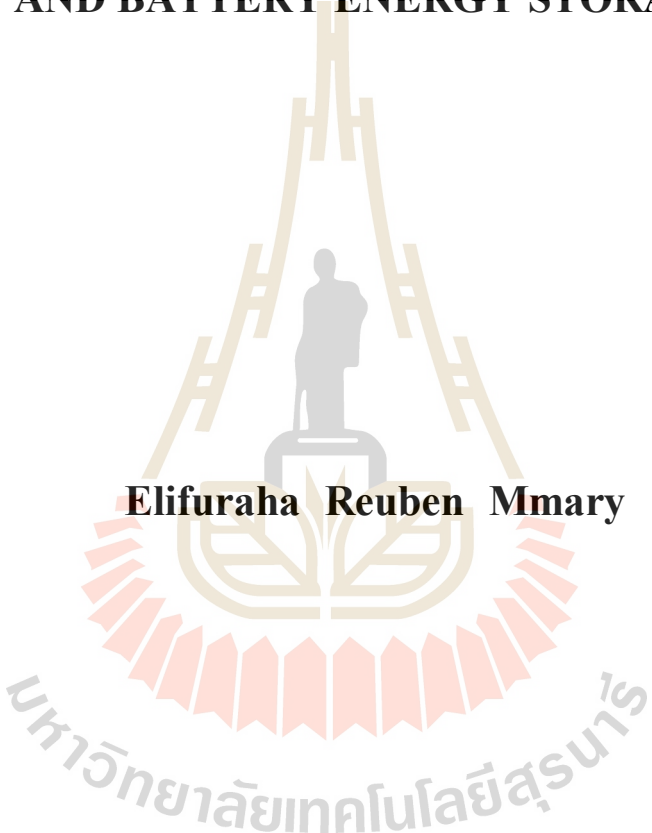


**PERFORMANCE ENHANCEMENT OF POWER
DISTRIBUTION NETWORK INTEGRATED WITH
HYBRID RENEWABLE ENERGY SOURCE
AND BATTERY ENERGY STORAGE**

Elifuraha Reuben Mmary

The logo of Suranaree University of Technology is a watermark in the background. It features a central figure of a person standing on a pedestal, flanked by two stylized 'H' shapes. Below this is a circular emblem with a book and a flame. The entire logo is surrounded by a decorative border of red and orange triangles. The Thai text 'มหาวิทยาลัยเทคโนโลยีสุรนารี' is written in a circular path around the bottom of the logo.

**A Thesis Submitted in Partial Fulfillment of the Requirements for
the Degree of Master of Engineering in Electrical Engineering**

Suranaree University of Technology

Academic Year 2017

การเพิ่มประสิทธิภาพของระบบจำหน่ายไฟฟ้าที่ติดตั้งระบบผลิตพลังงาน
แบบไฮบริดและแบตเตอรี่



นาย อธิฟูราฮา รุบีเอน เอ็มมารี

วิทยานิพนธ์นี้เป็นส่วนหนึ่งของการศึกษาตามหลักสูตรปริญญาวิศวกรรมศาสตรมหาบัณฑิต

สาขาวิชาวิศวกรรมไฟฟ้า

มหาวิทยาลัยเทคโนโลยีสุรนารี

ปีการศึกษา 2560

**PERFORMANCE ENHANCEMENT OF POWER DISTRIBUTION
NETWORK INTEGRATED WITH HYBRID RENEWABLE
ENERGY SOURCE AND BATTERY ENERGY STORAGE**

Suranaree University of Technology has approved this thesis submitted in partial fulfillment of the requirements for a Master's Degree.

Thesis Examining Committee


(Assoc. Prof. Dr. Keerati Chayakulkheeree)

Chairperson


(Asst. Prof. Dr. Boonruang Marungsri)

Member (Thesis Advisor)


(Asst. Prof. Dr. Padej Pao-la-or)

Member


(Asst. Prof. Dr. Kaan Kerdchuen)

Member



(Prof. Dr. Santi Maensiri)

Vice Rector for Academic Affairs
and Internationalization



(Assoc. Prof. Flt. Lt. Dr. Kontorn Chamniprasart)

Dean of Institute of Engineering

อิลิฟูราธา รูบีเอน เอ็มมารี : การเพิ่มประสิทธิภาพของระบบจำหน่ายไฟฟ้าที่ติดตั้งระบบ
ผลิตพลังงานแบบไฮบริด และแบตเตอรี่ (PERFORMANCE ENHANCEMENT OF
POWER DISTRIBUTION NETWORK INTEGRATED WITH HYBRID RENEWABLE
ENERGY SOURCE AND BATTERY ENERGY STORAGE) อาจารย์ที่ปรึกษา :
ผู้ช่วยศาสตราจารย์ ดร.บุญเรือง มะรังศรี, 172 หน้า.

การผลิตไฟฟ้าแบบกระจายด้วยพลังงานหมุนเวียนแบบผสมผสาน (Hybrid renewable distributed generation) ได้รับการยอมรับว่าเป็นวิธีการที่มีประสิทธิภาพในการใช้แหล่งพลังงานทดแทนในเครือข่ายการจำหน่ายพลังงานไฟฟ้า อย่างไรก็ตาม การเพิ่มประสิทธิภาพของปัญหาคำนวณวิศวกรรมที่แท้จริงมีวัตถุประสงค์ที่ขัดแย้งกัน ด้วยการเพิ่มความต้องการของโหลดและระบบผลิตไฟฟ้าแบบกระจายด้วยพลังงานหมุนเวียนแบบผสมผสานที่มีประสิทธิภาพสูงทำให้เกิดประสิทธิภาพการทำงานของเครือข่ายจำหน่ายไฟฟ้า และเปลี่ยนแปลงการวางแผนและการออกแบบระบบอย่างมาก ในงานวิจัยนี้ได้มีการพิจารณาการเพิ่มประสิทธิภาพแบบหลากหลายซึ่งรวมถึงพลังงานสูญเสียและปัญหาเสถียรภาพแรงดันไฟฟ้าที่มีระบบผลิตไฟฟ้าแบบกระจายด้วยพลังงานหมุนเวียนแบบผสมผสานทำงานร่วมกัน อัลกอริทึมอาณานิคมผึ้งเทียมแบบใหม่ซึ่งมีความสามารถในการแก้ปัญหาทั้งสองอย่างที่ได้กล่าวมา ได้ถูกนำมาเสนอแนวทางในการแก้ปัญหาการเพิ่มประสิทธิภาพของการวางแผนระบบจำหน่ายไฟฟ้า คุณลักษณะที่สำคัญของอัลกอริทึมอาณานิคมผึ้งเทียม คือ มีความสามารถในการให้ผลลัพธ์ที่ดีที่สุดในการเพิ่มประสิทธิภาพ ระบบพลังงานหมุนเวียนแบบผสมผสานที่นำเสนอ ได้แก่ พลังงานแสงอาทิตย์ (Solar PV) กังหันลม และระบบกักเก็บพลังงานแบบแบตเตอรี่ (BES) เพื่อจ่ายพลังงานให้กับระบบทดสอบ ได้แก่ ระบบทดสอบ IEEE 33 โหนด ระบบทดสอบ IEEE 34 โหนด และระบบทดสอบ IEEE 69 โหนด โดยใช้รังสีอาทิตย์เฉลี่ย 2.7 กิโลวัตต์ต่อตารางเมตรต่อวัน และความเร็วลมเฉลี่ย 4.84 เมตรต่อวินาที ประสิทธิภาพและความสามารถในการทำงานของวิธีการที่เสนอมานี้เปรียบเทียบกับระบบทดสอบ IEEE 6 บัส และระบบทดสอบ IEEE 37 บัส ผลการวิจัยชี้ให้เห็นว่าแนวทางที่เสนอนั้นเป็นเครื่องมือเฉพาะที่มีประสิทธิภาพและเป็นประโยชน์มากในการแก้ปัญหาหลายรูปแบบ อย่างไรก็ตาม ผลการจำลองจะถูกเปรียบเทียบกับงานวิจัยอื่น ๆ ที่กล่าวถึงในวรรณกรรม ผลการวิจัยนี้แสดงให้เห็นว่าปัญหาเสถียรภาพแรงดันไฟฟ้าและปัญหาพลังงานสูญเสียที่เกิดจากการทำงานร่วมกันของระบบผลิตไฟฟ้าแบบกระจายด้วยพลังงานหมุนเวียนแบบผสมผสานจะมีผลกระทบของตำแหน่งที่เหมาะสมและการปรับขนาดแหล่งพลังงานทดแทน

สาขาวิชาวิศวกรรมไฟฟ้า

ปีการศึกษา 2560

ลายมือชื่อนักศึกษา

ลายมือชื่ออาจารย์ที่ปรึกษา

Mary

Om

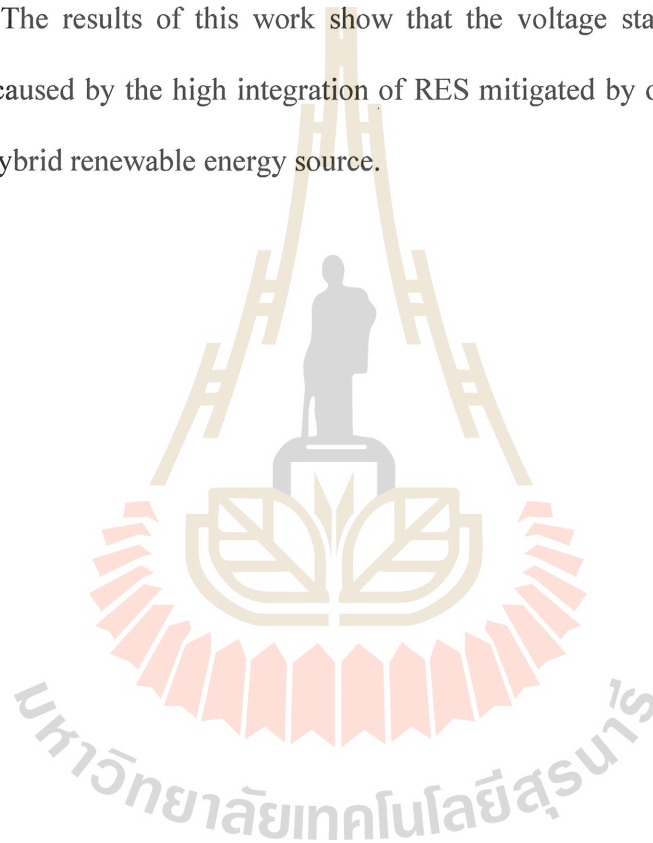
ELIFURAHA REUBEN MMARY : PERFORMANCE ENHANCEMENT
OF POWER DISTRIBUTION NETWORK INTEGRATED WITH HYBRID
RENEWABLE ENERGY SOURCE AND BATTERY ENERGY STORAGE.
THESIS ADVISOR : ASST. PROF. BOONRUANG MARUNGSRI, D.ENG,
172 PP.

RADIAL DISTRIBUTION NETWORK/RENEWABLE DISTRIBUTED
GENERATION /MULTIOBJECTIVE OPTIMIZATION/ABC

Hybrid renewable distributed generation (RDG) are recognized as effective means of exploit renewable energies source in power distribution network. However, optimization of real engineering problems contains more than one objectives that are generally conflicting each other. With the increasing of load demand and high penetration of renewable distributed generation (RDG) perturb performance of the conventional radial distribution network (RDN), and dramatically change the system planning and design. In this research work, performance enhancement of active RDN through multi-objective optimization is considered which include solving of power loss and voltage stability problem simultaneously.

A new artificial bee colony (ABC) algorithm which is capable of solving two objectives simultaneously, is proposed to solve the optimization problem of distribution system planning. Among the essential features of ABC algorithm are its robustness and ability to provide best results in optimization processes. A proposed hybrid system includes solar PV, wind turbine, and BES to supply power to IEEE 33-nodes, modified IEEE 34-nodes, and IEEE 69-nodes.

Average solar radiation of $2.7\text{kWh/m}^2/\text{day}$ and wind speed of 4.84m/s were used during simulation. The efficacy and functionality of the proposed method tested using IEEE 6-buses, and IEEE 37-nodes. The results suggest that the proposed approach is a unique, effective, and most practical tool for solving multi-objective problems. However, the simulation results compared with other research works mentioned in the literature. The results of this work show that the voltage stability and power loss problems caused by the high integration of RES mitigated by optimal placement and sizing of hybrid renewable energy source.



School of Electrical Engineering

Academic Year 2017

Student's Signature

EMary

Advisor's Signature

gms

ACKNOWLEDGEMENT

Firstly, I would like to express thanks to my heaven God for good health and enabling to accomplish research work in a School of Electrical Engineering, the Suranaree University of Technology here in Thailand.

I would like to express my sincere gratitude towards my advisor, Assistant Professor Dr. Boonruang Marungsri for his invaluable guidance, advice, and encouragement which made my research work possible for the accomplishment. I extend my thanks to the supervisory committee members, Assoc. Prof. Dr. Keerati Chayakulkheeree, Asst. Prof. Dr. Padej Pao-la-or and Assoc Prof. Dr. Kaan Kerdchuen for their valuable time of reviewing my thesis (research work). I would also like to thank the staffs of the School of Electrical Engineering at Suranaree University of Technology for their continuous help and guidance throughout the research study.

Last but not least, I would like to express special thanks to my parents for their relentless support and spiritually encouragement throughout the study of my research until the achievement of my study. Without them, I would not be the man I am today.

Elifuraha Reuben Mmary

TABLE OF CONTENTS

	Page
ABSTRACT (THAI).....	I
ABSTRACT (ENG).....	II
ACKNOWLEDGMENT.....	IV
TABLE OF CONTENTS.....	V
LIST OF TABLES.....	XI
LIST OF FIGURES.....	XIII
CHAPTER	
I INTRODUCTION.....	1
1.1 The research background.....	1
1.2 The motivation of the research.....	5
1.3 Research question.....	7
1.4 Problem statement.....	7
1.5 Research objectives.....	8
1.6 Limitation of the research.....	9
1.7 The significant of the research.....	10
1.8 Research structure.....	11
1.9 Chapter summary.....	12
II LITERATURE REVIEW.....	13
2.1 Introduction to literature review.....	13
2.2 Voltage control in RDN.....	14
2.3 Technology of Renewable DG.....	15

TABLE OF CONTENTS (Continued)

	Page
2.4 Solar photovoltaic system.....	16
2.4.1 Solar irradiance.....	16
2.5 Wind turbine.....	18
2.5.1 Driver for the grid development.....	21
2.5.2 Induction and Synchronous Generator.....	23
2.6 Emerging of energy storage system.....	29
2.6.1 Pumped hydro energy storage.....	30
2.6.2 Compressed air energy storage.....	30
2.6.3 Battery energy storage system.....	31
2.6.4 Choice of battery technology.....	32
2.6.5 Sizing and siting of BES	33
2.6.6 Modeling of BES.....	34
2.6.7 Ancillary services provided by battery energy storage....	35
2.7 Power flow analysis in RDN.....	36
2.8 Multiobjective power optimization.....	37
2.8.1 Priority goal programming.....	38
2.8.2 Pareto based multiobjective algorithm.....	39
2.8.3 Classical optimization techniques.....	40
2.9 Technical benefits of RDG in RDN.....	41
2.9.1 Power and energy loss.....	42
2.9.2 Voltage stability Index.....	43
2.9.3 Existing radial distribution network (RDN) model.....	43

TABLE OF CONTENTS (Continued)

	Page
2.9.4 Sink and source of reactive power in RDN.....	46
2.10 Renewable Distributed Generation.....	46
2.10.1 Optimization of RDG in RDN.....	50
2.10.2 Smart distribution network.....	53
2.10.3 Renewable DG in radial distribution network.....	54
2.10.4 Impact of RDG in voltage profile of RDN.....	54
2.10.5 Impact of RDG in power losses of RDN.....	55
2.10.6 Schematic diagram of proposed hybrid RDG.....	56
2.11 Summary of the chapter.....	57
III METHODOLOGY.....	58
3.1 Introduction to methodology.....	58
3.2 Mathematical formulation.....	60
3.2.1 Power flow analysis in RDN.....	60
3.2.2 Newton-Raphson power flow algorithm.....	61
3.2.3 Real power flow analysis.....	61
3.2.4 Reactive power flow.....	62
3.3 Modeling of Renewable DG source and load data.....	62
3.3.1 Modeling of wind turbine.....	65
3.3.2 Modeling of Solar PV.....	66
3.3.3 Modeling of storage battery capacity.....	67
3.4 Problem formulation.....	68
3.4.1 Multiobjective optimization problem.....	69

TABLE OF CONTENTS (Continued)

	Page
3.4.2 Multiobjective problem with weight factor.....	69
3.4.3 Decision variables.....	70
3.4.4 Power loss.....	71
3.4.5 Voltage stability index.....	71
3.4.6 Problem constraints.....	71
3.4.7 Equality constraints.....	72
3.4.8 Inequality constraints.....	72
3.5 Optimization method.....	72
3.5.1 Analytical methods.....	74
3.5.2 Performance index.....	74
3.5.3 Computational methods.....	75
3.5.4 Artificial Intelligent Techniques.....	75
3.5.5 Artificial Bee Colony Technique.....	77
3.5.6 Algorithm of ABC.....	77
3.5.7 Pseudo code of the main body of ABC Algorithm.....	80
3.5.8 Control parameters of ABC.....	80
3.5.9 Overview of ABC algorithm.....	81
3.6 Multiobjective ABC (MOABC).....	82
3.6.1 Main steps of the MOABC Algorithm.....	83
3.6.2 Mathematical Algorithm of MOABC.....	84
3.7 Chapter summary.....	85
IV SIMULATION RESULTS.....	89

TABLE OF CONTENTS (Continued)

	Page
4.1 Introduction.....	89
4.2 Simulation results based on types of RDG.....	90
4.2.1 Solar PV resources	90
4.2.2 Wind resources	91
4.2.3 Validation of proposed method.....	93
4.2.4 Test model of IEEE 6-bus.....	92
4.2.5 Test model of IEEE 37-nodes.....	94
4.3 Distribution system model.....	99
4.4 Simulation of IEEE 33-nodes system.....	99
4.4.1 Simulation results for case 1: Power loss.....	98
4.4.2 Simulation results case 2: Multiobjective optimization....	99
4.4.3 Integrating of RDG in IEEE 33-nodes systems.....	103
4.5 Simulation of IEEE 69 nodes system.....	106
4.5.1 Simulation results for case 1: Power loss.....	105
4.5.2 Simulation results case 2: Multiobjective optimization....	106
4.5.3 Integration of RDG in IEEE 69-nodes systems.....	107
4.6 Existing IEEE 34-nodes radial feeder model.....	110
4.6.1 Load model	111
4.6.2 Shunt capacitor.....	111
4.6.3 Transformer.....	112
4.7 Real system of 34 nodes system.....	112
4.7.1 Simulation of real system without RDG.....	113

TABLE OF CONTENTS (Continued)

	Page
4.7.2 Simulation results for case 1: Power loss.....	113
4.7.3 Simulation results case 2: Multiobjective optimization...	114
4.7.4 Sizing of BES in real distribution system	115
4.7.5 Integration of RDGs in real distribution systems.....	122
4.8 Chapter summary.....	122
V CONCLUSION AND FUTURE WORK.....	123
5.1 Conclusion.....	123
5.2 Benefits of research work.....	124
5.3 Future work.....	124
REFERENCE.....	125
APPENDICES.....	136
APPENDIX A Research Publication	136
APPENDIX B Branch data for IEEE 33 nodes	163
APPENDIX C Load data for IEEE 33 nodes	164
APPENDIX D Branch data for real system of 34 nodes	165
APPENDIX E Load data for real system of 34 nodes	166
BIOGRAPHY.....	167

LIST OF TABLES

Table		Page
2.1	Energy output from different RDGs	16
2.2	Technical specification of solar PV	17
2.3	Technical specification of WT	22
2.4	The classification of WT	25
2.5	Classifications of wind turbine	26
2.6	Characteristics of wind turbine	26
2.7	Comparison of battery technologies	35
2.8	Source and sink of reactive power	46
4.1	Line data of six bus system	92
4.2	Control variable	93
4.3	Validation of results	94
4.4	Validation in IEEE 37-nodes	96
4.5	Results of IEEE 33-nodes at base case without RDG	100
4.6	Multiple RDGs considering power loss	102
4.7	Optimization with single RDG (Injecting P only)	103
4.8	Optimization with single RDG (Injecting P and Q)	103

LIST OF TABLES (Continued)

Table		Page
4.9	Multiple RDGs considering MOOP	104
4.10	Results of IEEE 33 nodes with RDGs	104
4.11	Control variable limits and optimal solution in IEEE 33 nodes	105
4.12	Results of IEEE 69 without RDGs	107
4.13	Multiple RDGs by considering power loss only.....	108
4.14	Optimization with multiple RDGs.....	109
4.15	Load model of IEEE 34 nodes	111
4.16	Control variable limits and optimal solution in 34-nodes	113
4.17	Results of real system without RDG.....	114
4.18	Multiple RDG considering single objective	115
4.19	Optimization with single RDG with both P and Q	116
4.20	Optimization with multiple RDGs with both P and Q	116
4.21	Results of real system with RDGs	117
4.22	Proposed capacity of BES	118
4.23	Results of VSI in real system without RDG	120
4.24	Results of VSI with RDG into real system of 34 nodes	121

LIST OF FIGURES

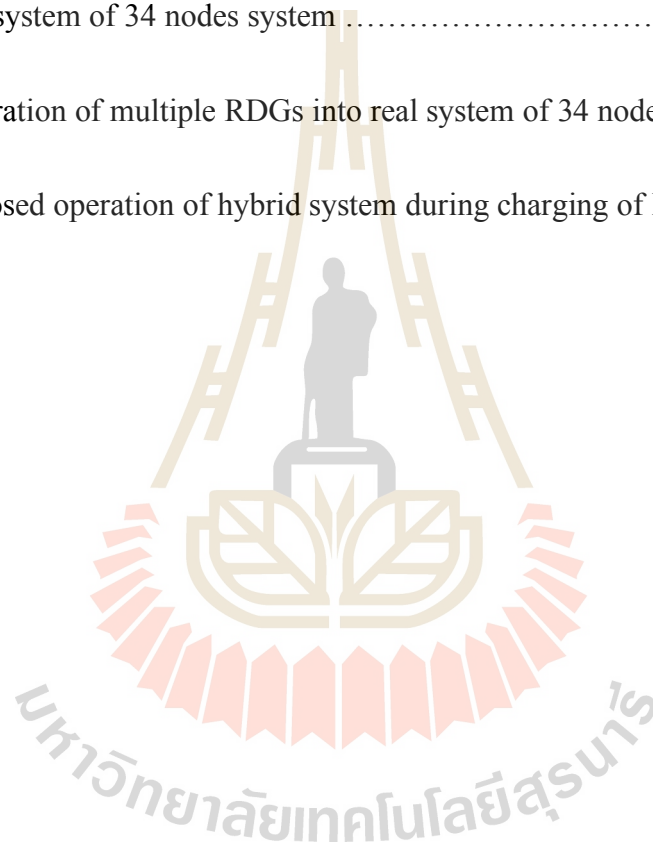
Figure	Page
2.1 Solar PV	16
2.2 On-shoe wind farm.....	19
2.3 Off-shoe wind farm.....	19
2.4 Details of wind turbine	20
2.5 Power characteristics of wind turbine.....	25
2.6 Construction scheme of sodium Sulphur cell.....	29
2.7 Lithium ion batteries.....	30
2.8 Variety of energy storage.....	32
2.9 The optimum compromise solution.	40
2.10 Existing IEEE 34 nodes radial distributed network model	45
2.11 Smart grid with RDGs	52
2.12 Schematic diagram of proposed hybrid RDGs with BES	57
3.1 Normalized daily WT and solar PV output	63
3.2 Proposed schematic of hybrid system.....	68
3.2 Flow chart of ABC Algorithm	79

LIST OF FIGURES (Continued)

Figure	Page
4.1 Power output from solar PV	90
4.2 Solar irradiation	90
4.3 Curve of power converted from solar PV.....	91
4.4 Power output from WT.....	92
4.5 Normalized load demand curve	92
4.6 Test network of IEEE 6 bus	96
4.7 Fitness curve of ABC and PSO.....	97
4.8 IEEE 37 nodes system	98
4.9 Fitness curve of ABC in IEEE 37-nodes.....	99
4.10 IEEE 33 nodes system.....	100
4.11 Fitness function considering P only	102
4.12 Multiple RDGs injecting both P and Q	104
4.13 Integration of multiple RDGs in IEEE 33 nodes.....	106
4.14 Voltage and VSI of 33 nodes	106
4.15 Line diagram of the IEEE 69-nodes test system.....	107
4.16 Fitness curve for multiple RDG considering power loss only	108

LIST OF FIGURES (Continued)

Figure		Page
4.17	Fitness curve by multiple RDGs (Injecting both P and Q)	109
4.18	Existing IEEE 34-nodes system	110
4.19	Real system of 34 nodes system	114
4.20	Integration of multiple RDGs into real system of 34 nodes.....	117
4.21	Proposed operation of hybrid system during charging of BES.....	119



CHAPTER 1

INTRODUCTION

1.1 The Research Background

The widespread of using fossil fuels energy source for power plant industries caused rising in air pollution and high temperature. However, increased population and depletion of fossil fuels in the world make the necessity of finding alternative energy resources for generation of power to suit increased load demand. Wind and solar are clean, accessible, abundant availability in nature, eco-friendly and cost-effective energies. In other words, wind and solar energy are efficient enough to either generate power on distribution network or supply demand on the remote area where the electricity costs through the present distribution network are high. Hybrid systems are proposed to increase the reliability, stability and reduce implementation cost of the wind turbine (WT) and solar PV. In a publication of (Vafaei et al., 2012) demonstrated that the hybrid systems are usually more reliable and less costly than systems that use only a single source of energy.

The hybrid power system enables to overcome the limitations in the wind and solar resources since their performance characteristics depend upon the unfavorable changes in environmental conditions. It is probable to endorse that hybrid generation systems are usually more reliable, stable and less costly than systems that depend on a single source of energy. On the other hand, one environmental condition can make one type of RDG more profitable than other. For example, solar PV system is ideal

for locations having more solar illumination levels and Wind power system is ideal for locations having better wind flow conditions.

The power system model comprises three essential components namely generation, transmission line, and distribution system. The components are interdependent to ensure the generated power can be transmitted from the generation to the customer via the distribution system and transmission line. Also, the power system is designed to work with unidirectional power flow due to lack of power source except in the generation component only. However, as the demands are expected to escalate in the future, one of the possible solutions could be done to upgrade the entire power system performance. Concerning this solution, it will require intensive planning to the components of the radial distribution network (RDN); thus, increasing the overall cost of the power system. On the contrary, the introduction of the concept of microgrid offers an exciting solution by integrating renewable distributed generation (RDG) in the distribution system instead of relying solely on centralized generation schemes, thereby reducing the necessary improvements made in the generation and the transmission lines.

Emerging of the RDG has changed the fundamental nature of the operation in the power systems, particularly the distribution networks where the status has changed from passive to an active network. This means that the RDG can actively participate in the distribution system to provide additional support to the main grid in fulfill load demands. Also, numerous benefits have been identified by other researchers, for instances enhance voltage profile, reduction of greenhouse gases, improve reliability, stability and also reduce power loss. The reduction of power losses is an important task that can be done to maintain the efficiency of the distribution system. There several

approaches which are commonly proposed by researchers to reduce the power losses; either by installing of series and shunt capacitors, installing of RDGs and network reconfiguration. However, the advantage of these approaches can be achieved if they are carefully coordinated in the distribution system.

Many countries around the world are introducing programs aimed at reducing the emissions produced by the fossil power plants and increasing the utilization of RDG. Among different types of renewable energy technologies, wind power is expected to be one of the most popular types of renewable in the near future. Wind energy has some advantages such as no pollution, relatively low capital cost and a short gestation period. As mentioned above wind power has many advantages. However, it also causes intermittent and volatile characteristics which may impact on power system security and stability. High penetration of wind power can introduce new challenges such as reduce the power system dispatch and economic efficiency (Bilal et al.,2010). As a result, the decreasing power system stability margins will lead to unacceptable operating conditions and power system collapses. Also, the uncontrollable nature of wind power will lead to an additional cost of managing the intermittency as the intermittency of wind can cause strain on the electricity grid.

One way to overcome this inherent variability of RES with a wind turbine and solar PV is by integrating energy storage especially battery energy storage (Berrada & Loudiyi, 2016). If there existed an efficient and cheap method at a scale of hundreds of MWh to store the energy generated from these renewable sources, then this source could be used on a dispatchable basis much like natural gas plants, allowing a generation to match demand. Incorporating such forms of energy storage with wind and solar technologies would enable the largescale integration of renewable and non-

emitting generation to the electricity grid. To make the integration of RDG possible, Recently, a combination of the battery energy storage (BES) together with RDG has been proposed to provide economic and technical benefits to power systems (Paska, Biczal, & Klos, 2009). Energy storage systems have been shown to be quite suitable for mitigating the adverse impacts resulting from the integration of RDG. To reduce the fluctuation of the wind energy output, a battery energy storage system (BES) integrated into the renewable energy generation system. BES can also act as a means of mitigating the intermittency of power from RDG.

Energy storage technologies include flywheel storage, pumped hydro, compressed air, battery storage and many more. Although the supremacy of one over the other can be arbitrarily discussed, what is sure about each one of them is that they can also provide ancillary services to the system, some of which are: stabilization of voltage and frequency, power quality improvement, islanded operation, reduction of losses and many others. All of these applications serve to increase the reliability and the stability of the grid (Mohandas, Balamurugan, & Lakshminarasimman, 2015).

From the technical aspect, ancillary services are defined as those services performed by the electrical generating, transmission, system control and distribution system equipment and people that support the essential services of generating capacity, energy supply, and power delivery. The following figure presents the ancillary services BES can provide.

There are several research groups which have been used to solve optimization problems of RDG into RDN such as analytical, heuristic and meta-heuristic technique, where each of the group has its own merits and demerits. Among these groups, the meta-heuristic are more prominent in solving the coordination problems due to

robustness and simple to implement. There are numerous of techniques that have been introduced under the meta-heuristic methods such as Genetic Algorithm (GA) (Mohandas et al., 2015), Particle Swarm Optimization (PSO), and Artificial Bee Colony (ABC). Additionally, some authors have also proposed hybridized optimization methods by combining two optimization techniques to cancel out the discrepancies of each for achieving better solutions.

Recently, some studies have been done by some researchers to harmonize between the two approaches as an example to solve coordination between the DG and the capacitors, simultaneously. Means, the location and size of the RDG and the BES are determined simultaneously by using one approach. One significant advantage when combining this approach is the reduction of the power loss can be obtained more than if executed separately. Therefore, investigation of optimal coordination between the WT and Solar PV with BES should be carried out to achieve better performance in the distribution system. This research aims to find a solution that can harmonize high penetration of RDG with BES coordination to further reduce the power loss and improvement of voltage stability in the radial distribution network.

1.2 The motivation of the research

Power of solar PV and a wind turbine farm highly dependent on the meteorological conditions, and therefore it shows high fluctuations in power generation. Optimal HRES and BES could, therefore, be an option to best match the load curve and intermittent of RES. In recent years, the hybrid generation system has become significant because of the complementary characteristics of the RES. In many regions, when BES, solar PV, and wind turbine combined for power generation, they

complement each other using daily and seasonal variations. This combination reduces the dependence on one environment parameter thus providing the reliable power, cheap electricity, and is more efficient than utilization of single renewable energy source. Hybrid, wind turbine and solar PV offer higher reliability than any one of them alone because the energy supply does not depend on entirely one alternate source. HRES can operate either in grid-connected or stand-alone mode. Therefore, the primary motivation for this research is to study and analyze the hybrid renewable energy system (HRES) with energy storage into distribution networks.

The main drawbacks of power from RES are nature dependent power supply, and the occasion of energy production is not necessarily in line with the time when energy is precisely needed. These drawbacks could be overcome by including BES into the system. BES are frequently used with RES systems for compensating the power during outages and with the objective of storing the energy generated by the RES when there is reasonable weather condition. Then the stored power in batteries can deliver it to electrical loads when it is needed.

From a fundamental perspective, the main disadvantage of wind energy is the intermittent nature of wind. Wind is extremely unreliable, equally likely to blow as to not blow during peak hours. Although daily and seasonal wind patterns exist, the wind is still highly unpredictable when it comes to timing and strength. The intermittency and uncertainty of wind make the dispatch of wind energy a difficult task. High penetration of RES could impact the system stability and reliability of power grid. In order to reduce the power fluctuation of the WT and solar PV, a BES integrated into the system. Wind farms and solar PV combined with BES can enhance system reliability, stability, and efficiency.

The installation of WT and solar PV (RDGs) units is becoming more prominent in distribution systems due to their overall positive impacts on power networks. Some significant advantages of integrated DGs include reducing power losses, improving voltage profiles, reducing emission impacts and improving power stability. Because of these benefits, utility companies have started to change their electric infrastructure to adapt to the introduction of RDGs in their distribution systems.

Nonetheless, to maximize benefits, solution techniques for RDG deployment should be obtained using optimization methods, since installing RDG units at non-optimal places and in inappropriate sizes may cause increase power losses and costs. Moreover, installing RDGs is not straightforward, and thus the placement and sizing of RDG units should be carefully addressed. The primary motivation of the present thesis research is investigating optimization problem by considering multiobjective optimization problems.

1.3 Research question

Numerous research questions which may arise when scrutinizing the effect of integrating RDG in the distribution network are listed below:

- a) What is the suitable method that can be applied to solve the optimization problems?
- b) Which combination of RDG gives the best impact on the distribution network?
- c) What happens to the performance of voltage stability index when the optimization performed on the system?

1.4 Problem statement

The continuously increasing penetration of renewable distributed generation (RDG) in Tanzania requires a detailed assessment of the impact on the electric power grids. Most importantly, one key driver of establishing the need for research in performance enhancement of distribution grid is present intermittent of the renewable energies sources (RES). The available RES in this research includes solar PV and wind turbine. Most of the optimization problem in the real world are multiobjective optimization problems (MOOP) into which the primary goal of MOOP is to find optimum solutions for all objectives simultaneously. In MOOP problem solver suggest set of solutions to decision maker according to the importance of the problem type. Since the set of optimum solutions is a Pareto-optimal set which is not worse than each other.

Renewable Distribution Generations (RDG) play an essential role in delivering the power into the power distribution network. However, power losses and voltage stability must take into consideration to enhance the performance of power delivered to the consumer. Non-optimal location, number, configuration, and sizing of RDG units may lead to losses increase together with lousy effect on voltage magnitude. However, to introduce BES to existing grid while maximizing the benefits, this can yield optimal sizing and placement needs to be determined. On the other hand, it is not possible to install a significant amount of energy storage in power systems to solve all grid problems, as this increases the overall costs substantially.

Taking into account the facts presented so far, the problem, which constitutes the motivation of this research work defined as follows: 'Performance enhancement of power distribution network connected with optimal hybrid RDG and BES in a LV distribution grid. Many optimization techniques have been used to minimize the power

losses and improve voltage magnitude by considering the optimal sizing and location of RDG. For this research, ABC together with performance index is used to find the optimal sizing and location of RDG in IEEE-33-nodes and modified IEEE 34-nodes distribution network.

1.5 Research objectives

Most of the researchers have been done in the area of conventional DG with RDG. However, by examining the literature, it was determined that there research gaps, namely, multiobjective optimization of BES with enabling high penetration of HRES in the distribution network. This research aims to investigate the optimal placement and sizing of RES with BES in distribution networks in a way that to reduce power losses and improve voltage stability of an LV network simultaneously. The optimization technique used for this problem is Artificial Bee Colony (ABC) compared with the Genetic Algorithm (GA) and power-word software for testing effectiveness of ABC.

To achieve the primary purpose of research the following specific objectives addressed as follows:

- a) To study power flow by using Newton Raphson method and optimization technique of RDG using ABC Algorithm
- b) Formulation of a multi-objective optimization and performance index taking into consideration of voltage stability index.
- c) Develop an optimization model to determine the optimal placement and sizing of RDG and BES with IEEE 33-nodes and modified IEEE 34-nodes using MATLAB.

1.6 Limitations of the Research

The motivation for the proposed thesis is to study the benefits of having RES and BES in smart distribution networks with high solar PV and penetration of WT. A particular interest is to fill the gap of sizing and siting of hybrid RDG and BES maximize the benefits of RDG in the radial distribution network. To archive the objectives of the research, several essential sub-tasks need to be undertaken; this includes the following:

- a) Understand the optimal power flow studies initiated in the process; namely, the Newton-Raphson method.
- b) Familiarize with the topics related to the research; Renewable Distributed Generation (DG), Battery energy storage system, ABC Algorithm and the MATLAB software.
- c) Literature reviews of related research work.
- d) Develop a program to solve the optimization problem of RDG in MATLAB programming based on the ABC Algorithm.
- e) Test the program on the IEEE 33-nodes and IEEE-37-nodes test system to confirm its eligibility and applied to modified IEEE 34-nodes radial distribution network.

1.7 The significance of the Research

The prime inspiration of this research is to determine the optimal sitting and sizing of RDG with BES coordination, to enhance the performance of RDN regarding total power loss reduction, voltage stability and increase the voltage profile improvement as well. Installation of the optimal RDG in the distribution has helped to improve the overall system efficiency especially reduction of power losses. This

research will contribute to the evaluation and implementation of BES and HRES in the radial distribution network. It will suggest the best configuration technologies for a given network and the potential of the BES and RDG for performance enhancement of RDN. Thus, specific contributions become:

- a) Analysis of primary implications of using ABC for solving optimal placement and sizing problem of RDG concerning the power loss reduction and voltage stability improvement in RDN
- b) In this thesis, multi-objective optimization model proposed for the optimal placement and sizing of hybrid RDG and BES in RDN.
- c) The results obtained in this can be used for comparative analysis of RDGs and BES in future of Smart Distribution Network.

1.8 Research Structure

The outlines of this thesis are as follows:

Chapter 1 provides an introduction, Problem Statement, research objectives, limitation of the research and Structure of the research.

Chapter 2 explains a review of radial distribution system, optimization techniques, features of radial distribution network and RES as well. This chapter gives the background of the electrical system, renewable DG, BES, hybrid RES.

Chapter 3 illustrates the AI Techniques and modeling of an essential element of RDG including solar PV, BES and wind turbine based PMSG.

Chapter 4 exhibits the outcomes for the simulation results of power-world and ABC Algorithm. It also showed the optimum variables with the help of AI optimization techniques in MATLAB software.

Chapter 5 discusses the obtained simulation results and their usefulness in minimizing power losses and voltage profile improvement in RDN.

Chapter 6 concludes the results of the smart distribution system against penetration of RES and BES for performance enhancement and recommends actions to be carried out.

1.9 Chapter Summary

This chapter explained the general introduction about RDN with their different type of RDG as RES. Also, it described in short about Electrification System of Tanzania and its components. In the problem statement, it showed how intermittent of RES affect the stability and reliability of RDN. Lastly, it direct to the objective, and limitation of research including an outline of the thesis have been mentioned in this chapter.



CHAPTER 2

LITERATURE REVIEW

2.1 Introduction to the literature review

This section presents a comprehensive review of the fundamental theory of voltage control in the radial distribution system, review and application of RDG in power distribution system, and modeling of RDG in load flow studies. Also, due to the natural intermittency of renewable resources such as wind speed and sunlight, storage devices and their applications are introduced later in this section to mitigate the variability of power output from RDG.

Battery energy storage can allow higher amounts of renewable generation to be integrated by the smoothening power output of RES; time shifting generated energy to follow demand and increase hosting capacities through peak shaving (Weitemeyer, Kleinhans, Vogt, & Agert, 2015). Power quality related issues due to the intermittency of RES can be mitigated by controlling the storage's charging patterns to respond to grid variables (Sadwick, 2016). For optimal utilization and maximum storage value, several applications should be within the operational constraints of the storage unit. Several battery technologies which have been developed and tested for such applications including lead acid, sodium sulfate, and lithium-ion are presented (Paska et al., 2009).

2.2 Voltage control in RDN

To maintaining the voltage of the PQ nodes within permissible limits, several means must be provided to control the voltage (Aman, Jasmon, Bakar, & Mokhlis, 2013). There is numerous way of improving the voltage regulation in power distribution network:

- a) Use of voltage regulators
- b) Application of voltage regulation equipment's in substation of PDN
- c) Application of capacitor in the distribution substation of PDN
- d) Balancing of loads on primary feeders
- e) The increase of feeder conductor size
- f) Change of single section to multisession of feeder
- g) Transfer of loads to new feeders
- h) The increase of primary voltage level
- i) Installation of a new substation and primary feeder
- j) Application of voltage regulators out on primary feeders
- k) Application of series and shunt capacitor on the primary feeder

The selection of techniques depends upon the particular system requirement. However, automatic voltage regulation is always provided by regulation at the substation, feeder regulation and additional regulation along the main by regulators mounted on poles. Distribution substation is equipped with load tap changing transformer (LTC) that operate automatically (Yan & Saha, 2012).

In case of customers located at long distances from the substation, additional regulator or capacitor located at the selected point of the feeder. Many utility companies have experienced the most economical way of regulating the voltage within the required

limits to apply both step voltage regulator and shunt capacitor. However, installation of these equipment does not match with an increased load in term of active power. Since, compensation made by the voltage regulator, LTC, and capacitors is reactive power only. Hence, to control voltage and minimize power losses in RDN, it needs to install RDG near to customer to minimize copper losses and regulate voltage as well.

2.3 Technologies of Renewable DG

Renewable RDG defined as small-scale generating units located close to the loads that are being served. It is possible to classify RDG technologies into two broad categories: renewable and nonrenewable energy resources. The former comprises biomass, wind turbine, solar PV, geothermal, hydropower and tide power plants. The latter includes reciprocating engines, combustion gas turbines, micro-turbines, and fuel cells. The next section provides a review of renewable technologies of solar PV, energy storage and a wind turbine to be considered in this research.

The power and energy outputs from a given area are summarized in Table 2.1. It is evident that solar PV is very competitive concerning land use, even if the capacity factor is relatively low for the actual area.

Table 2. 1 Energy output from different Renewable DG (Jones & Olsson, 2017)

	Hydropower	Wind Turbine	Solar PV
Power density in (MW/km ²)	0.1-17	5-8	20-110
Capacity factor	0.6	0.3	0.2
Output in GWh/km ²	0.5 – 90	13 -21	35 -190

2.4 Solar Photovoltaic System

Solar PV technologies use some of the properties of semiconductors to convert sunlight into electricity directly as shown in Figure 2.1. The advantages are that these technologies are characterized by zero emissions, silent operation, and a long life service. They also require low maintenance and no fuel costs. Also, solar energy is redundant and inexhaustible. However, it is weather-dependent, intermittent and unavailable during the night (Hosenuzzaman et al., 2015). Given a high penetration level of PV together with demand variations, power distribution systems would experience power fluctuations along with unexpected voltage rise, high losses, and low voltage stability.

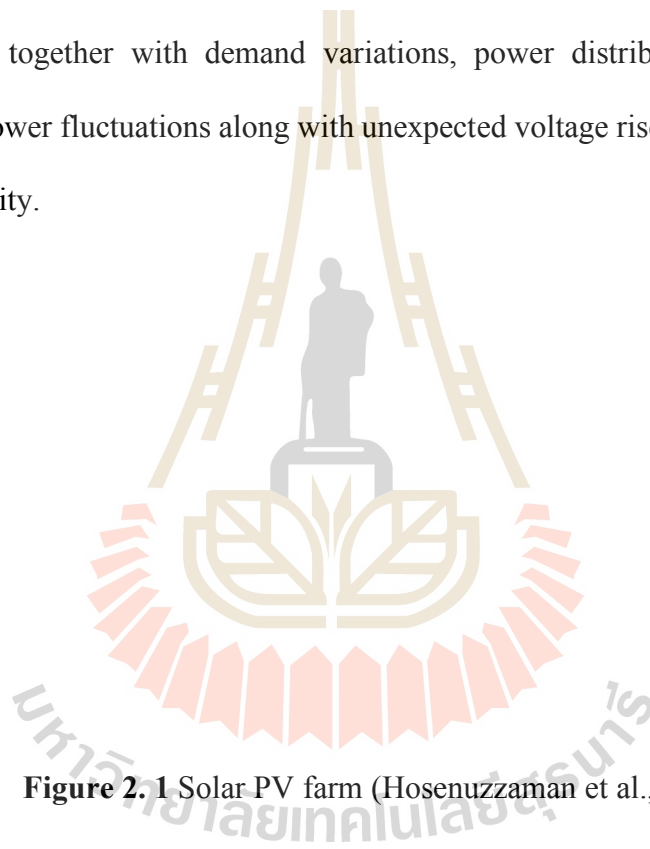


Figure 2.1 Solar PV farm (Hosenuzzaman et al., 2015)

2.4.1 Solar irradiance

The solar irradiance is mostly represented by the global horizontal irradiance (GHI) or direct normal irradiance (DNI). The GHI ($\text{kWh/m}^2/\text{a}$ or W/m^2) is the total amount of irradiation, consisting of a direct and a diffuse (scattered) proportion that is relayed onto a particular horizontal area. The inclined GHI is primarily used for power estimation purposes related to a solar PV with a fixed inclined angle. The DNI

value (kWh/m²/a or W/m²) represented the direct, perpendicular to a predefined surface, beaming component of the sun only and measured by tracking the measuring instrument. Diffuse irradiation is excluded entirely from such a calculation (Bilal et al., 2010).

The power output of a solar PV depends on the area (A) of the PV panel, solar irradiance $\mu(t)$ and efficiency of the solar PV panel β . However, Ileberi et al., (2016) describe technical specification that can be used for engineer to estimate power output from solar PV as shown in Table 2.2

$$P_{PV}(t) = \eta_m * [1 - \beta(T_c - T_{ref})] * A * G(t) \quad (2.1)$$

Where

P_{PV} is power of solar PV, T_c is temperature of the cell

T_{ref} is reference temperature

Table 2.2 Technical specification of solar PV (Ileberi Gbalimene1 et al 2016)

S/N	Description	Details
1	Rated power per solar PV panel (MW)	0.8
2	Efficiency at standard test condition %	13
5	Normal operating temperature °C	40
6	Life time (years)	30

2.5 Wind Turbine

Wind turbines are devices that convert kinetic energy from the wind into electricity. They can be categorized into two brands: vertical axis wind turbines and horizontal axis wind turbines. Like solar PV, wind turbines are emissions-free and require no fuel costs. Wind energy is also redundant and inexhaustible. However, the main challenges are that wind turbines have an unpredictable and intermittent output

and a high-capital investment cost. Also, the simultaneous occurrence of excessive wind generation and low demand could lead to the possibility of encountering voltage rise, high losses and low voltage stability in power distribution systems (Kharrich, Akherraz, & Sayouti, 2017).

Wind turbines transform wind energy into electricity. The wind is a highly variable source, which cannot be stored. Thus, it must be handled according to this characteristic. The main parts of a WT are the tower, the rotor, turbine blade, generator and the nacelle. The nacelle accommodates the transmission mechanisms and the generator. The rotor may have two or more blades. Wind turbine captures the kinetic energy of wind flow through rotor blades and transfers the energy to the induction generator side through the gearbox.

Output power from wind turbine vary based on installed location, which is either on-shoe wind farm or off-shoe wind farm as shown in Figure 2.2 and Figure 2.3 respectively. However, more output power expected from off-shoe wind farm.



Figure 2. 2 On-Shoe Windfarm (Ayodele and Ogunjuyigbe 2015; Zhao et al., 2009)



Figure 2. 3 Off-Shore Windfarm

(Ayodele & Ogunjuyigbe, 2015; Zhao, Li, Hao, Zhang, & Lu, 2009)

The output power of a WT is determined by several factors such as wind velocity, size, and shape of the turbine. The power developed is given by (Zhao et al., 2009).

$$P = \frac{C_p \rho V^3 A}{2} \quad (2.2)$$

Where

P is power output (W),

C_p is power coefficient, pair density (kg/m^3),

V is wind speed (m/s), and A is swept area of rotor blades (m^2).

Power coefficient C_p gives a measure of the amount of energy extracted by the turbine rotor. On the contrary, variable speed wind turbine systems provide much smoother output power and more stable bus voltage with lower losses. However, a significant problem of WT is the intermittent nature of generation. A general scheme of a wind turbine is shown in Figure.2.4 where its main components are presented. In the most

common system, the generator system gives an AC output voltage that is dependent on the wind speed.

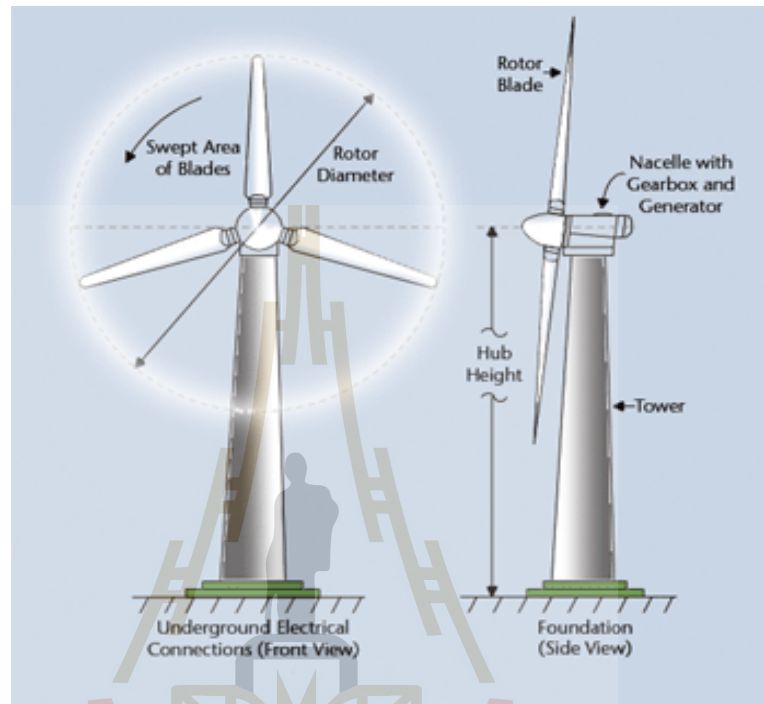


Figure 2. 4 Details of the wind turbine (Berrada & Loudiyi, 2016)

A German physicist Albert Betz concluded, no wind turbine can convert more than $16/27$ of the kinetic energy of the wind into mechanical energy turning a rotor. The theoretical maximum power efficiency of any design of wind turbine is a wind turbine can extract 59% of the energy carried by the wind. This is called maximum power coefficient ($C_{pmax} = 0.59$).

Among the renewable sources of energy available today for generation of electrical power, wind energy stands foremost because of the no pollution, relatively low capital cost involved and the short gestation period required. Wind-powered systems have been widely used since the tenth century for water pumping, grinding

grain, and other low-power applications. There were several early attempts to build large-scale wind-powered systems to generate electricity.

According to Global Wind Energy Council (GWEC), global wind power capacity has increased from 7600MW at the end of 1997 to 159,215MW by 2009. Most of the countries producing electricity from wind are U.S., China, Germany, Spain, Thailand and India, having their installed capacities 35159MW, 25770MW, 25105MW, 19149MW, 224.5 and 3000MW, respectively, by 2014 (Girard, Bossavy, & Kariniotakis, 2011). This ranked Thailand 46th in the world by installed capacity as of 2015. Today, wind power accounts for about 0.4% of the world's electricity demand.

2.5.1 Factor that affects power output of wind turbine

Wind energy is undoubtedly one of the cleanest forms of producing power from a renewable source. There is no pollution, there is no burning of fossil fuels but it's not like erection of a wind turbine anywhere and it will start generating power. There are some factors that can make an impact on the amount of energy generated out of WT as depicted in Table 2.3.

Table 2.3 Technical specification of WT (Ileberi Gbalimene1 et al. 2016)

S/N	Description	Details
1	Rated power per WT (MW)	2.1
5	Hub-height (m)	155
6	Blade length (m)	50
7	Lifetime (years)	30

2.5.1.2 Wind speed

It being a wind turbine, its output first most depends on the wind speed. Both the speed and force of the wind can be deciding factors. Different regions have different wind speeds. You can gather the available wind dynamics data and using a model like Weibull Distribution.

2.5.1.2 Hub Height of WT

Places of higher altitudes have more wind due to various atmospheric factors. Besides, at higher places there is less obstruction from the surrounding hills, trees and building. In fact the height and radius of blade length are so important that alternative energy scientists and engineers are trying to use to estimate generated wind power.

2.5.1.3 Rotor of WT

The amount of energy produced by your wind turbine is proportional to the size of the rotor used, when all other factors have been taken into consideration. A bigger rotor certainly generates more power. Although it may cost more, in the long run, whenever you are getting a wind turbine erected, go for a big a rotor as possible.

2.5.2 Induction and Synchronous Generator

The induction generator needs reactive power to build up the magnetic field, taking it from the mains. Therefore, the operation of the asynchronous machine

usually is not possible without the corresponding three-phase mains. In that case, reactive sources such as capacitor banks would be required, making the reactive power for the generator and the load accessible at the respective locations. Hence, induction generators cannot be easily used as a backup generation unit, for instance during islanded operation (Senjyu et al., 2006)

The synchronous generator operates at specific synchronous speed and hence is a constant-speed generator. In contrast with the induction generator, whose operation involves a lagging power factor, the synchronous generator has variable power factor characteristic and therefore is suitable for power factor correction applications. A generator connected to a vast electrical system will have little effect on frequency and voltage.

Usually, a change in the field excitation will cause a change in the operating power factor, while a change in mechanical power input will change the corresponding electrical power output. Thus, when a synchronous generator operates on infinite bus bars, over-excitation will cause the generator to provide power at lagging power factor, and during under-excitation, the generator will deliver power at leading power factor. Thus, synchronous generator is a source or sink of reactive power.

In general, the electrical power output is calculated by using the following equation (Seifert, 2012):

$$P = \frac{\rho}{2} \cdot C_p \cdot \eta \cdot A \cdot V^3 \quad (2.3)$$

However, taking into account the cut-in speed, rated speed and cut-out speed the formula will be as shown in (2).

$$P(t) = \begin{cases} P(t); V_{in} \leq V \leq Vr \\ P_r; V \leq V \leq V_{out} \\ 0; V > V_{out} \text{ or } V < V_{in} \end{cases} \quad (2.4)$$

$P(t)$ in the first case could be calculated by using (9) if all variables are known.

Hence, $P(t)$ is calculated in this study according to equation (11):

$$P(t) = P_r \cdot \frac{V^3(t)}{V_r^3} \quad (2.5)$$

The power output of WT is proportional to the kinetic energy, air density, etc. which is depicted in Figure 2.5. Precise values can be obtained from manufacturer's data sheet for the respective limits as tabulated in Table 2.1

$$P_{WT}(t) = 0.5\alpha\rho AV^3(t) \quad (2.6)$$

Where

α is the Albert Betz constant, ρ is air density, A is area swept by turbine rotor, and $v(t)$ is wind speed. The energy sources of RDGs can be categorized into stable and unstable energy sources, Fuel cell and Micro-gas turbine are some of the stable energy sources, Wind and Solar are most commonly used in unstable energy sources. Different energy sources (wind turbines) show individual output characteristics when combining with different energy converters. However, based on different types of RES, Girard et al.,(2011) classify WT based on its rating, features and application as shown in Table 2.4. Also, Mohamed et al., (2016) describe characteristics of WT based on different type of manufactures, power rating, diameter of rotor, hub height and its wind speed in m/s as tabulated in Table 2.5

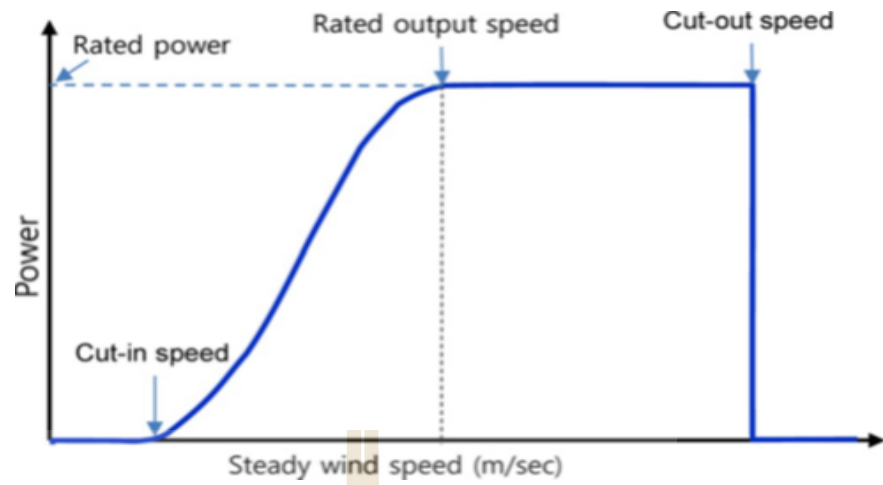


Figure 2. 5 Power characteristics of wind turbine

Table 2. 4: Classification of Wind turbine (Girard et al., 2011)

Type	Rating	Features	Application
Micro	Less than 3kW	Direct drive PMSG	Battery charging, rural load
Small	3 to 30kW	Low maintenance	Remote area/ Residential area
Medium	30 to 200kW	Wound rotor	Hybrid system, RDG
Large	≥ 200 kW	Wound, variable speed	Offshore wind farm

Table 2. 5: The characteristics of WT (Mohamed, Eltamaly, & Alolah, 2016)

Manufacturer	P_r (kW)	D (m)	u_c (m/s)	u_r (m/s)	u_f (m/s)	h (m)
--------------	------------	---------	-------------	-------------	-------------	---------

Enercon-1	330	34	3	13	34	50
ACSA-1	225	27	3.5	13.5	25	50
Fuhrlander-3	250	50	2.5	15	25	42
Ecotecnia-2	600	44	4	14.5	25	45
ITP-1	250	30	3	12	25	50
NEPC-3	400	31	4	15	25	36
Southern Wind	225	29.8	4	15	25	45
Enercon-2	330	33.4	3	13	34	37
NEPC-2	250	27.6	4	17	25	45

2.6 Emerging of energy storage system

More importantly, energy storage can support to accommodate a high penetration level of intermittent renewable RDG. Energy storage is being developed in a variety of solutions such as batteries, flywheels, ultra-capacitors and superconducting energy storage systems. BES has recently emerged as one of the most promising near-term storage technologies for power applications. There are some leading battery technologies such as lead-acid, nickel cadmium, nickel-metal hydride, and lithium iron. Different energy storage technologies have been developed by using various energy converting strategies (Etxeberria et al., 2010). For example, energy is stored in water reservoirs as the gravitational potential energy, as the compressed air in caverns, as electrochemical energy in batteries and flow batteries, like the chemical energy in fuel cells, as kinetic energy in flywheels, as the magnetic field in inductors and as an electrical field in capacitors.

2.6.1 Pumped Hydro Energy Storage

The operating principle of the pumped hydro storage uses the potential energy of water keeps in a reservoir. Water is pumped from lower reservoir to upper reservoir to store energy when the power demand is low. Then, when the power demand is high, water flows from the upper reservoir to lower one, activates the turbine and generates electrical energy. The stored energy capacity of this system is proportional to water volume of upper reservoir and height. This energy storage technology is a large-scale and long-term storage system with a lifetime of 30-50 years.

2.6.2 Compressed Air Energy Storage

In this energy storage technology, conventional gas turbine technology is used. Energy is stored as compressed air in an underground storage chamber. When the power demand is low, the air is pumped to the chamber, and excess energy is stored. The compressed air in the chamber is converted to the electrical energy via a gas turbine. The compressed air is heated and converted to the mechanical energy via a set of low and high-pressure turbines. The air is also mixed with natural gas and combusted. Electrical generators coupled with turbines generate electrical energy. Also, turbine exhaust is used to heat the compressed air and to improve the efficiency. Also, nowadays, this topology attracts much interest. The compressed air storage technology also has a long lifetime about 40 years, and it is considered as long-term storage technologies compatible and competitive with the pumped hydro energy storage systems (Beaudin, Zareipour, Schellenberg, & Rosehart, 2014).

2.6.3 Battery Energy Storage Systems

Batteries are the most common energy storage technologies in which energy stored in a battery cell as electrochemical energy (Kaldellis, 2010). The battery cells are connected in series or in parallel to reach the desired voltage, current and capacity values. A battery cell composes two electrodes called anode and cathode, and the electrolyte. The electrolyte and electrodes are placed in a closed and sealed container. The electrolyte enables the exchange of ions between the electrodes, and electrons flow through the external circuit in (Sortomme & El-Sharkawi, 2009).

The lead-acid batteries are the oldest battery energy storage technology and invented in 1859. In the conventional lead-acid battery, lead dioxide (PbO_2) used as an anode, sponge lead (Pb) used as a cathode, and sulfuric acid (H_2SO_4) used as the electrolyte. There are two types of lead-acid batteries: flooded batteries and valve-regulated batteries. The cycle life of the conventional lead-acid batteries is about 1200-1800 cycle because of the deterioration of electrodes due to the reversible redox reactions.

However, their long charge times, low cycle life, low energy density, low specific energy density and specific power density values, toxic nature of sulfuric acid and lead limit the usage of this type of batteries in grid-scale energy storage systems. However, the conventional lead-acid battery technology is modified to improve their performances. Lead-carbon electrodes are introduced to increase the specific power density, energy density and cycle life of the lead-acid batteries. The lead-acid batteries used for power stabilization, back-up, and phase shifting of renewable power generation systems, with these improved specifications.

Sodium-Sulphur (Pan, Hu, & Chen, 2013; Vrettos & Papathanassiou, 2011) accepted modern rechargeable high-temperature battery technology as shown in Figure 2.6. The sodium-Sulphur batteries have advantages such as high operating temperature (300-350°C), the high energy density of 150kW/m³. With these features, the sodium-sulfur batteries are suitable for non-mobile large-scale energy storage applications, especially for grid-scale energy storage systems including load leveling, peak-shaving, and renewable energy management applications

NaS batteries have the beneficial property of being able to be used for power and energy applications simultaneously. Their primary function is energy storage for more extended periods but their short response time of around one millisecond and pulse power ability makes them suitable for power quality applications as well.

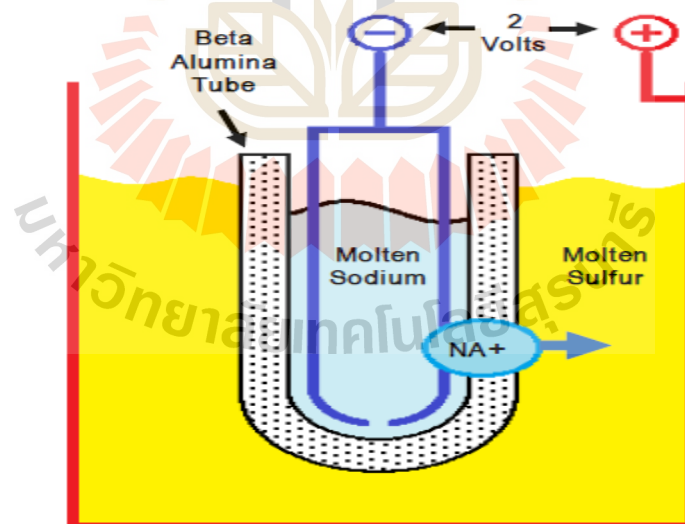


Figure 2. 6 Construction scheme of a sodium-sulfur cell (Pan, Hu, & Chen, 2013)

Lithium-ion batteries shown in Figure 2.7 have been commonly used in mobile consumer electronics, telecommunication tower and electric vehicle and hybrid electric

vehicle applications attract attention to be a possible solution of large-scale energy storage systems. Different chemistries are investigated to obtain high power density, high energy density, high specific energy density, long cycle life values. There are three types of lithium batteries in the market: cobalt, manganese, and phosphate. The energy density and specific energy density values of lithium-ion batteries are high as 170-300Wh/l and 75-125Wh/kg, respectively. Also, they have fast charge and discharge capability, high efficiency (about 70 - 80%). Therefore, in grid-scale applications, lithium-ion batteries are used for regulation and power management services for minutes of runtime.



Figure 2. 7 Lithium-ion batteries (Connolly et al., 2012)

2.6.4 Choice of battery technology

From the battery technology point of view, is not only essential to know the capacity and energy output, but also battery technology which suits the application

are to be considered. It is also important to know that battery technology are still in the development phase with possible future cost and operational improvements. Many battery technologies are sufficiently commercial with beneficial cost development in both the short and long term perspective. There are a few factors to consider when choosing among the different battery technologies such as technical, market, and cost.

The technical maturity is a measurement of how much of the potential technical improvements have been realized. New technologies have an enormous potential for improved performance and costs, but they also come with a more significant of uncertainty for estimations of cost. Figure 2.8 and Table 2.7 shows some storage technologies in comparison to their anticipated research and development cost. While it is essential to have technical maturity in mind, such comparison can be biased as it refers to the application for smart grids. While NaS batteries have been deployed already, other technologies such as lithium ion are still in demonstration phase when it comes to grid energy storage applications and therefore described as immature. However, NaS have almost exclusively been manufactured for grid storage demonstrations only, and production volumes are low. Lithium-ion batteries, on the other hand, have significant production volumes and a commercial market due to automobile and consumer electronic applications

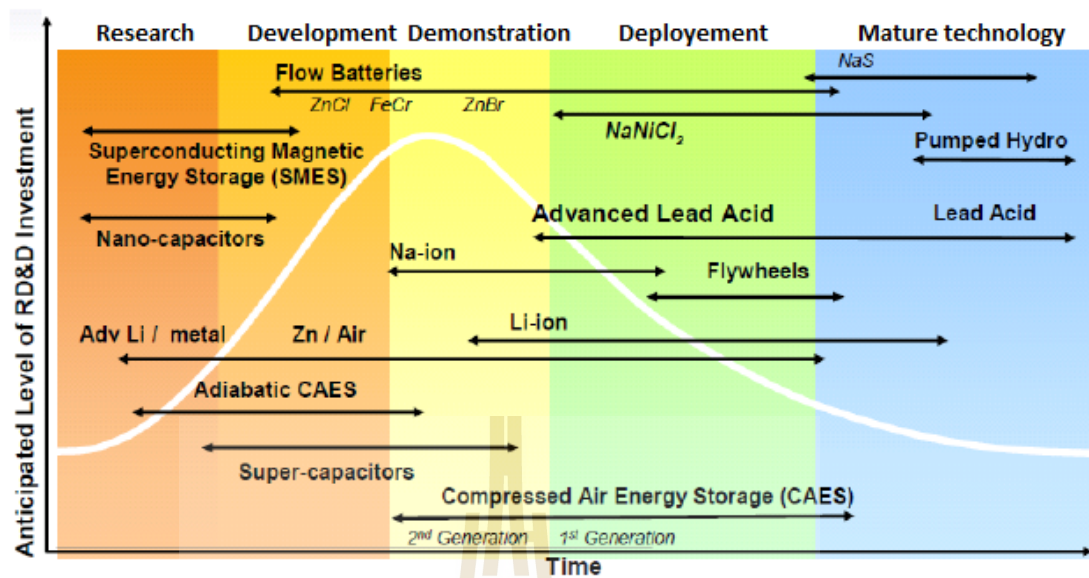


Figure 2. 8 Variety of Energy Storage Technologies

(Dunn, Kamath, & Tarascon, 2011).

Table 2.6 Technologies of BES (Zidar et al.,2016)

Specification	Lead Acid	Ni_Cd	NaS	Flow BES	Li-Ion
Wh/kg	30-50	45-120	80-140	20 -45	90 -190
Life time (yrs)	3 - 15	15 - 20	12 - 20	5 -20	8 -15
Recharge t in hrs	8 – 16	2 - 4	9	4	2 - 4
Discharge rate	5%	20% to 30%	62 % -70%	58% -70%	< 10%
Cell voltage	2	1.2	2	1.4	3.6
Temp ($^{\circ}$ C)	-20 to 50	-20 to 65	300-360	-5 to 55	-20 to 60
Toxicity	Very high	Very high	High	High	Low

2.6.5 Sizing and Sitting of BES.

Let E_{batt} be the average energy requirement for the battery per day in kWh per day. It is estimated from the determined power deficit ($P_{diff}(t)$) calculated as

below where $P_{dem}(t)$ is the power that is to be dispatched over a time period Δt . Let N the number of days in the simulation period (Vrettos & Papathanassiou, 2011).

$$P_{diff}(t) = P_{gen}(t) - P_{dem}(t)$$

$$E_{batt}(kWh) = \max \left\{ \sum_{i=1}^N P_{diff} \cdot \Delta t \right\} \quad (2.7)$$

The model needs to take into account the depth of discharge (DOD), days of autonomy (D), and battery aging. DOD is optimally selected for each battery to ensure its longevity and efficiency. Storage system is characterized by the following parameters which are defined as:

a) Maximum energy capacity

This is the maximum amount of available energy in the storage system in a fully charged state.

b) Minimum energy capacity

It is the minimum amount of available energy in the storage system below which the storage is not discharged to complement supply generation in meeting the grid load.

c) Maximum power capacity

The maximum amount of energy that can be injected into or withdrawn from the storage system at any instant. Though the maximum power of charge and discharge may be sized differently, the two are set equal for this analysis.

d) Cycle efficiency

The product of the charging and discharging efficiencies of the storage system is the cycle efficiency. For this study, the charging or discharging efficiency is obtained by finding the square root of the cycle efficiency.

e) Total discharge time

It is the duration at which the stored energy capacity is exhausted at maximum power discharge. In the model, this is obtained as the ratio of the energy capacity to the power capacity. However, in practical systems, this depends on the depth of discharge and operational conditions of the system. Separating the power and energy dimensions of storage systems is not trivial, and this presents a challenge in choosing the optimum time constant for most storage technologies.

f) Self-discharge

This is the rate at which the storage system intrinsically discharges/loses its available capacity whether it is being used or not. It represents an inherent loss of the storage system. It is dependent though on many factors including environmental conditions

2.6.6 Modeling of BES

The battery is charged when the energy generated by the wind or the PV array and the PW exceeds the local load demand at any time during the day. However, when the load is higher than the energy generated by the sources of wind or PV arrays, the battery is discharged to cover the deficit. BES published in (Sinha 2015) mentioned to store surplus generated energy, regulated system voltage and supply load in case of insufficient power generation from the hybrid RDGs. Sizing of BES depends on the maximum depth of discharge (DOD), temperature and battery life.

During charging process

$$S_c(t+1) = S_c(t)[1 - \sigma(t)] + [I_B(t) \eta_c / C_B] \quad (2.8)$$

$$S_c(t+1) = S_c(t)[1 - \sigma(t)] - [I_B(t) \Delta t \eta_d / C_B] \quad (2.9)$$

Where

S_c State of charge

σ Discharge rate

I_B Current of the battery

C_B Capacity of the battery

η_c Efficiency which ranges between 0.65 to 0.85

η_d Discharged efficiency.

$$1 - DoD \leq S_c(t) \leq 1 \quad (2.10)$$

Where,

DoD = depth of discharge

2.6.7 Ancillary services provided by battery energy storage systems

Transient voltage stability refers to the ability of the system to maintain a synchronous operating a significant after it has been affected by a significant disturbance. (Usually a connection or disconnection of large generators). Authors in (Bahmani-Firouzi & Azizipanah-Abarghooee, 2014; Yang et al., 2012), BES was used for mitigation of voltage disturbance caused by the connection of the doubly-fed induction generator wind turbine to the grid.

Voltage Control is a system service under which the voltage sags, swells and other voltage related problems are monitored and controlled with the use of BES. Publication of optimal voltage control in (Jamian, Mustafa, Mokhlis, & Baharudin,

2014), propose a strategy of using battery energy storage. The focus is on the grids that have renewables distributed generation. Methodology presented in (Saif et al., 2010) proposed GA for optimal placement of BES in the distribution grid. The Power loss minimization is achieved by optimally placing the BES within the network

2.7 Power flow analysis in RDN

The power flow (also known as load flow) problem models the nonlinear relationships among bus power injections, power demands, and bus voltages and angles, with the network constants providing the circuit parameters. It is the heart of most system-planning studies. Also, power flow solution is required for many other analyses such as rotor-angle stability, voltage stability, and contingency studies. This section provides a formulation of the power flow problem and its associated solution strategies.

There are three popular numerical methods for solving the power flow equations. These are the Gauss-Seidel (G-S), Newton-Raphson (N-R), and fast-decoupled (F-D) methods (Glover et al., 2012; Saadat, 2010; Weedy et al., 2012). The N-R method is superior to the G-S method because it exhibits a faster convergence characteristic. However, the N-R method suffers from the disadvantage that a "flat start" is not always possible since the solution at the beginning can oscillate without converging toward the solution. To avoid this problem, the power flow solution is often started with the G-S algorithm followed by the N-R algorithm after a few iterations.

According to research made by Mmary et al., (2018), there are several traditional load flow methods used in transmission and distribution networks, such as the Gauss-Seidel, Newton-Raphson and Fast Decoupled techniques. These methods fail

to meet requirements in both performance and robustness aspects in the distribution system applications due to complexity, size, and characteristics of RDN.

2.8 Multi-Objective power optimization

In the real world, many optimization problems contain more than one objectives that are generally conflicting with each other to be either minimized or maximized at the same time. For example, the excellent design for bridge construction is represented by lower mass and higher strength. A plane design needs to optimize fuel efficiency, weight, and cargo simultaneously. Likewise, in power system optimization it needs solution sets which will enable operator and designer to decide according to the importance of the problem.

It is not possible to find a single optimal solution (an example of power loss reduction only) that can ensure compliance with all other objectives problems. The best solution means that it is not the worst one for each objective and it is better than the others for one objective at least. In other words, an optimal solution is not dominated by any other solutions in the search space. It is called a non-dominated solution or Pareto optimum, while an image formed by Pareto-optimal solutions under the space of objective functions is known as a Pareto front (Figure 2.9).

Single objective optimization yields solutions of a single aspect which may not be acceptable to the utilities. Therefore, multi-objective approaches are required to solve the problem. The use of multi-objective optimization (MOO) techniques have some advantages such as more accessible to decide at the end or before running the optimization based on the view that system operator takes. On the other hand, multiple objectives might not be optimized simultaneously because of inherent conflicts existing

between them. To grab this problem, there are three approaches to consider multi-objectiveness (Celli, Ghiani, Mocci, & Pilo, 2005; Kong & Jeyasurya, 2009).

As the widely adopted inventive search method, the artificial bee colony (ABC) algorithm is a powerful search technique that drew inspiration from the natural foraging behaviors observed in bee colony (Abido, 2011). Due to its simplicity and efficiency, ABC has become a high competitor in solving the MO problems. Many researchers have presented several existing multiobjective algorithms such as (Abido, 2011; Chaouachi, Kamel, Andoulsi, & Nagasaka, 2013). However, these proposed algorithms still suffer from low convergence rate and lack the diversity of swarm.

2.8.1 Priority Goal Programming

This approach is built on the conventional techniques for generating trade-off surfaces. The objectives are aggregated into a single parameterized objective function, and trade-offs are determined based on the weighting coefficients values. The weighting factor method in (Nangia et al., 2005), is used to aggregate cost of generation function and system transmission losses to study the correlation between each objective and its weight factor in an optimal power flow problem. In the work of (Yun et al., 2010), authors solved a voltage control problem by an extension of the simplex known as goal programming simplex by ranking the priority of the control objectives. Several objectives such as adjusting the reactive power of generators are considered to increase the reliability and stability operation of a power system. The publication in (Abou El-Ela et al., 2011), weighting factors are applied to obtain overall maximal composite benefits of added RDGs. Priority goal programming is an easy and efficient approach

to implement but requires extensive sensitivity analysis if the prior assessment of weights is going to be used.

2.8.2 Pareto-Based Multi-Objective Algorithms

In Pareto based multi-objective programming no single optimal solution simultaneously optimizes all the objective functions, so in some literature, it is referred to as non-deterministic approach. In such cases, the decision makers are looking for the most desirable solution. In Pareto-based multi-objective algorithms, as shown in Figure 2.9, all objectives are optimized at the same time and solutions which are not dominated by another solution are chosen and illustrated in n-dimensional space as represents the number of objectives. In other words in this methods multi-objective problem is directly addressed through the use of separate objectives and produce an optimum set of points.

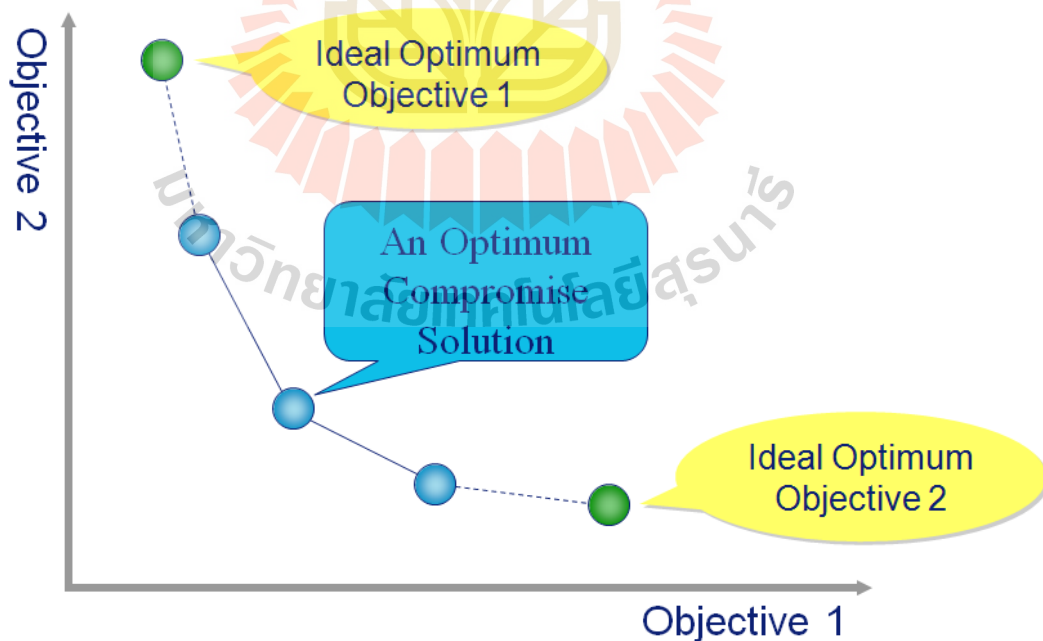


Figure 2. 9 The optimum compromise solution

2.8.3 Classical optimization techniques

Solving of the optimization problem in the reactive power and voltage control, several classical optimization techniques have been proposed. These conventional optimization techniques include the gradient method, Quadratic programming, nonlinear programming, linear programming and interior point method. Although these techniques have been successfully applied to solve the reactive power optimization problem (RPOP) these are still associated with some difficulties such as handling of the multi-modal characteristic of the problems, nonlinear and non-convex nature of the RPOP. These classical techniques also suffer from the problem of a local optimum.

In the recent years, global optimization techniques based on artificial intelligence like GA, and PSO have been proposed to solve the RPOP. These global optimization techniques overcome the above difficulties of classical optimization and do not suffer from the problem of a local optimum. If the optimization problem involves more than one objective functions, then the process of determining more solutions are called multi-objective optimization. Due to the presence of conflicting multiple objectives, the multi-objective optimization results in some optimal solutions, known as Pareto- optimal solutions. The following are a fundamental goal in multi-objective optimization: To find a set of solutions as close as possible to the Pareto-optimal front.

In this research (thesis) presents a new ABC algorithm based on the intelligent foraging behavior of honey bee swarm for solving multi-objective power optimization problem. The multi-objective problem formulated as a nonlinear constrained multi-

objective optimization problem with two competing objectives, i.e., power loss reduction and maximizing voltage stability.

2.9 Technical benefits of RDG in RDN

2.9.1 Power and Energy Losses

The distribution system is well-known for its high R/X ratio and significant voltage drops that could cause substantial power losses along the feeders. It is added that the distribution loss usually is higher than the transmission loss. Consequently, power loss reduction in RDN has been one of the most significant challenges to power distribution utilities worldwide. Studying the reduction of power loss at the distribution system level is necessary. RDG planning, the loss reduction can lead to positive impacts on system capacity release, voltage profiles, and voltage stability. RDG planning methods for minimizing losses can be classified into two groups, namely power and energy losses. The optimal placement and sizing of RRDG for minimizing power losses in RDN have attracted considerable attention in recent years. Most traditional methods have assumed that RDG units are dispatchable and placed at the peak load. Typical examples for such researchers are analytical methods, numerical approaches and a wide range of heuristic algorithms such as GA, PSO, and Artificial Bee Colony (ABC) Algorithm (Karaboga & Basturk, 2007; Mohandas et al., 2015).

Also, the relevant literature review shows that most of the existing studies have assumed that RDG units operate at pre-specified power factor, usually unity power factor under the current standard IEEE 1547. In such researches, only the location and

size have been considered, while the optimal power factor for each RDG unit that would be a crucial part of minimizing energy losses has been neglected. Depending on the characteristics of loads served, each RDG unit that can deliver both active and reactive power at optimal power factor may have positive impacts on energy loss reduction.

The total power loss includes real and reactive power loss as given in equations below:

$$P_{loss} = \sum_{i=1}^n \sum_{j=1}^n \left[a_{ij} (P_i P_j + Q_i Q_j) + b_{ij} (Q_i P_j - P_i Q_j) \right] \quad (2.11)$$

$$Q_{loss} = \sum_{i=1}^n \sum_{j=1}^n \left[c_{ij} (P_i P_j + Q_i Q_j) + d_{ij} (Q_i P_j - P_i Q_j) \right] \quad (2.12)$$

$$a_{ij} = \frac{R_{ij}}{V_i V_j} \cos(\delta_i - \delta_j) \quad (2.13)$$

$$b_{ij} = \frac{R_{ij}}{V_i V_j} \sin(\delta_i - \delta_j) \quad (2.14)$$

$$c_{ij} = \frac{x_{ij}}{V_i V_j} \cos(\delta_i - \delta_j) \quad (2.15)$$

$$d_{ij} = \frac{x_{ij}}{V_i V_j} \sin(\delta_i - \delta_j) \quad (2.16)$$

Where

- n is the number of nodes
- P_i is the power flow at the node in kW
- Q_i is reactive power flow at node i in kVAr
- P_j is the real power flow at node j in kW

Q_j is reactive power flow at node j in kVAr

R_{ij} is the resistance of the line connecting node i and j in ohms

X_{ij} is reactance of the line connecting node i and j in ohms

V_i and V_j the voltage magnitude at node i and j

δ_i and δ_j are the bus voltage magnitude at node i and j

a_{ij} , b_{ij} , c_{ij} and d_{ij} are the function of loss coefficient between node i and j

2.9.2 Voltage Stability Index

Problems related to voltage stability in power systems are one of the significant concerns in power system planning and operation. Voltage stability is concerned with the ability of a power system to maintain acceptable voltages at all nodes in the system under normal condition and after being subject to a disturbance. Voltage instability occurs under heavily loaded system conditions together with deficient reactive power support, and this may lead to voltage collapse. At the distribution system level, the voltage instability has been identified for the last decade. Another study has reported that under critical loading conditions in a particular industrial area, the distribution network experienced voltage collapse. In recent years, due to high intermittent renewable penetration, sharply increased loads and the demand for higher system security, it is necessary to study the voltage stability at the distribution system level (Mohandas et al., 2015).

According to the European standard EN 50160, ANS C84.1, IEEE 1547 (Weitemeyer et al., 2015), voltage characteristics of electricity supplied by electricity networks under normal operating conditions, which excludes period with faults or

interruption, it is stated that the supply voltage variations should not exceed $\pm 10\%$ of the nominal voltage. This applies to high voltage and medium voltage networks. Regarding the low voltage distribution grids standard IEC 60364-5-52 low voltage electrical installations, it is specified that the maximum allowed voltage drop is $\pm 3\%$ for lightning circuits and $\pm 5\%$ for all other circuits (Saint, 2011; Silva, Funmilayo, & Bulter-Purry, 2007).

2.9.3 Existing IEEE 34-Nodes Radial Distributed Network Model

For the addition of RDG and BES to a distribution network, the existing IEEE 34 nodes network was adopted as a test case. The IEEE Distribution Analysis Subcommittee has data for numerous test cases, and hence the data for IEEE 34 bus was chosen for the radial distribution feeder. The original system is 60Hz, 24.9kV, 12 MVA with various fixed loads and distributed loads connected to a primary utility substation. The load type includes constant current, constant impedance and constant power models (three phase and single phase). The line impedances are calculated from their geometric data and given as configurations which contain details of impedance and capacitance matrices in ohms/mile and Siemens/mile. The entire configuration is as shown below in Figure 2.10 and the model details are found in the same description (Mwakabuta & Sekar, 2007; Silva et al., 2007).

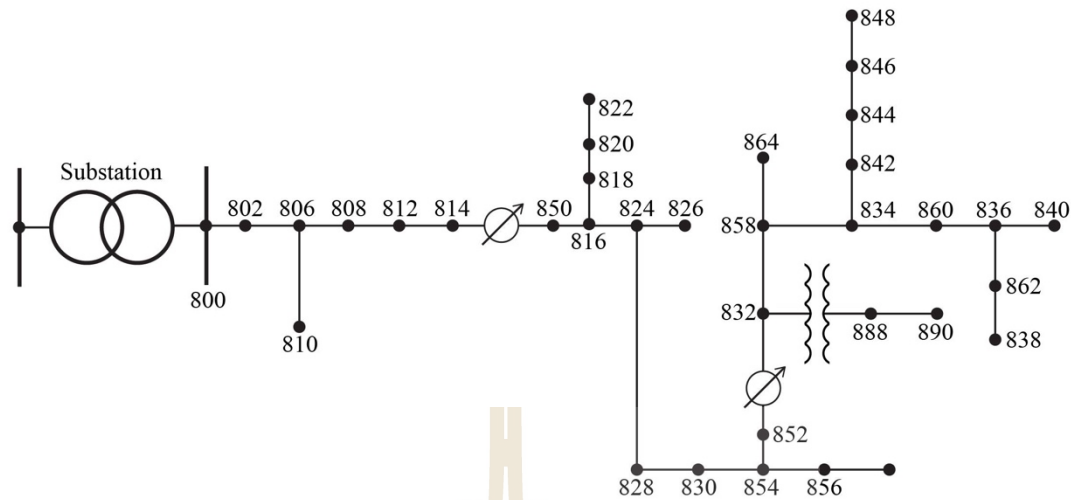


Figure 2. 10 Existing IEEE 34-Nodes Radial Distributed Network Model

From the IEEE distribution feeder committee, the information 34-nodes line impedances, transformer connection impedances, and load data are obtained. The nominal voltage feeder is 24.9 kV which is an actual feeder located in Arizona. It is characterized by:

- a) Very long and lightly loaded
- b) Two in-line regulators required to maintain a good voltage profile
- c) In-line transformer reducing the voltage to 4.16 kV for a short section of the feeder
- d) Unbalanced loading with both spot and distributed loads. Distributed loads are assumed to be connected at the center of the line segment
- e) Shunt capacitors

Because of the length of the feeder and the unbalanced loading it can have a convergence problem.

2.9.4 Sinks and Sources of Reactive Power

Balancing the reactive power means that the sum of the reactive power production, consumption and losses must be zero at all times. This section gives a brief overview of some of the reactive sources and sinks which can be found in distribution networks as shown in Table 2.8. A thorough description of the problem of reactive power can be found in (Mamandur & Chenoweth, 1981; Yang et al., 2012), reactive power problems related to solar PV power are treated in (Aghatehrani & Golnas, 2012) and reactive power related to power shown in (Zhao et al., 2009)

Table 2. 8 Source and sink of reactive power

Source	Sink	Controllable
Underground cable	Transformer	Synchronous generator
Overhead lines at low load	Overhead lines at high load	Switchable capacitor
Fixed capacitor	Induction motor	Switchable reactor
	Wind turbine, Fixed reactor	STATCOM, SVS

2.10 Renewable Distributed Generation

Recently, some publication has proposed a solution to determine both the location and size of the RDG in simultaneous. Some of the methods above are Genetic Algorithm, Particle Swarm Optimization, Artificial Bee Colony and Evolutionary Programming. As identified by Lopes et al., (2008), the primary benefits of integrating RDGs correctly behind the rapid growth of RDG units, are:

- a) Environmental sustainability

One of the primary drivers behind the growth of RDG units is the use of renewable energy and CHP to limit greenhouse gas (GHG) emissions by the use of renewable energy. Another significant driver for RDG from the environmental perspective is the avoidance of construction of new transmission lines and large power plants.

b) Commercial

In the competitive market environment and the uncertainty associated with it, small capacity generations are preferred. Another commercial driver is that RDG units can have a beneficial impact on power quality and reliability such as improve voltage profile, reduce line losses and reduce network congestion since it is distributed around the network close to customers.

2.10.1 Optimization of RDG in Radial Distribution Network

RDG planning is the process of optimizing RDG type, size, and location to achieve a set of objectives. It also includes some nonlinear optimization objectives, such as line loss minimization. Recently, diverse methods for optimizing the location, size, and type of RDG have been proposed, with particular emphasis on RDG placement and sizing. Such optimization methods can be summarized into two categories. The first group of RDG planning methods focuses on the optimization of a single objective. One of the most common objectives found in the literature is the minimization of line losses. Other single-objective RDG planning approaches focus on the minimization of total cost. Cost can be aggregated from different points-of-view. Hence, these techniques formulate the problem either from the perspective of RDG

developer or the perspective of a distribution system operator. These methods are based on the use of traditional mathematical optimization techniques and genetic algorithms.

The second group of the proposed optimization techniques is a multi-objective method. The solution methods of multi-objective problems to are divided into two main types. The first type makes use of single-objective techniques, and the solution set is identified by changing the master objective iteratively. The weighted-sum method is one of the most common methods of this type. The second type of multi-objective optimization methods is based on Evolutionary Algorithms (Singh & Verma, 2009).

Researchers from all over the world are studying the formerly mentioned problems and have featured various techniques and methodologies for selecting the optimum sitting and sizing of DGs to improve voltage profiles and minimize or even eliminate power losses of modern distribution networks with distributed generation. Subsequent is a presentation of the most essential latest studies published in the technical literature.

Publication of multiple types of optimization techniques in (Jamian et al., 2014) used to regulate the RDG's output to compute its optimal size. Comparative studies of a new proposed rank evolutionary particle swarm optimization method with evolutionary particle swarm optimization and traditional particle swarm optimization were conducted. The implementation of evolutionary programming and particle swarm optimization allowed the entire particles to move toward the optimal value more rapidly. Their applied technique has shown a reduction in power losses which can be achieved when an optimal DG size is selected. Another conclusion made, was that evolutionary particle swarm optimization showed better results than the conventional

particle swarm optimization due to its reduced iteration numbers and minor consumed computing time.

A study conducted in (Baghaee, Jannati, Vahidi, Hosseinian, & Rastegar, 2008) used genetic algorithms to optimize the location and size of different RDG units. Three primary objectives have been selected, i.e., voltage, real and reactive power losses, and RDG size, aiming to reduce the total power losses and improve the voltage profiles. A 69-node radial distribution test system has been used in their study for testing and verification purposes. The proposed methodology suggested that the installation of three RDG units of the same size in three different positions of the 69-nodes radial distribution test system resulted in the reduction of power losses and voltage profiles enhancement.

Publication in (Naik, Khatod, & Sharma, 2013) presents a method that aimed to minimize power losses and improve voltage profiles of a distribution system with a RDG unit coupled. They have chosen a 33-nodes distribution system to apply their method on. Initially, a voltage sensitivity index was calculated for all the buses, and then the bus with the lowest sensitivity index was chosen as the optimum place for the RDG unit installation. Subsequently, several RDG sizes were tested to identify the one that would result in the least possible power losses. In this study, the forward-backward sweep algorithm was selected to perform the load flow analysis.

An analytical study for the calculation of the optimum size and the allocation of RDG units at optimal positions was presented by (Hung, Mithulananthan, & Bansal, 2013; TN Shukla, Singh, Srinivasarao, & Naik, 2010). The technique that aimed to reduce the power losses and to improve the voltage profiles of distribution systems has used a sensitivity index to identify the best location for the connection of the RDG. The

13-bus IEEE radial distribution test system has been used for verification purposes, and the main conclusion of this work was that minimum loss, and a better voltage profile can be achieved with integrating a single RDG unit of optimum size and in an optimum location rather the integration of several RDG units.

The published results in (Fadaee & Radzi, 2012; Fetanat & Khorasaninejad, 2015) explored the penetration of hybrid distributed generation technologies to a medium voltage power distribution network. Power flow and short-circuit analyses were carried out to determine the changes caused by the RDG penetration to the currents, losses, voltage profiles and short-circuit levels of the examined network. Their general conclusion was that arbitrary RDG accommodation leads not only to network sterilization but also to the violation of technical constraints.

Wang et al., (2015) used multi-objectives PSO algorithm to optimize a hybrid PV/wind/battery energy system on the basis of cost, reliability, and emission criteria without power loss and voltage stability. To the best of our knowledge, there has been a few research works on integrating RDG and BES into the radial distribution network, bridging the gap between traditional distribution planning frameworks and methods for siting RDG within the distribution system.

2.10.2 Smart Distribution Network.

Smart distribution networks are based on two-way digital communication between the consumers and suppliers as illustrated in Figure 2.11. It allows better monitoring and control of the supply chain with the aim of reducing the energy consumption, power loss, maximizing voltage profile and reduction of costs (Bruce, 2007). There is a tendency to expand existing grids with digital technology to

build smart grids which would react to the local changes better and would play a vital role in the integration of RDG and BES. Modern distribution grid should have the following features:

- a) Enabling informed participation of customers
- b) Accommodating emerging of RDG and BES
- c) Enabling new services, and markets
- d) Providing the power quality

The significant technical benefits of employing RDG are as follows (El-Khattam & Salama, 2004):

- a) Reduced line losses.
- b) Voltage profile improvement.
- c) Increased overall energy efficiency.
- d) Enhanced system reliability and security.
- e) Improved power quality.

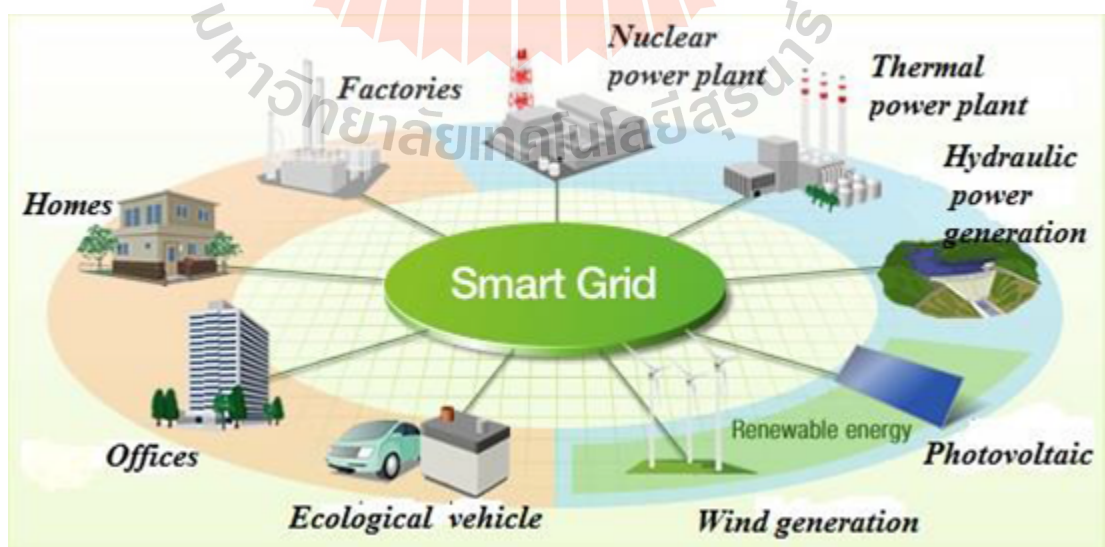


Figure 2. 11 Smart grid with RRDG (Basso & DeBlasio, 2011)

2.10.3 Renewable DG in Radial Distribution Network

Distribution system design and planning problems have been studied and researched since the very beginning. However, these problems have faced a significant change in paradigm over the past decade due to deregulation of the power industry, policy changes and advancements in RDG technologies. In the beginning, the research focused on traditional planning problems such as the placement of substations and routing of feeders to minimize costs and losses to the LDC. Since then, the research has advanced keeping in step with the changes in the tools available to researchers, changes to distribution systems, advancement in technology and changes in policy. This section discusses various proposals for optimal distribution planning in the deregulated environment.

Publication of (Devi & Geethanjali, 2014) presents an optimization method for radial distribution network planning based on a combination of the steepest descent and the simulated annealing approaches. The optimization procedure starts by applying the steepest descent approach continued by applying the method of simulated annealing. The method takes into account the capital recovery, energy loss, and undelivered energy costs.

A multi-objective model for placing RDG under load uncertainty proposed by the publication of (Niknam, Narimani, Aghaei, & Azizipanah-Abarghooee, 2012) where minimization of investment, operation cost of RDG units and cost of losses and risks of voltage violation were considered. The output of the algorithm is a set of Pareto-

optimal multi-objective RDG placement solutions, and the planners select the most satisfactory Pareto-optimal solution by their experience.

Paper of (Payasi, Singh, Singh, & Singh, 2015) consider a multi-objective performance index-based size and location determination of distributed generation in distribution systems. While most of the studies assumed a constant power (real and reactive) load model, Singh et al. examined the use of different load models, finding that the choice of models has a significant impact on the optimal planning of RDG. The proposed technique was based on genetic algorithm (GA).

In the publication of (Reddy, Reddy, & Manohar, 2016) a multi-objective optimization applied to determine the placement and sizing problem of RDG resources into existing distribution networks. The procedure, based on the application of GA, allows the planner to decide the best compromise solution for his particular requirements. The voltage stability improvement, cost of energy losses and power losses are included in the objectives function of the research study.

Optimization of RDGs is a research field with significant areas to be explored, such as the formation of new methodologies that could help to notify decision makers in the design stages of projects. These methodologies provide support tools for system sizing due to their ability to tackle non-linear problems with relatively high calculation speeds. For example, cost optimization of either grid-connected or stand-alone HRESs using HOMER optimization software (Etinski & Schülke, 2013) which is based on the analytical simulation of several scenarios. Others develop heuristic methodologies, relying on evolutionary algorithms to optimize microgrid according to cost, reliability, power loss, stability parameters. However, few of them deal with solar-, wind-, and

BES hybridization in a grid-connected scheme, such as the case proposed in the present work considering MOOP of power loss and maximization of voltage stability.

This work proposes an improvement to a grid-connected solar PV-wind, which was proposed in a previous publication of (Fetanat & Khorasaninejad, 2015). This improvement consists of adding a certain degree of autonomy given by BES, which is a controllable source. Also, these sources of energy are recognized to be the RES with higher social, technical, economic, and environmental benefits.

2.10.4 Impacts of RDG in voltage profile of RDN

Distributed generation is supposed to support and improve the system's voltage, but the question that is raised is up to what extent is this statement accurate since it has been demonstrated that the penetration of RDGs in the distribution system may cause overvoltage or under-voltages. Furthermore, specific RDG technologies vary their output power level over time, as in the case of photovoltaics and wind generators. As a consequence, voltage fluctuations occur that in turn deteriorate the power quality delivered to consumers (Yan & Saha, 2012).

Moreover, over-voltages and under-voltages in distribution networks with RDG have been reported due to the incompatibility of RDGs with the existing voltage regulation methods. In general, the distribution networks are regulated with the help of voltage regulators, capacitors and the tap changing of transformers. These methods were designed for radial (unidirectional) power flow and had been proved to be very reliable and efficient in the past. However, nowadays, the installation of RDGs in distribution networks had a substantial impact on the voltage regulation methods performance due to the meshed (bidirectional) power flow, introduced by RDGs to the

networks. On the other hand, the implementation of RDG had a positive impact on the distribution networks for the reason that they contribute to the reactive compensation for voltage control, to frequency regulation and they operate as a spinning reserve in the case of primary system's fault indices.

2.10.5 Impacts of RDG in power losses of RDN

Several studies, most of which were presented earlier, demonstrated that the location and size of RDG unit play an essential role in the power losses elimination. Consequently, the specific location of an RDG in a distributed network and RDG's specific capacity resulting in minimum power losses are in general identified as the optimum location. The allocation process is very similar to the capacitor allocation procedure aiming at the power losses reduction. The main difference between the two processes is that RDG units exhibit impact upon both real and reactive power, while the capacitor banks influence only the reactive power flow. It has been proven, that in the case of networks with increased power losses, installing a relative small distributed generation unit strategically connected to the network, may result in substantial power losses reduction (Passey et al., 2011)

In summary, although many heuristic optimization methods have been used in several studies and deliver promising results, most of these studies focus on one issue like the sizing of conventional DG, reliability, cost only and they didn't address multi-objectives with multi-constraints analysis of HRES. Furthermore, all of the optimization approaches used in the above studies didn't take into account the smart grid applications like load shifting, renewable DG, metering infrastructure, communication, intelligent dispatching, power network topology and demand-side

management relied on the consumer's endeavors, which makes it hard to be accomplished. Most of these approaches depend on the presence of a real-time pricing tariff for cost or peak demand reduction which is not an ideal solution. In addition, the above studies ignored the dummy energy and didn't provide approaches to exploit it

In this thesis, an optimal sizing, and placement algorithm based on smart grid applications is introduced to determine the optimum hybrid PV/wind/battery energy systems so as to meet the load requirements with minimum power loss and highest voltage stability.

2.10.6 Schematic diagram of proposed hybrid RDG

In several studies of optimization delivers promising results, most of these studies focus on one objective function with one source of RDG. In this research work, two sources of RES was considered in on-grid hybrid RDG as shown in Figure 2.12.

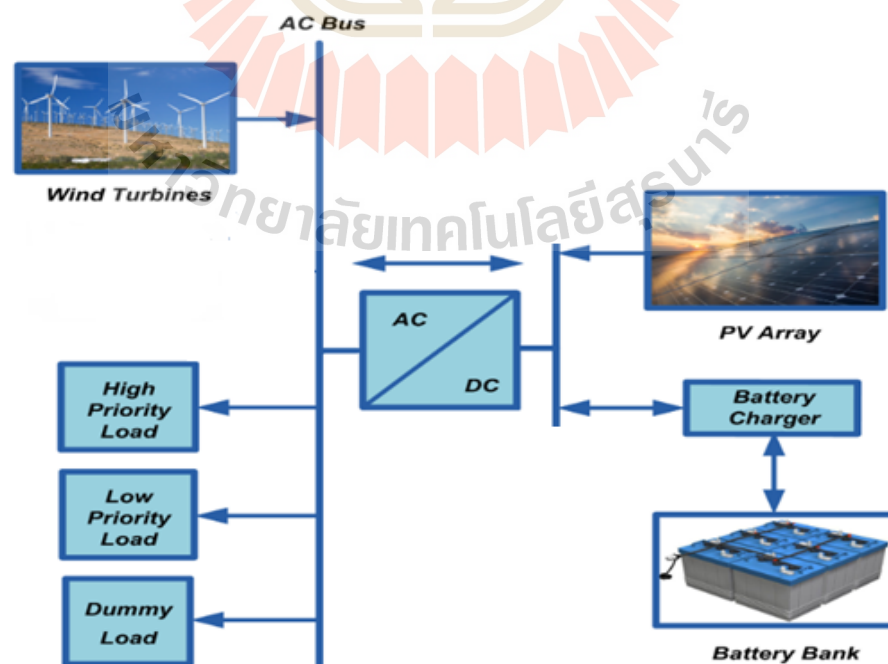
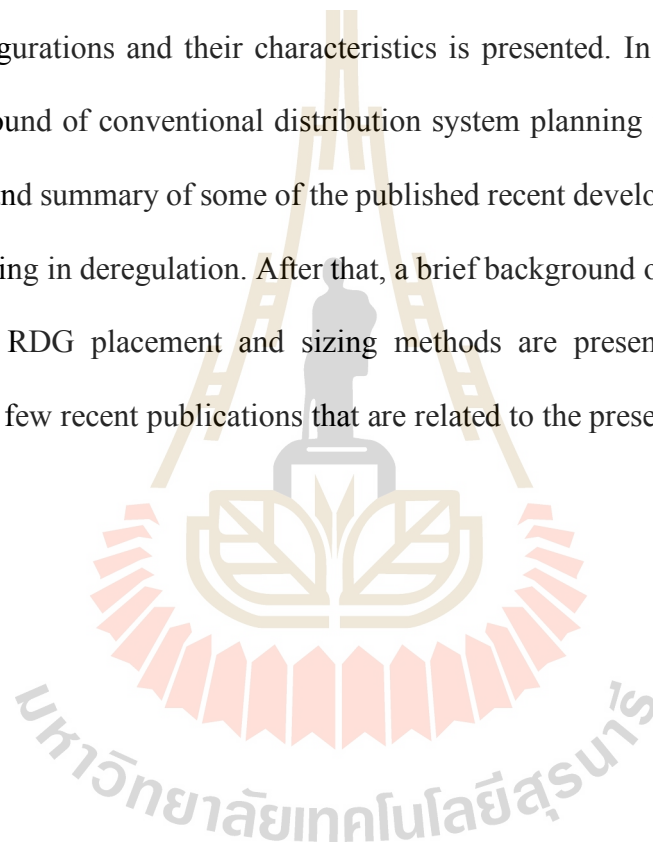


Figure 2. 12 Schematic diagram of proposed hybrid RDG with BES

2.11 Summary of the chapter

In this chapter, an attempt has been made to discuss and review some of the published literature on distribution system planning. In the first section, a brief background of the electric power system and distribution system including distribution system configurations and their characteristics is presented. In the second section, a brief background of conventional distribution system planning is presented, followed by a review and summary of some of the published recent developments in distribution system planning in deregulation. After that, a brief background of RDG types, benefits and optimal RDG placement and sizing methods are presented. The last section discusses the few recent publications that are related to the presented work.



.CHAPTER 3

METHODOLOGY

3.1 Introduction

As described in Chapters 1 and two distribution systems design and planning are facing a significant alteration in paradigm due to the deregulation of the power industry and with the rapid penetration of RDG sources. A proper distribution system design and planning is the key to determining the best expansion strategies to provide reliable and stable services to the customer. In this chapter, a comprehensive optimizing framework of RDG in RDN from the utility company perspective is presented. It incorporates RDG units as an option for upgrade plans for feeders and substations.

In Section 3.2, the mathematical modeling of the optimization framework is described. This is followed by the description of the 34-nodes radial distribution system and the computational details in Sections 3.3 and 3.4 respectively. Finally, a summary of this chapter presented in Section

3.2 Mathematical Formulation

In this section, the mathematical model for planning RDG in RDN is presented.

3.2.1 Power Flow Analysis in Radial Distribution System

The simplicity Z-bus method is used for power flow analysis (Sharma & Vittal, 2010). Since the distribution system with RDG needs to be modeled with PV buses and sensitivity matrix approach. Sensitivity matrix deduced from the impedance matrix Z . The sensitivity matrix deduced;

$$M \Delta Q = \mathbb{K} \quad (3.1)$$

Where

ΔQ is reactive power mismatch

ΔV is the voltage mismatch of PV nodes

Since PV nodes have a voltage nearly 1.0 p.u, the reactive power mismatch will be approximately equal to injected current increment, and hence matrix M calculated as:

$$M = \begin{bmatrix} |Z_{11}| & |Z_{12}| & \dots & |Z_{1n}| \\ \vdots & \vdots & \ddots & \vdots \\ |Z_{n1}| & |Z_{n2}| & \dots & |Z_{nn}| \end{bmatrix} \quad (3.2)$$

3.2.2 Newton-Raphson Power Flow Algorithm

As depicted in (3.3-3.11), N-R algorithm is used to solve power flow calculation. For the network with some nodes, the power injection measurement of nodes i can be written as follows:

$$I_i^* = \sum_{j=1}^n Y_{ij}^* V_j^* \quad (3.3)$$

$$S_i = V_i I_i^* = V_i \left(\sum_{j=1}^n Y_{ij}^* V_j^* \right) = V_i \sum_{j=1}^n Y_{ij}^* V_j^* \quad (3.4)$$

$$Y_{ij} = G_{ij} + jB_{ij} \quad (3.5)$$

$$V_i = |V_i| \angle \theta_i = |V_i| (\cos \theta_i + j \sin \theta_i) \quad (3.6)$$

The complicated equation of power rewritten as follows

$$S_i = P_i + jQ_i = V_i \sum_{j=1}^n Y_{ij}^* V_j^* = \sum_{j=1}^n |V_i| |V_j| (\cos \theta_{ij} + j \sin \theta_{ij}) (G_{ij} - jB_{ij}) \quad (3.7)$$

Resolving into the real and imaginary part as balancing equation

$$P_i = \sum_{k=1}^n |V_i| |V_k| (G_{ik} \cos \theta_{ik} + B_{ik} \sin \theta_{ik}) = P_{Gi} - P_{Di} \quad (3.8)$$

$$Q_i = \sum_{k=1}^n |V_i| |V_k| (G_{ik} \sin \theta_{ik} - B_{ik} \cos \theta_{ik}) = Q_{Gi} - Q_{Di} \quad (3.9)$$

By neglecting line charging capacitance, power flow between two nodes can use voltage magnitude and phase angle to express

$$x = \begin{bmatrix} \theta_2 \\ Q_n \\ |V_2| \\ |V_n| \end{bmatrix}; \quad f(x) = \begin{bmatrix} P_2(x) - P_{G2} + P_{D2} \\ P_n(x) - P_{Gn} + P_{Dn} \\ Q_2(x) - Q_{G2} + Q_{D2} \\ Q_n(x) - Q_{Gn} + Q_{Dn} \end{bmatrix} \quad (3.10)$$

The Jacobian Matrix determined by differentiating each function concerning each variable as:

$$J(x) = \begin{bmatrix} \frac{\partial f_1(x)}{\partial x_1} & \frac{\partial f_1(x)}{\partial x_2} & \frac{\partial f_1(x)}{\partial x_n} \\ \frac{\partial f_2(x)}{\partial x_1} & \frac{\partial f_2(x)}{\partial x_2} & \frac{\partial f_2(x)}{\partial x_n} \\ \frac{\partial f_n(x)}{\partial x_1} & \frac{\partial f_n(x)}{\partial x_2} & \frac{\partial f_n(x)}{\partial x_n} \end{bmatrix} \quad (3.11)$$

3.2.3 Real Power Flow Analysis

The real power flow in a line connecting two nodes i and j expressed as follows;

$$P_i = V_i V_j Y_{ij} \cos(\theta_{ij} + \delta_j - \delta_i) \quad V_i^2 Y_{ij} \cos \theta_{ij} \quad (3.12)$$

$$\Delta P_{ij} = \frac{\partial P_{ij}}{\partial \delta_i} \Delta \delta_i + \frac{\partial P_{ij}}{\partial \delta_j} \Delta \delta_j + \frac{\partial P_{ij}}{\partial V_i} \Delta V_i + \frac{\partial P_{ij}}{\partial V_j} \Delta V_j \quad (3.13)$$

$$\frac{\partial P_{ij}}{\partial \delta_i} = -V_i V_j Y_{ij} \sin(\theta_{ij} + \delta_j - \delta_i) \quad (3.14)$$

$$\frac{\partial P_{ij}}{\partial \delta_j} = V_i V_j Y_{ij} \sin(\theta_{ij} + \delta_j - \delta_i) \quad (3.15)$$

$$\frac{\partial P_{ij}}{\partial V_i} = V_j Y_{ij} \cos(\theta_{ij} + \delta_j - \delta_i) - 2V_i Y_{ij} \cos \theta_{ij} \quad (3.16)$$

$$\frac{\partial P_{ij}}{\partial V_j} = V_i Y_{ij} \cos(\theta_{ij} + \delta_j - \delta_i) \quad (3.17)$$

Where

V_i and V_j are the maximum magnitudes at buses i and j respectively

δ_i and δ_j are the voltage angles at buses i and j respectively

Y_{ij} is the size of j^{th} element of the Y_{bus} matrix

Y_{ii} is the magnitude of the i^{th} element of the Y_{bus} matrix

θ_{ij} is the angle of the j^{th} element of the Y_{bus} matrix

θ_{ii} is the angle of the i^{th} element of the Y_{bus} matrix

3.2.4 Reactive Power Flow Analysis

The reactive power flow in a line connecting two nodes, node i and nodes j expressed as follows:

$$Q_i = -V_i V_j Y_{ij} \sin(\theta_{ij} + \delta_j - \delta_i) - V_i^2 Y_{ii} \sin \theta_{ii} \quad (3.18)$$

$$\Delta Q_{ij} = \frac{\partial Q_{ij}}{\partial \delta_i} \Delta \delta_i + \frac{\partial Q_{ij}}{\partial \delta_j} \Delta \delta_j + \frac{\partial Q_{ij}}{\partial V_i} \Delta V_i + \frac{\partial Q_{ij}}{\partial V_j} \Delta V_j \quad (3.19)$$

Where,

$$\frac{\partial Q_{ij}}{\partial \delta_i} = -V_i V_j Y_{ij} \cos(\theta_{ij} - \delta_{ij}) \quad (3.20)$$

$$\frac{\partial Q_{ij}}{\partial \delta_j} = V_i V_j Y_{ij} \cos(\theta_{ij} + \delta_{ij}) \quad (3.21)$$

$$\frac{\partial Q_{ij}}{\partial \delta_i} = -V_i V_j Y_{ij} \sin(\theta_{ij} + \delta_{ij}) - 2V_i Y_{ij} \cos \theta_{ij} - V_i Y_{sh} \quad (3.22)$$

$$\frac{\partial Q_{ij}}{\partial V_j} = -V_i Y_{ij} \sin(\theta_{ij} - \delta_{ij}) \quad (3.23)$$

3.3 Modeling of Renewable DG Source and Load data

In this research, two types of renewable DG units described in Chapter 2, namely wind power and solar PV are considered. The outputs of the wind turbine and solar PV-based DG are assumed to follow the normalized average output curve depicted in Figure 3.1. Each curve provides an hourly generation output as a percentage of the daily peak output itself. Also, the load assumed to be normalized with maximum load demand occurred in given 24 hours.

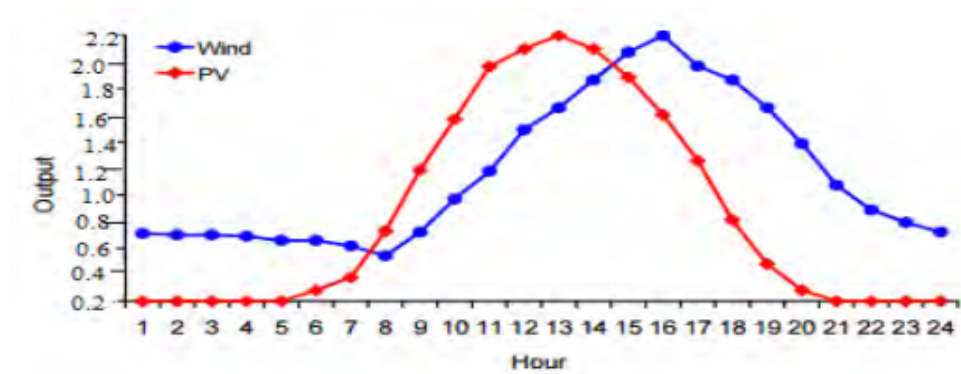


Figure 3. 1 Normalized daily WT and solar PV output

The average monthly data of the wind speed, and solar radiation, for Dodoma and Tanga region in Tanzania, are used as a case study. These sites represent the climatic conditions variety in Tanzania with different solar radiation and wind speed potentials. A load demand of these regions is used for the system under study and has the steady state (hourly) demand as shown in Appendix D. This load is assumed to be the same on each sites under study.

3.3.1 Modeling of wind turbine

Wind energy is extracted through wind turbine blades and then transferred through a gearbox and the rotor hub to the mechanical energy in the shaft. The shaft drives the generator to convert the mechanical energy to electrical. The turbine model is based on the output power characteristics, expressed as

- a. If the wind speed range is below the cut-in speed for the turbine, then output power is zero.
- b. If the wind speed range is between the cut-in and the rated speed for the turbine, then the power output is the maximum extractable from the wind based on the C_p and wind speed relation for the turbine.

- c. If the wind speed range is between the rated and cut-out speed for the turbine, then the power generated is the rated output of the plant.
- d. If the wind speed range is above the cut-out speed, then the power generated is zero

$$P = 0.5C_p A \rho V^3 \quad (3.24)$$

Where

V represents the wind speed

A represent area of the rotor

C_p represent performance coefficient of WT

Production from a wind turbine depends on wind speed, the density of the air and the swept area of the rotor. Therefore, the maximum power available from the wind can be expressed by equation (3.24) above.

The wind speed provided corresponds to an anemometer placed in height H_o , so it must be extrapolated to actual height H_a by using the power law to wind turbine hub height, as below

$$V_a = H_a [H_o]^{-1} [V_o] \quad (3.25)$$

3.3.2 Modeling of Solar PV.

The power in MW of the Solar PV depends on the technical parameters such as ambient temperature and solar irradiation. The expression (3.26) and (3.27) used to calculate the power output of the solar PV and average temperature of the cell

$$P_{PV} = \frac{P_{STC} I_S}{1000} [1 + \mu(T_C - 25)] \quad (3.26)$$

Where

P_{STC} is maximum power of Solar PV at Standard Test Condition (STC) in Watts,

I_s is solar irradiance on the Solar PV surface (W/m^2),

μ is solar PV temperature coefficient,

T_c is photovoltaic cell temperature ($^{\circ}C$).

The photovoltaic module temperature calculated as a function of solar irradiance and ambient temperature based on the module's nominal operating cell temperature (N_{OCT}) (Arai et al., 2018)

$$T_c = T_a + \frac{I_s}{1000} (T_{NOCT} - 20) \quad (3.27)$$

Where

T_a is ambient temperature ($^{\circ}C$), and

T_{NOCT} is the nominal operating temperature of solar PV

3.3.3 Modeling of storage battery capacity

According to the publication of (Brown, Lopes, & Matos, 2008) present calculation of the battery capacity into which amount of power generation with multiple points of solar PV and WT are calculated for a given one year. The required ratio of power generated capable of supplying the demand for one year obtained as follows

$$R_m = D_y P_r * (W_y)^{-1} \quad (3.28)$$

$$B_c = R_m N_p \quad (3.28)$$

Where

D_y is load demand for a given one year (kWh)

P_r is ratio of power from solar PV to WT

W_y is generated electric energy of solar PV and WT in one year (kWh)

N_p is nominal power of solar PV and WT in one year (kW)

According to publication Sinha et al., (2015), mention that BES store surplus generated energy and it supply power to the load in case of insufficient power generation from the hybrid system. Battery sizing depends on the maximum depth of charge, temperature and battery life. In this research, schematic diagram in Figure 3.2 used to illustrate layout of proposed hybrid RES with BES.

During charging process

$$S_c(t+1) = S_c(t)[1 - \sigma] + [I_B(t) \Delta t \eta_c C_B^{-1}] \quad (3.29)$$

During discharging process

$$S_c(t+1) = S_c(t)[1 - \sigma] - [I_B(t) \Delta t \eta_D C_B^{-1}] \quad (3.30)$$

$$[1 - DD] \leq S_c \leq 1 \quad (3.30)$$

Where

C_B Nominal battery capacity

S_c State of charge of the battery

DD Depth of discharge

σ Self-discharge rate of the battery

According to Mohamed et al., (2016), the state of charge (SOC) of the BES after a certain time (t) calculated based on the energy balance between the WT, solar PV and the load as shown in the following equations:

$$E_B(t+1) = E_B(t)(1 - \sigma) + \text{Surplus power} \cdot \eta_{BC} \quad (3.31)$$

$$E_B(t+1) = E_B(t)(1 - \sigma) - \text{Deficit power} \cdot \eta_{BD} \quad (3.31)$$

Where,

E_B Energy of the battery,

η_{BD} and η_{BC} are discharging and charging efficiency of the battery

σ Self-discharge rate of the BES

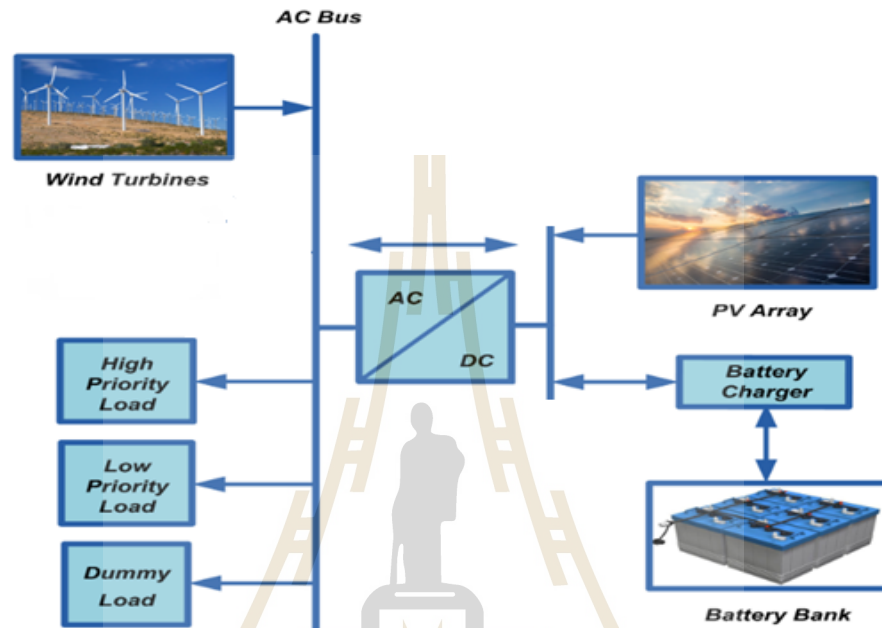


Figure 3. 2 Proposed schematic diagram of hybrid RDG

Feeding dummy load

Dummy load can be used to absorb the surplus power from hybrid RDG that exceeds the LPL demand, and battery demand as shown in the following equations:

$$P_{dummy}(t) = P_w(t) + P_{PV}(t)\eta_{inv} - P_{LHP}(t) - P_{LLP}(t) \quad (3.32)$$

Where

P_w is power from WT

P_{PV} is power from solar PV

P_{LLP} is low priority load

P_{LHP} is high priority load and P_{dummy} is dummy power

Feeding low priority load

If $P_{RDG}(t) > P_{LHP}(t)$ & $SOC(t) \geq E_{Bmax}$ then:

$$P_{LLP}(t) = P_w(t) + P_{PV}(t)\eta_{inv} - P_{LHP}(t) \quad (3.33)$$

Where

P_{RDG} is power from RDG

SOC is state of charge

E_{bmax} is maximum energy storage of the battery

3.4 Problem Formulation

This section deal with the development of a mathematical model for OF/MOF and different constraints for RDN in the presence of RDG

3.4.1 Multi-Objective Optimization Problem

A non-linear constrained multi-objective optimization problem aggregate the objectives and constraints to be optimized simultaneously. The problem can be mathematically formulated with some equality and inequality constraints as follows:

$$\text{Minimize } [J_1(x,u), J_2(x,u)] \quad (3.34)$$

Subjected to constraints:

$$g(x, u) = 0 \quad (3.35)$$

$$h(x, u) \leq 0 \quad (3.36)$$

Where

J is a multi-objective function,

x and u are vectors of dependent and control variables (independent), respectively. State variable x is dependent variables shown in (3.35) consists of the active power of slack bus, load bus voltages, reactive power of generators, and thermal limit of the transmission line. Hence x can be expressed as:

$$x^T = [P_{slack}, V_i, S_{ij}, Q_{RDGi}] \quad (3.37)$$

Where

P_{slack} represent active power generated at the slack bus

V_i represent voltage at node/load node

Control variables vector u are shown in equation (3.36) consists of power output except at the slack bus, generator voltages, and transformer tap setting and reactive power injections. Hence u can be expressed as:

$$u^T = [V_{RDGi} \dots V_{RDGn}, T] \quad (3.38)$$

Where,

V_2 is voltage at node except node one

T is transformer tap settings

3.4.2 Multi-objective problem with a weight factor

The calculation of multiobjective function required to achieve the performance of RDN integrated with optimal RDG is given by;

$$J = \min[(w_l f_1) + (w_v f_2)] \quad (3.39)$$

$$w_l + w_v = 1 \quad (3.40)$$

Where

f_1 is function of power loss

f_2 is function of voltage stability index

3.4.3 Decision Variables

- a) The voltage at PV nodes in p.u
- b) Tap changer of the transformer in p.u
- c) Size of RDG in MW

3.4.4 Power Loss

The aim is to reduce power losses in the system calculated as follows:

$$P_{loss} = \sum_{i=1}^n \sum_{j=1}^n \left(a_{ij} (P_i P_j + Q_i Q_j) + b_{ij} (Q_i P_j - P_i Q_j) \right) \quad (3.41)$$

3.4.5 Voltage Stability Index

VSI proposed by (Murty & Kumar, 2015) used in this research as second objective function and for identifying the potential node expressed in (3.42).

$$\begin{cases} VSI_i = |V_j|^4 - 4(P_j X_i - Q_j R_i)^2 - 4(P_j R_i - Q_j X_i) |V_j|^2 \\ f_2 = (1 + VSI)^{-1} \end{cases} \quad (3.42)$$

The node at which VSI has the lowest value is prone to collapse. Where VSI_{max} is the maximum value, and f_2 is the objective function for VSI.

3.4.6 Problem Constraints

Typical limitations in the optimal placement and sizing of RES problem include:

- a) Power balance equality constraints of the power flow equations
- b) Voltages constraints of nodes
- c) Power boundaries of RDG

These are parameters that define the limits of the existing system to which they subjected to the power loss equation, voltage profile improvement, and voltage stability.

3.4.7 Equality constraints

It represents real power limitations and reactive power constraints as follows:

$$P_{Slack} + P_{RDGi} - P_{Di} - P_i = 0 \quad (3.43)$$

$$\begin{cases} P_i = P_{RDGi} - P_{Di} \\ P_i = |V_i| \sum_{j=1}^N |Y_{ij}| |V_j| \cos(\delta_i - \delta_j - \theta_{ij}) \end{cases} \quad (3.44)$$

Where

P_D is real power load demand

P_{RDG} is outputs power from RDG.

3.4.8 Inequality constraints

It represents typical dependent variables such as transfer power limits of RDN and nodes voltage as follows;

$$\begin{cases} S_{ij} \leq S_{ij}^{\max} \\ P_{RDG}^{\max} \leq P_D^{\max} \end{cases} \quad (3.45)$$

$$\begin{cases} V_i^{\min} \leq V_i \leq V_i^{\max} \\ 0 \leq P_{RDG} \leq P_{RDG}^{\max} \end{cases} \quad (3.46)$$

$$P_{RDG,disch} = P_{RDG(t)} - P_{storage} \quad (3.47)$$

3.5 Optimization Method

The combination of RDGs sizing has been addressed in several publications using PSO, GA and other inspired methods as well. Other few researchers they did in sitting of RDG considering multi-objective optimization. In this research work, a MOOP of RDG sizing and placement is also included in the problem. Furthermore, the multi-objective optimization problem of power losses and maximization of voltage stability through the use of weighting factors assigned to the elements of the objective function.

There are two methods for sizing and placement of RDG in the distribution network (Bouktir & Guerriche, 2015). The first method is traditional based such as optimal power flow (OPF), SI, PLI, and VSI. In the second method, the artificial intelligent (AI) is used to apply with RDG placement and sizing like Genetic Algorithm (GA), Differential Evolution (DE) and Particle Swarm Optimization (PSO) and Artificial bee colony (ABC). Many research studies have been carried out in the recent years to present methodologies in placement and sizing of RDGs (Aman et al., 2013; Devi & Geethanjali, 2014; Reddy et al., 2016). ABC algorithm was introduced to determine the optimum size and location of a single RDG unit to minimize the real power losses of the system (Mohandas et al., 2015).

In recently, much effort has been contributed to solving the optimal RDG placement problem, utilizing different algorithms and considering different objectives. The placement and sizing problem of RDG could be formulated as an optimization

problem. Various algorithms are used to solve the problem. The methods used to solve problem divided into three categories;

- a) Analytical Methods
- b) Computational Methods
- c) Artificial Intelligence Methods

3.5.1 Analytical Methods

Although the analytical methods suffer from many drawbacks, they are still used in optimizing the location and size of RDGs in distribution systems. Total loss was minimized by optimal placement of RDG unit exclusively at the various optimal location of the test system. They iteratively increased the size of the RDG unit at all nodes and then calculated the losses; based on VSI calculation, the top-ranked nodes are considered for placement of RDG units. Also, (Murty & Kumar, 2015) proposed the use of power flow and power loss sensitivity factors in identifying the most suitable zone and then optimized the solution by maximizing the voltage improvement and minimizing the line losses in the network.

$$\begin{cases} P_i = [\alpha_{ii}]^{-1} [\beta_{ii} Q_i + \sum_{j=1, j \neq i}^n (\alpha_{ij} P_j - \beta_{ij} Q_j)] \\ \alpha_i = \frac{\partial P_L}{\partial P_i} = 2 \sum_{j=1}^n (\alpha_{ij} P_j - \beta_{ij} Q_j) \end{cases} \quad (3.48)$$

$$\begin{cases} Q_{RDGi} = Q_{Di} - [A_{ij}]^{-1} \sum_{j \neq i}^n (A_{ij} Q_j - \beta_{ij} P_j) \\ P_{RDGi} = P_i + P_{Di} \end{cases} \quad (3.49)$$

3.5.2 Performance Index

Performance index introduced to minimize the search space during optimization (Aman, Jasmon, Mokhlis, & Bakar, 2012; Murty & Kumar, 2015; Ochoa, Padilha-Feltrin, & Harrison, 2005; Yang et al., 2012). In this case, the voltage stability index (VSI) shown in (3.49 and 3.50) calculated for all of the nodes, since the nodes with max voltage stability index near to zero are prone to voltage instability, and it is essential to distinguish weak nodes. A node with VSI near to one is more stable than other below or near 0.6

$$VSI_i = |V_j|^4 - 4(P_j X_i - Q_j R_i)^2 - 4(P_j R_i - Q_j X_i) |V_j|^2 \quad (3.50)$$

3.5.3 Computational Methods

Another class of techniques used for optimizing the location and size of RDGs in a power system is the computational methods. Although these methods are fast compared to the other classes of techniques, their drawback is that they are complicated and reproduction of their results may be difficult or sometimes impossible. (Shukla, Singh, & Naik, 2010) Addressed the issue of optimizing RDG planning regarding size, number, and location to reduce line losses in radial distribution networks. Their optimization methodology, which was based on the Sequential Quadratic Programming algorithm, assessed the compatibility of different generation schemes upon the level of power loss reduction and RDG cost (Kothari, 2012)

3.5.4 Artificial Intelligence Methods

Artificial Intelligent Techniques such as DE, ABC (Varadarajan & Swarup, 2008) are adaptive heuristic search algorithms based on the evolutionary ideas

of natural selection and genetics. Artificial intelligent represent rational exploitation of solving optimization problems through a random search. In the recent past, much effort has been contributed to resolving the optimal RDG problem, utilizing different algorithms and considering different objectives. The optimal placement and sizing of RDG could formulate as an optimization problem.

The general idea of the ABC technique is that it starts with random solutions and repeatedly attempts to find better solutions by searching the neighborhoods of the current best solutions and abandoning the weak solutions. The current problem solutions represented as food sources that are each associated with an employed bee. It is evident from the description above that the standard ABC algorithm has only three control parameters that need to be set appropriately for the given problem. First, the population size, Second, the local search abandoning limit and third, the maximum number of search cycles. Various algorithms used to solve optimal power flow problem (Adaryani & Karami, 2013): GA tend to converge towards local optima or even arbitrary points rather than the global optimum of the problem. Hence there needs to combine a method that has good convergence to obtain a robust solution for the problem at hand.

The following are demerits of PSO:

- a) They produce less accurate results at regulation speed; this is because they quickly suffer from partials optimism
- b) Non-coordinate problems such as the solution to the energy field and the moving rules of the particles in the energy field, application of the method may not work out correctly.

3.5.5 Artificial Bee Colony Technique

The ABC algorithm approach is established from foraging behavior of real honey bees developed by Karaboga (2005) as a new heuristic method for solving multidimensional optimization problems. ABC Technique as meta-heuristic optimization applied for solving MOOP by (Abu-Mouti & El-Hawary, 2011). Since most of the meta-heuristic methods are independent of the initial solutions and are derivative-free, they overcome the main limitations of deterministic or conventional optimization methods which are getting trapped in local extremes and divergence situations respectively. The colony of ABC consists of three groups: employed, onlookers, and scout bees. The merit of ABC are listed as follows:

- a) ABC does not converge prematurely.
- b) It can discover good solution more rapidly.
- c) It produces a good solution at the reasonable time.
- d) Accuracy

3.5.6 Algorithm of ABC

Step1: Initialize solutions population X_i , as shown in (3.50)

$$X_{i,j} = x_j^{\min} + rand(0,1)(x_j^{\max} - x_j^{\min}) \quad (3.50)$$

Step 2: Calculate the fitness values using (3.51)

$$Fitness = (1 + Objective Function)^{-1} \quad (3.51)$$

Step 3: Update new position (solutions) for the bees by using (3.52).

$$v_{ij} = x_{ij} + f_{ij}(x_{ij} - x_{kj}) \quad (3.52)$$

Step 4: Apply selection process between X_{ij} and V_{ij} .

Step 5: Determine the values $P_{(X_{ij})}$ for the solutions X_{ij} using (3.53)

$$P(x_{ij}) = F(x) \left(\sum_{i=1}^n F(x_i) \right)^{-1} \quad (3.53)$$

Step 6: Generate the new solutions V_i from the solutions x_i , by considering selection process between X_{ij} and V_{ij} .

Step 7: Calculation of the solution for the scout bees, and replace it with an entirely novel resolution and weigh them as shown in equation (3.54)

$$X_{i,j}^{new} = x_j^{\min} + rand(0,1)(x_j^{\max} - x_j^{\min}) \quad (3.54)$$

Step 8: If cycle = MCN, stop and print result. Else, follow Step 3.

The flow chart from step 1 to step 8 illustrated in Figure 3.3.

Employed bees: Randomly search for food source positions (solutions) and then share the information that is nectar amounts by dancing with the bees waiting in the hive. Duration of dance depends on the nectar amount (fitness value) of the food source.

Onlooker bees: Watch dances of variously employed bees and chose the excellent food source position according to the quality of that food source. Scout bees: An employed bee of the source which is abandoned becomes a scout and starts to search a new food source randomly. Onlookers are placed on food sources by using probability-based selection, as the nectar amount increases on source onlooker bees prefer that source too.

Scout bees are the explorers and have no guidance while looking for food. That creates the possibility of both low or rich quality sources may be discovered. In ABC one of the employed bees is selected as the scout bee, and a parameter limit controls this selection.

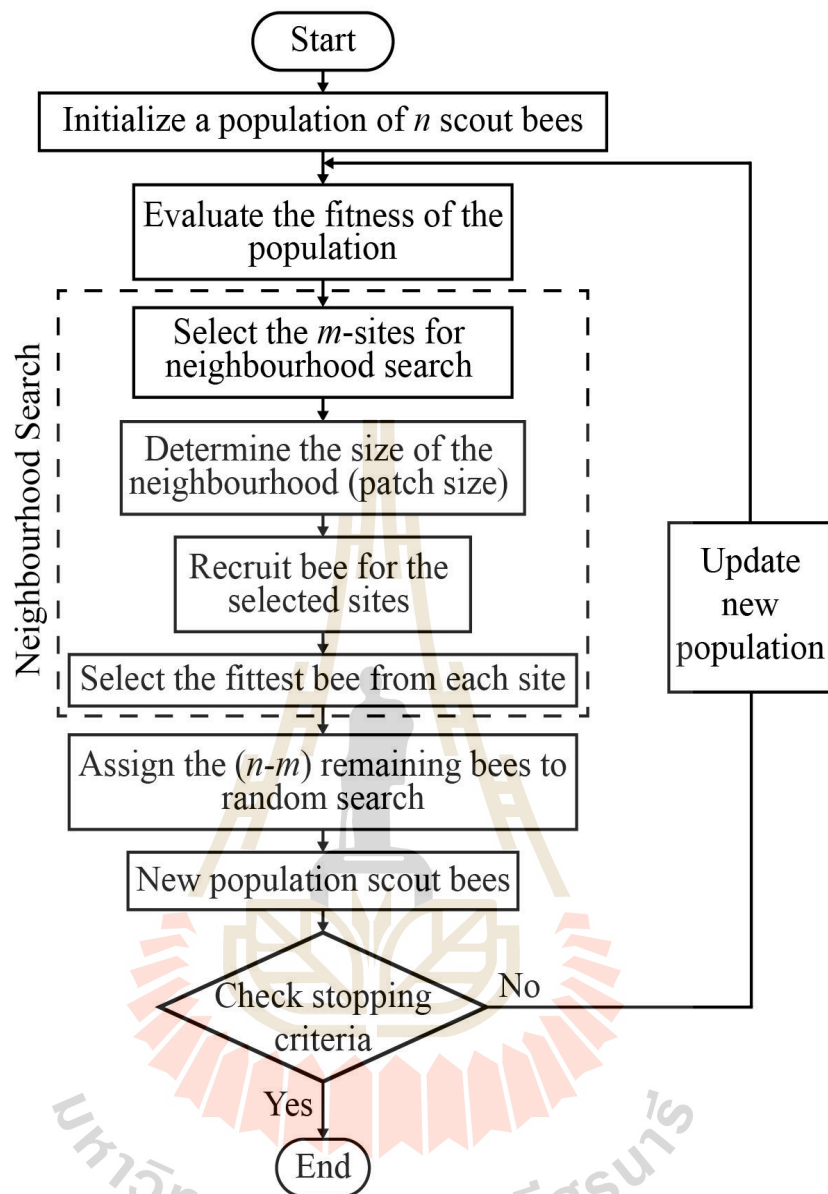


Figure 3. 3 Flowchart of ABC Algorithm

If a predetermined number of trials does not improve the food source (solution), its employed bee abandons the source, and it converts to a scout. So limit is the number of trials before leaving a food source.

3.5.7 Pseudo-code of the main body of ABC algorithm

- a) Initialization
- b) Evaluation

- c) cycle = 1
- d) repeat
- e) Employed Bees Phase
- f) Calculate Probabilities for Onlookers
- g) Onlooker Bees Phase
- h) Scout Bees Phase
- i) Memorize the best solution achieved so far
- j) cycle = previous cycle + 1
- k) Until cycle = Maximum Cycle Number

3.5.8 Control parameters of ABC

- a) Colony size (CS) = 20:

It represents the total number of bees present. One half of CS represents the number of employed bees and second half stands for the number of onlooker bees.

- b) Limit value = 100:

It represents the number of trials for a food-source position (solution) to be abandoned.

- c) Maximum cycle number (MCN) = 300:

It is the maximum number of times the search process has to be repeated.

3.5.9 Overview of ABC Algorithm

In the ABC algorithm, the colony of artificial bees contains three groups of bees: employed bees, onlookers, and scouts. A bee waiting on the dance area for

making the decision to choose a food source is called an onlooker, and a bee is going to the food source visited by it previously is named an employed bee. A bee carrying out random search is called a scout. In the ABC algorithm, the first half of the colony consists of employed artificial bees and the second half constitutes the onlookers.

For every food source, there is only one employed bee. In other words, the number of employed bees is equal to the number of food sources around the hive. The employed bee whose food source is exhausted by the employed and onlooker bees becomes a scout. In the ABC algorithm, each cycle of the search consists of three steps:

- a) Sending the employed bees onto the food sources and then measuring their nectar amounts.
- b) Selecting of the food sources by the onlookers after sharing the information of employed bees and determining the nectar amount of the foods.
- c) Determining the scout bees and then sending them to possible food sources.

At the initialization stage, a set of food source positions are randomly selected by the bees, and their nectar amounts are determined. Then, these bees come into the hive and share the nectar information of the sources with the bees waiting on the dance area within the hive. At the second stage, after sharing the information, every employed bee goes to the food source area visited by her at the previous cycle since that food source exists in her memory and then chooses a new food source by means of visual information in the neighborhood of the present one. At the

third stage, an onlooker prefers a food source area depending on the nectar information distributed by the employed bees on the dance area. As the nectar amount of a food source increases, the probability with which that food source is chosen by an onlooker increase, too. Hence, the dance of employed bees carrying higher nectar recruits the onlookers for the food source areas with higher nectar amount.

Visual information is based on the comparison of food source positions. When the nectar of a food source is abandoned by the bees, a new food source is randomly determined by a scout bee and replaced with the abandoned one. In our model, at each cycle at most one scout goes outside for searching a new food source and the number of employed and onlooker bees were equal.

The probability P_i of selecting a food source i is determined using the following expression:

$$P_i = \frac{fit_i}{\sum_{N=1}^{S_N} fit_N} \quad (3.55)$$

Where

fit is the fitness of the solution represented by the food Source i and

S_N is the total number of food source

The main advantage of ABC algorithm is that: It does not require external parameters such as crossover rate and mutation rate as in case of genetic algorithms, differential evolution, and other evolutionary algorithms. The other advantage is that

the global search ability in the algorithm implemented by introducing neighborhood source reduction mechanism which is similar to mutation process.

3.6. Multiobjective ABC (MOABC)

In a real world, many optimization problems deal with the simultaneous optimization of two or more objectives. That means, most of the real world problems are associated with the simultaneous optimization of several objective functions. Generally, these objective functions are non-commensurable and conflicting in nature. The conflicting natures of these objective functions give rise to a set of optimal solutions, instead of one optimal solution. The reason for the optimality of many solutions is that there is no one can be better than any other concerning all objective functions. These optimal solutions are called Pareto- optimal solutions.

3.6.1 Main steps of the MOABC algorithm

- i. Cycle = 1
- ii. Initialize the food source positions = solutions $\mathbf{x}_i, i = 1, \dots, S_N$
- iii. Evaluate the nectar amount fitness fit_i of food sources
- iv. The initialized solutions are sorted based on non-domination
- v. Store non-dominated solutions in the external archive evolution algorithm (EA)
- vi. Repeat
- vii. Onlooker Bees Phase

For each onlooker bee

Randomly chooses a solution from EA

Produce new solution v_i by using expression 4.1

Calculate the value $fit\ i$

Apply greedy selection mechanism in Algorithm 3 to
decide which solution enters EA

End of *for* loop

- viii. The solutions in the EA sorted based on non-domination
- ix. Keep the non-domination solutions of them staying in the EA
- x. If the number of non-dominated solutions exceeds the allocated size of EA. Use crowding distance to remove the crowded members
- xi. Cycle = previous cycle +1.
- xii. Until cycle = Maximum Cycle Number

3.6.2 Mathematical Algorithm of MOABC

Generally, multi-objective optimization problem consists of some objectives simultaneously and is associated with some equality and inequality constraints which can be formulated as follows:

$$\text{Minimize } f_i(x) \quad i = 1, \dots, N_{obj} \quad (3.55)$$

Where

f_i The i^{th} objective function, x is the decision vector represents a solution.

N_{obj} The number of objectives.

Subjected to constraints

$$\begin{cases} g_j(x) = 0 & j = 1, \dots, M \\ h_k(x) \leq 0 & k = 1, \dots, K \end{cases} \quad (3.56)$$

For a multi-objective optimization problem, any two solutions x^1 and x^2 may have one of the two possibilities: either one dominates other, or none dominates other. For the problem of minimization a solution x^1 dominates x^2 if the following conditions satisfied:

$$f_i(x^1) \leq f_i(x^2) \quad (3.57)$$

If the above conditions are violated, the solution x^1 does not dominate the dominate x^2 . If x^1 dominates the solution x^2 , x^1 is called non-dominated solution. Non-dominant solutions within the entire search space are also known as Pareto-optimal solutions which constitute the Pareto-optimal set or Pareto-optimal front.

3.6.3 Choice of weights factor for MOOP

As mentioned earlier, the allocation of the various weights in a given multi-objective function varies according to the engineer's requirements. Thus, a study of the effect of the weights factor on the fitness done to determine the best weights combination to adopt in coming up with the multi-objective function. During this study, the values of the weights are assumed positive. Initialized from zero to one with the step of 0.1 which gives ten options for the given two weight factor to have optimized multiobjective function (MOF). In this research study, weight factor calculated by run Matlab code which guided with given MOF. Thus the weights factor chosen for power loss function and voltage stability function were 0.6 and 0.4 respectively in the multi objective function (MOF) given by equation (3.39).

3.7 Chapter Summary

This chapter discussed the OPF and optimization methods for allocation and sizing of RDG. It also reviewed and explained the theory of MOABC in power optimization. The next chapter will show simulation results on how ABC used to solve multi-objective optimization problem (MOOP).



CHAPTER 4

SIMULATION RESULTS AND DISCUSSION

4.1 Introduction

This chapter presents the results obtained using ABC algorithm and VSI method as well. The algorithm outlined in the previous chapter was implemented and programmed in Matlab 2014. Simulations carried out using MA TLAB software have been conducted on IEEE 33-nodes, IEEE 69-nodes and real system of 34 nodes shown in Figure.4.10, Figure 4.15, and Figure 4.19 respectively. In all test-feeder system, the bus 1 is considered as slack bus, while other nodes are taken as PQ nodes with the option of inserting RDG. Different scenarios of RES are considered to perform the computation. Section 4.3 demonstrate the simulation of IEEE 33-nodes, section 4.4 depicts a simulation of IEEE 69-nodes network under the different cases and section 4.5 illustrate the simulation of real distribution system with 34-nodes.

4.2 Simulation Results based on the type of RDG and Resources

4.2.1 Solar PV Resources

The annual mean value of global solar radiation (insolation) ranges from 4.5 to 6.0kWh/m² according to ground measurements. It reflects a good potential for solar energy conversion throughout the region. Small-scale use of solar photovoltaic technologies are expected to be adequate from approximation 4kWh/m

while larger installations such as solar thermal power plants require about 5kWh/m^2 according to Alfayo & Uiso, (2002). With the reference to Figure 4.1 and Figure 4.2, output power from solar PV vary based on its insolation.

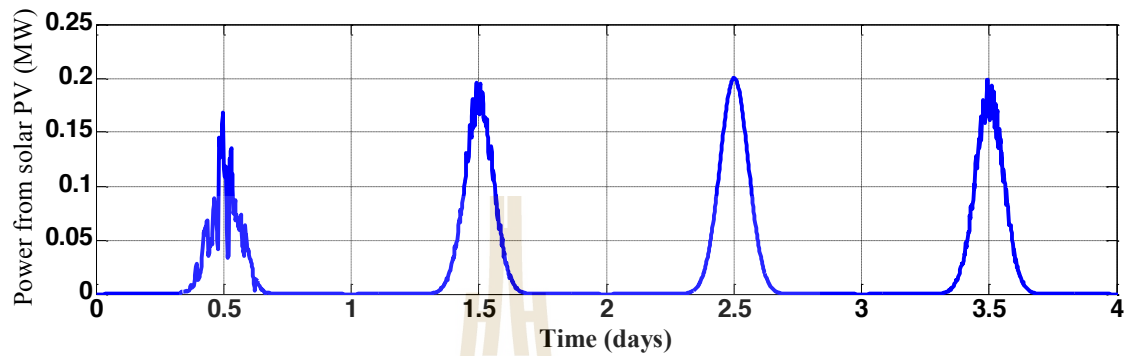


Figure 4. 1 Power output from solar PV

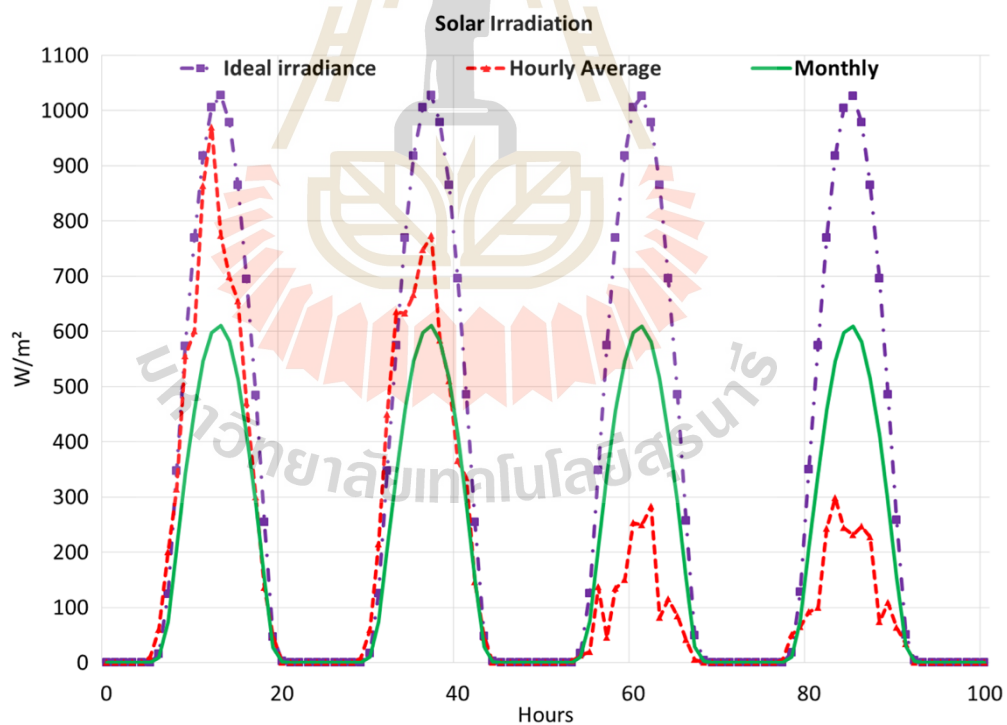


Figure 4. 2 Solar irradiation

From Figure 4.2, power density from solar PV vary from ideal, daily and even monthly.

For the estimation during designing sizing of RDG based on solar PV generator, it is

better to rely on monthly data. Jones et al., (2017) demonstrated how DC power from solar PV can be converted through inverter as shown in Figure 4.3.

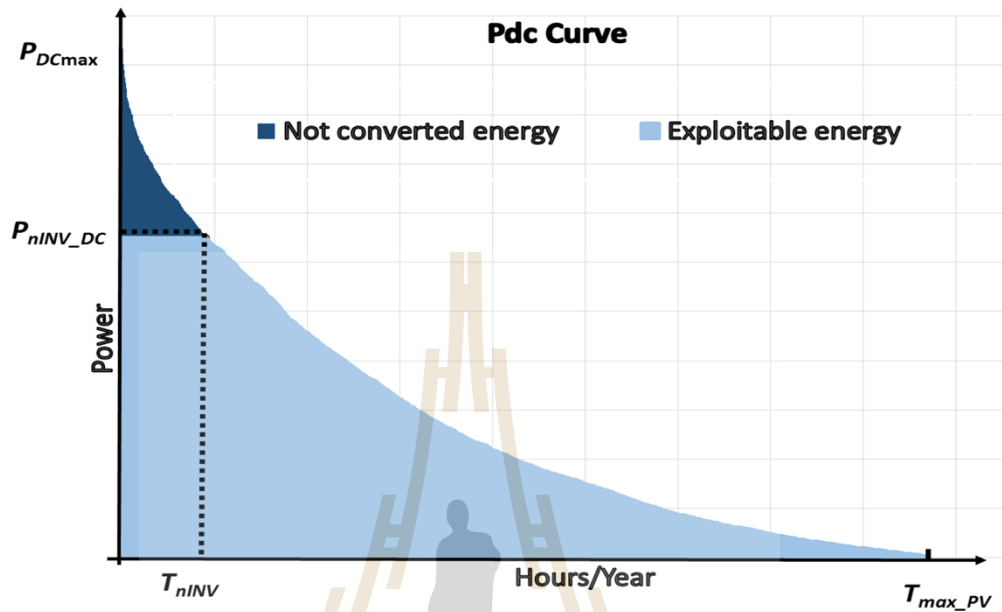


Figure 4. 3 Curve of Power converted from solar PV (Jones et al., 2017)

4.2.2 Wind Resources

Figure 4.4 illustrate how extraction of energy from WT vary for a given period of one year. Furthermore, measurements and modeling refer to 10m height and knowledge about wind speed at higher levels are less known.

In this research, two types of RDGs were used (solar PV and WT), the solar PV was made to generate active power while the latter can generate both active and reactive power.

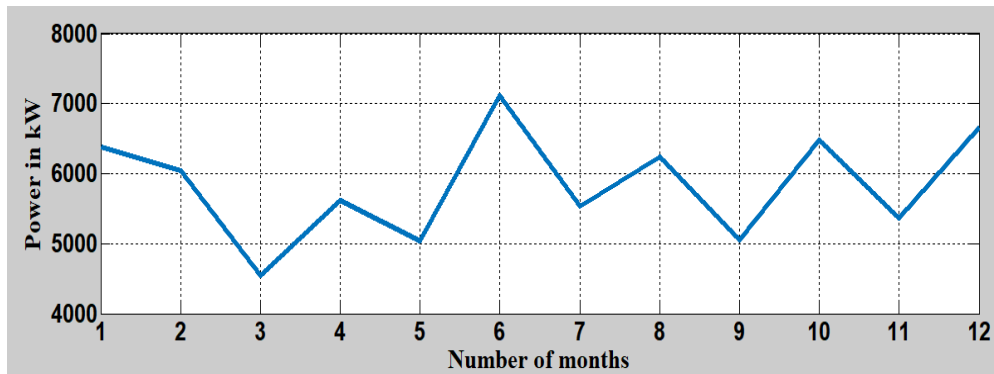


Figure 4. 4 Power output from the WT

4.2.3 Load modeling

The distribution system under study is assumed to follow the normalized 24-hour load profile of the IEEE system as shown in Figure 4.5 (Giradi et al., 2011 and Osaloni, 2016) The constant P and Q load in load characteristic incorporate through load factor LF in the equation below.

$$LF = \frac{\sum_{t=1}^{24} \text{load demand}(t) \text{ in p.u.}}{24} \quad (4.1)$$

Where

LF = Load factor

t = Time in hours

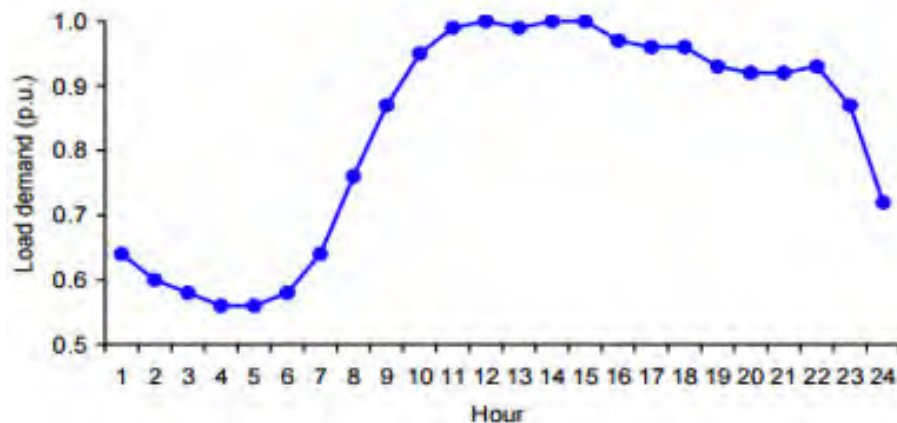


Figure 4. 5 Normalized daily load demand curve (Giradi et al., 2011)

4.2.4 Validation of proposed method

Distribution networks are sometimes considered as the critical infrastructure of a country, and detailed load data prompts privacy concerns. As a result, only a very few real networks are publically available for use as a test network. This has forced the research community to use only the available test feeders that are published in the literature so far, sometimes for purposes beyond the original intentions of the test feeder. For instance, the Institute of Electrical and Electronics Engineers (IEEE) Power and Energy Society (PES) published radial tests feeders providing references for the United States distribution system for the first time.

A test feeder is a distribution network model that is able to replicate the behavior of an actual distribution feeder. In this case, we say that the test feeder is representative of a particular actual network located in a particular area or country. A significant use of test feeders is benchmarking, allowing for researchers to evaluate the performance of new algorithms. For instance, in the OPF case, the computing time, the degree of optimality, or even a ratio between them can be used as a benchmark. With emerging widespread grid modernization efforts, testing the corresponding advanced optimization algorithms suggests a need for realistic large-scale distribution/transmission test networks. In addition to providing a valuable test platform, test networks are also essential to make consistent comparisons across different advanced algorithms.

This section details the validation process applied for validating the ABC algorithm as proposed in Chapter 3. In order to illustrate the effectiveness of the proposed methods in this research work, obtained results are compared with other approaches from published articles in the literature that deal with the same distribution

network. The validation studies have been carried out using two networks: First is six bus test systems designed with two set of generators, two transformers, two capacitors and three loads as detailed in Figure 4.6. Second, the network is IEEE 37-nodes designed with 36 branches, 37 nodes, and one transformer as detailed in Figure 4.8.

4.2.5 Test model of IEEE 6-bus

For the validity of the proposed ABC algorithm, the IEEE 6-bus in Figure.4.6 meshed distribution feeder system was considered in different cases. The network has a base value of 230kV, 100MVA and consists of 8 lines and 6 buses. The simulation is modeled by using GA and ABC as shown in Table 4.1 and compared with published results of PSO presented by Uthen et al., (2010). While in Table 4.2 depict the control variables used in IEEE 6 bus system. Figure 4.7 shows the comparison of convergence (fitness function) for ABC and PSO.

The simulations were performed using MATLAB software. The test carried out by solving the optimal power flow problem of the power loss objective in which variables limits are given in Table 4.2 as system constraints. The system was loaded with $50 + j10$ MVA, $30 + j18$ MVA, and $55 + j11$ MVA for bus number 3, 4 and 6 respectively. For comparison, 30 iterations applied for PSO, GA and that of ABC.

Table 4. 1 Line data of six bus with base values of 100MVA, 230kV

Line Number	Bus Number		Impedance (p.u)	
	From	To	R	X
1	1	6	0.123	0.518
2	1	2	0.000	0.300
3	2	5	0.282	0.640
4	3	4	0.000	0.133
5	3	5	0.723	1.050
6	4	1	0.097	0.407
7	4	6	0.080	0.370

Table 4. 2 Control Variables

Variables	Min	Max	GA	PSO	ABC
V_2 p.u	0.95	1.10	1.04	-	1.01
V_4 p.u	0.95	1.10	1.04	-	1.01
V_6 p.u	0.95	1.10	1.04	-	1.03
P_2 (MW)	20.00	45.00	25.02	-	25.04
Q_{C4} & Q_{C6} (Mvar)	0.00	50.00	24.01,18.01	-	24.0,18.0
T_{65} & T_{12} (p.u)	0.90	1.10	1.01,0.98	-	1.0,0.98

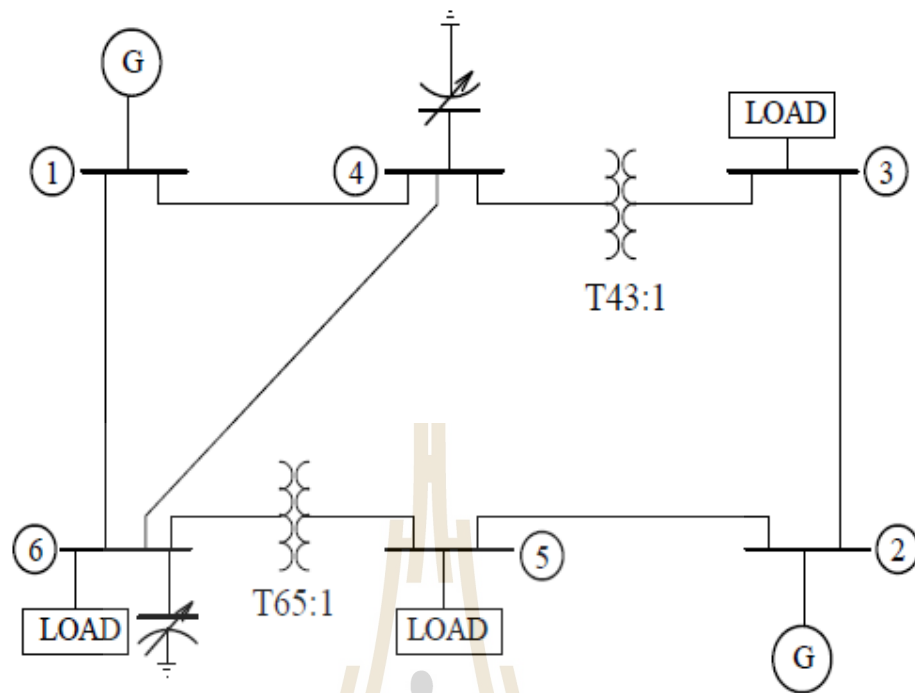


Figure 4. 6 Test network of IEEE 6-Nodes

Validation results for the proposed method demonstrated in Table 4.3 by considering different parameters.

Table 4. 3 Validation of Results

Methods	PSO	ABC
Active power loss (MW)	7.152	7.146
Reactive power losses (MVar)	-	4.04
Min voltage (p.u)	-	0.97
Max voltage (p.u)	-	1.04
VSImin	-	0.652
VSImax	-	0.872
Optimal size of G2 (MW)	-	4.46

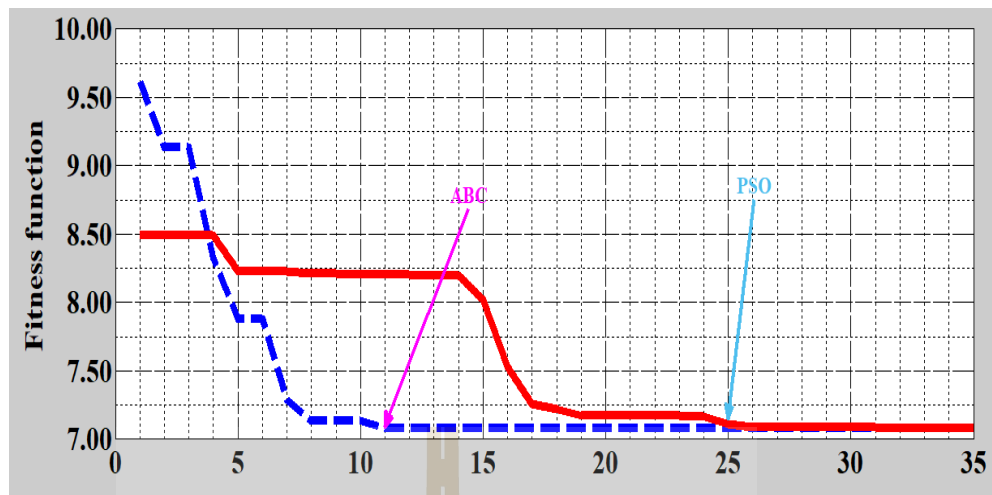


Figure 4. 7 Fitness curve of PSO and ABC

4.2.5 Test model of IEEE 37-nodes

The IEEE 37-nodes test system is an actual distribution network located in California. The characteristics of the feeder are:

- a) Three-wire delta operating at a nominal voltage of 4.8 kV
- b) All line segments are underground
- c) Substation voltage regulator consisting of two single-phase units connected in open delta.
- d) All loads are spot loads and consist of constant PQ, constant current and constant impedance
- e) The loading is very unbalance

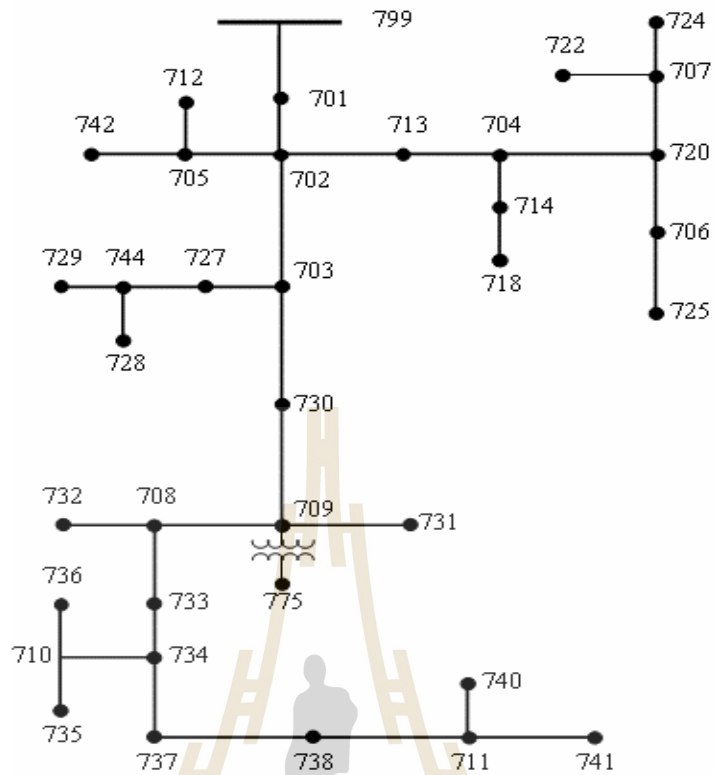


Figure 4. 8 IEEE 37-nodes system (Mmary et al., 2018)

In Table 4.4, results demonstrate the effectiveness of proposed method as compared with results of some published journals. Also, Figure 4.9 depicts convergence characteristics of proposed methods appeared in five iteration.

Table 4. 4 Validation in IEEE 37-nodes

Parameters	IEEE standard	Mmary et al,2018	ABC
Power loss (MW)	0.3679	0.3679	0.3482

From Table 4.4, results of published articles compared with results of prosed method.

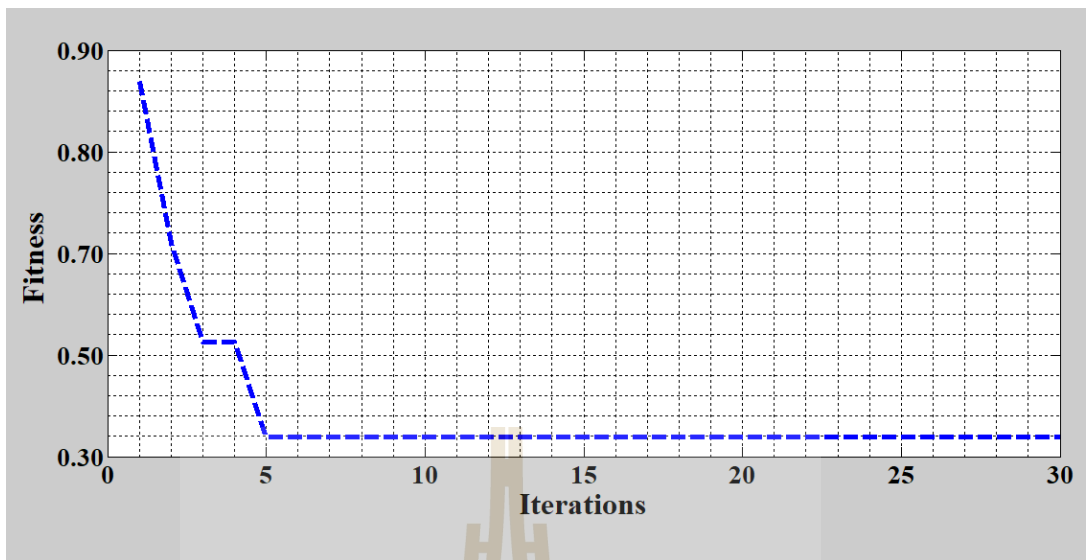


Figure 4. 9 Fitness curve of ABC in IEEE 37-nodes

4.3 Distribution System Model

The distribution system modeled are IEEE 33-nodes (Liu, Xu, Niu, & Xie, 2016), modified IEEE 34-node test feeder (Silva et al., 2007) and IEEE 69-node test feeder.

4.4 Simulation of IEEE 33-nodes system

In these results, the RDG was located in an IEEE 33-nodes test system. The test system is a radial system with a total load of 3.72MW +j2.3MVAR. The total real power loss 211.20kW and reactive power loss of 101.10kVAR are obtained using Newton-Raphson method. The diagram of this network is given in Figure 4.10 while its branch line and node data are as shown in Appendices B and C respectively. Results at base case are shown in Table 4.5.

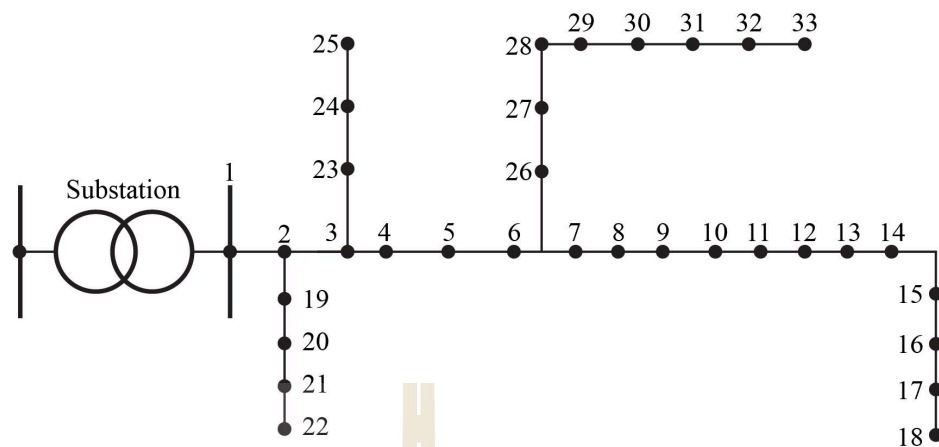


Figure 4. 10 IEEE 33-nodes system (Dufo-López et al., 2011; Liu et al., 2016)

Table 4. 5 Results of IEEE 33-nodes at the base case without RDG

S/N	Parameters	Value
1	Total reactive demand	2.295MVar
2	Total real demand	3.715MW
3	Min Voltage (node number)	0.9036 (17,18,32,33)
4	VSI min (node number)	0.6686 (17,18,32,33)
5	VSI max (node number)	0.8323 (1)
6	Total power loss	211.20 kW

The values of results given in Table 4.5 depict base case of IEEE 33 nodes without integration of RDGs. The following parameters were considered for evaluating performance of RDN: Total power loss of 211.2MW and voltage stability of 0.6686 were distinguished in RDN.

Also, the minimum voltage is 0.6686p.u. is bearing the node number 18 of the RDN. The system has a weak voltage profile at node 16, 17, to 18 due hugely loaded to the system. In this section, the results of optimal allocation two types of RDGs (WT and solar PV) in IEEE 33-nodes is given in this section considering the stochastic nature of their supply. The peak load is assumed to be within a period of 24-hours as presented in Chapter 4, Figure 4.5 were used. Also, results from ABC compared with the GA and PSO optimization method are presented. Finally, study cases are defined as case 1 with single objective optimization and case 2 with multiobjective optimization

4.4.1 Simulation result for case 1: Minimization of active power loss.

The base case was run using Newton-Raphson load flow to obtain the bus voltage magnitude, real and reactive power loss respectively. After the load flow, optimum size of RDG was identified using ABC and the approximate loss for each node and entire system was found using equation (2.11) and (2.12). By placing RDG at the corresponding location with the optimum sizing obtained from above, the performance of RDN were determined and tabulated in Table 4.6. As far as optimal location is concerned in a RDN, the optimal solution that minimizes the objective function was found to be at nodes 6, 20 and 31, with the size of the RDG being 0.50MW, 0.43MW, and 0.50MW respectively. Here, total real power losses reduced to 194.04kW from 211.20kW. Figure 4.11 demonstrate fitness function by considering one objective function. However, by considering single objective function there violation in some constraints found.

Table 4. 6 Multiple RDG considering power loss only

Ploss (MW)	Location	RDGs (MW)	VSI	VSI _{max}
0.1940	17,18,33	0.5, 0.43, 0.5	0.701	0.717

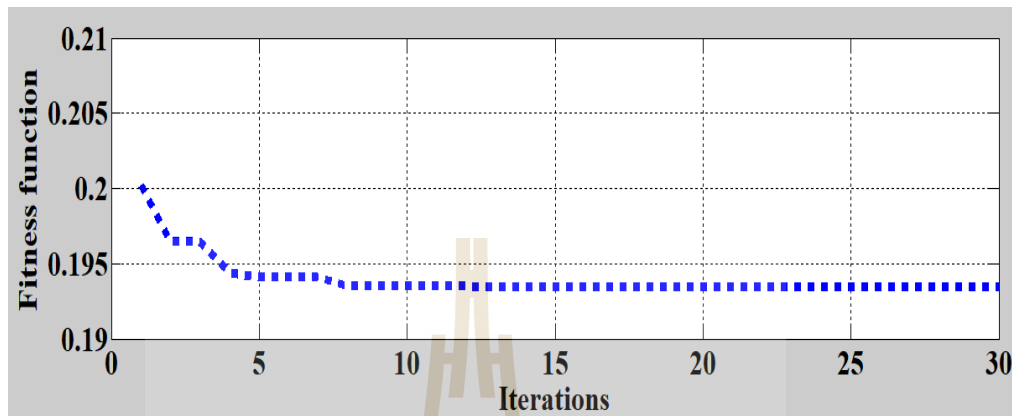


Figure 4. 11 Fitness function considering power loss only

4.4.2 Simulation result for case 2: Multi-objective Optimization

The placement and sizing of multiple RDG have been investigated by considering MOOP. That means, simultaneously of power loss reduction and maximization of VSI. In a given mathematical code in Matlab, setup of iterations was given in interval of 0.01 which gives 100 number of times/iteration for evaluating the optimal weight factor. The obtained weight factor was 0.55 in power loss and 0.45 in VSI.

Scenario 1: Optimization with single RDG (Injecting of P only)

Table 4.7 gives the comparison for scenario 1 of the case 2 with single RDG in the system optimally located at node 18 and sized using ABC.

Table 4. 7 Optimization with single RDG (Injecting of P only)

Ploss (MW)	Location	RDGs (MW)	VSI _{min}	VSI _{max}
0.144	18	4.72	0.713	0.729

Scenario 2: Optimization with single RDG (Injecting of P and Q)

In this case, wind turbine generator is considered in simulation. Since, selected location found through use of VSI.

Table 4.8 Optimization with single RDG (Injecting of P and Q)

Ploss (MW)	Location	RDGs (MW)	VSI _{min}	VSI _{max}
0.122	18	3.48	0.809	0.819

Table 4.8 gives the comparison for scenario 2 of the case 2 with a single RDG in the system optimally located at node 18 and sized using ABC. The VSI improved from 0.713 p.u to 0.809 p.u at node 18 as shown in Table 4.7 and Table 4.8 respectively. Furthermore, Figure 4.12 depicts the value of selected objective function at ten iterations which consider wound rotor synchronous generator (WRSC).

Scenario 3: Multiple RDGs considering MOP

Table 4.9 gives the comparison for scenario 3 of case number 2 with multiple RDGs in the system located at node 17, 18, 33. In this case, the VSI improved from 0.809 p.u lowest voltage at node 17, 18, 33 to 0.874 p.u as shown in Table 4.8 and Table 4.9 respectively. Finally the summary of results tabulated in Table 4.10. The fitness of simulated scenario demonstrated in Figure 4.12. The limits of decision variable used in IEEE 33 nodes and its optimal values are depicted in Table 4.13.

Table 4.9 Multiple RDG considering MOOP

Ploss (MW)	Location	RDGs (MW)	VSImin	VSImax
0.0840	17,18,33	1.84, 1.170, 1.59	0.874	0.977

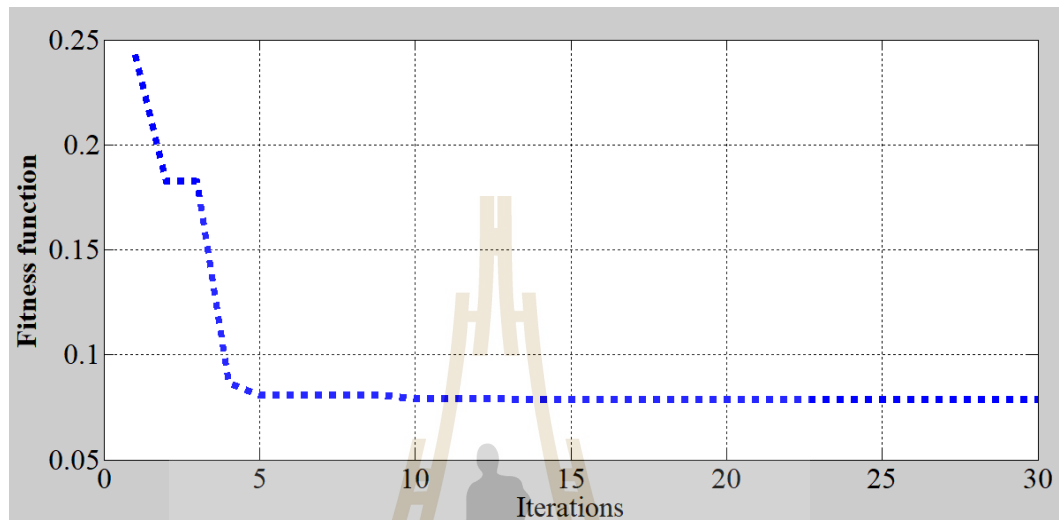


Figure 4. 12 Multiple RDGs (Injecting of P and Q)

Table 4. 10 Control variable limits and optimal values in 33-nodes

S/N	Control variable	Limit range		Optimal Value	
		Min	Max	GA	ABC
1	V_{18}	0.9	1.1	0.987	0.997
2	V_{17}	0.9	1.1	1.001	1.001
3	V_{33}	0.9	1.1	0.984	0.997

Table 4. 11 Results of IEEE 33 Nodes with RDGs

S/N	Parameters	Value
1	Total reactive demand (Mvar)	2.295
2	Total real demand (MW)	3.715
3	Min Voltage (node number)	0.9546 (18)

4	VSI min (node number)	0.879 (17,18,32,33)
5	VSI max (node number)	0.9972 (1)
6	Total power loss (kW)	84.01
7	Size of RDGs in (MW)	1.84, 1.17, 1.59
8	The output of Solar PV Module (Watt)	97.18
9	Number of PV module to form an array	8
10	Number of the array in solar PV panels	3
11	The output of WT (as per Table 2.1)	2.1
12	Number of WT	3

4.4.3 Integration of RDGs in IEEE 33-nodes system.

From the voltage stability analysis for IEEE 33 nodes, it is observed that node 7, 18, 32 and 33 are the best locations for the RDG. Voltage index graph for IEEE 33-nodes is shown in Figure. 4.14. From the graph, it has been observed that node 17, 18, 32 and 33 shows the minimum VSI which is the best location for RDG placement. The minimum voltages are highlighted. From Figure 4.14 it has been observed that the voltages improved from 0.9405, 0.9519, 0.9448 and 0.9495 in p.u (without RDG) to 0.9744, 0.9871, 0.9784 and 0.9879 in p.u. (with RDG) respectively. Hence, there is an improvement in the minimum voltage when compared before and after placement of RDG as shown in Figure 4.13. In case 2 of MOOP, three scenarios were considered during simulation. These results tabulated by considering single RDG which generate P only, single RDG which generate both P and Q to RDN and multiple RDG in Table 4.7, 4.8 and 4.9 respectively.

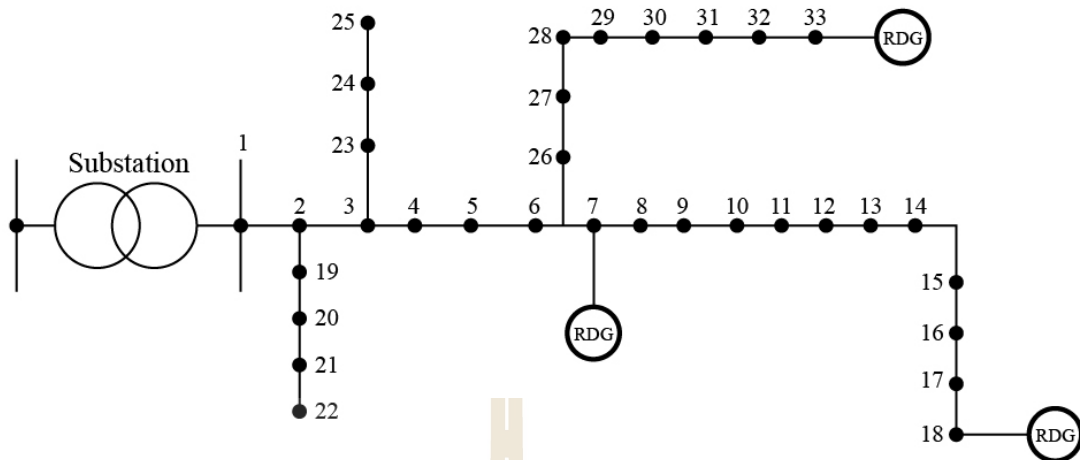


Figure 4. 13 Integration of multiple RDGs into IEEE 33-nodes.

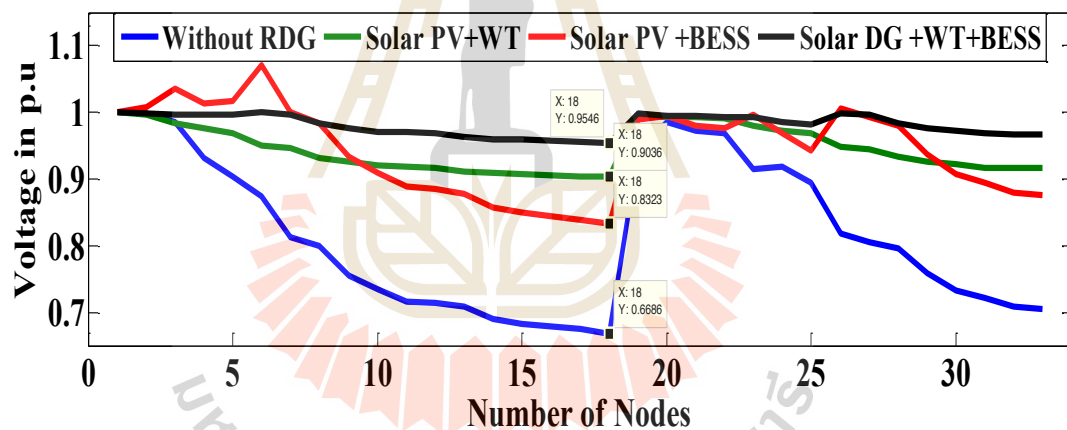


Figure 4. 14 Voltage profile of 33-nodes test system by integration of RDGs

4.5 Simulation of IEEE 69-nodes system

The system has a total load of 3.8MW and 2.69MVar and resulting power losses of 0.2250MW and 0.1022MVar. The algorithm implemented under MATLAB Software R2014b. Branch data and node data are found in (Grisales-Noreña, Gonzalez

Montoya, & Ramos-Paja, 2018) as illustrated in Figure 4.15. The primary objective of this section is to evaluate the benefit of the RDG on an IEEE 69-nodes radial distribution system in Figure 4.15 consists of several feeders at which are heavily loaded feeder. Simulation at base case shown in Table 4.12.

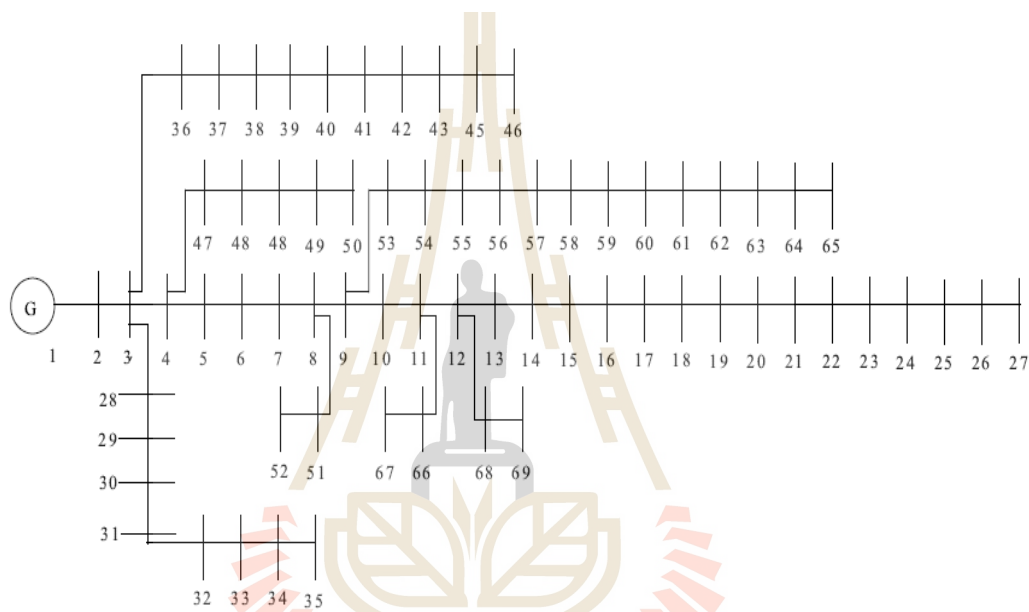


Figure 4. 15 Line diagram of the IEEE 69-nodes test system

Table 4. 12 Results of IEEE 69 Nodes without RDG

S/N	Parameters	Value
1	Load demand in Mvar	2.69
2	Load demand in MW	3.8

3	Min Voltage (node number)	0.904 (65)
4	Max Voltage (node number)	0.955 (1)
5	VSI min (node number)	26,27, 46, 63,65,69
6	Total power losses in MW	0.2250
7	Power losses in Mvar	0.1022

4.5.1 Simulation result for case 1: Minimization of active power loss.

The optimal solution (single objective) that minimizes the objective function was found to be at nodes 27, 65 and 69, with the size of RDG being 40kW, 34kW, and 25kW respectively. Here, total real power losses reduced to 0.191MW from 0.225MW as shown in Table 4.13 and ABC validated through its fitness curve in Figure 4.16 at fifth iteration.

Table 4. 13 Multiple RDG considering power loss only

Ploss (MW)	Location	RDGs (kW)	VSI	VSI _{max}
0.191	27,65,69	0.5, 0.43, 0.5	0.704	0.838

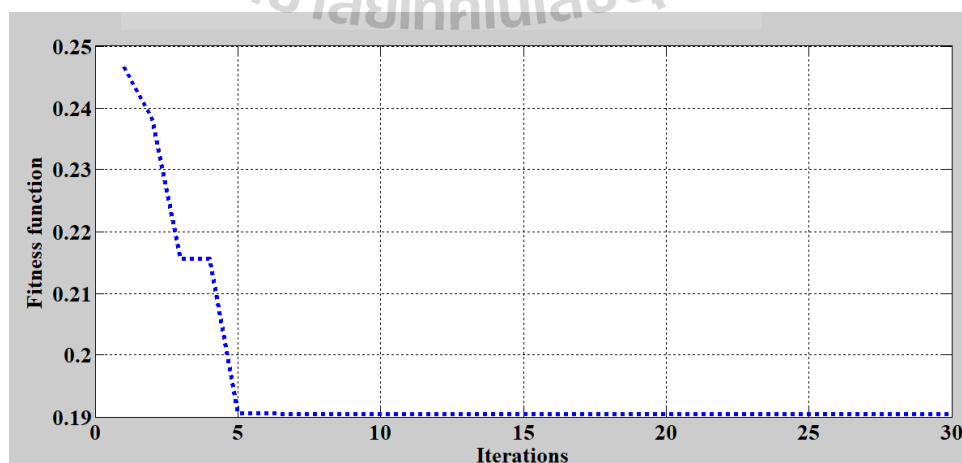


Figure 4. 16 Fitness curve for multiple RDG considering power loss only

4.5.2 Simulation result for case 2: MOO with multiple RDGs.

The optimal solution (multiobjective) that minimizes two objective functions were found to be at nodes 27, 46, and 65, with the size of RDG being 100kW, 114kW, and 217kW respectively. Here, total real power losses reduced to 0.094MW from 0.225MW as tabulated in Table 4.14. Its fitness curve of ABC by considering multiple RDGs (Injecting both P and Q) shown in Figure 4.17.

Table 4. 14 Optimization with multiple RDGs (Injecting both P and Q)

Ploss (MW)	Location	RDGs (kW)	VSImin	VSImax
0.05367	27,46,65	100, 114, 217	0.902	0.944

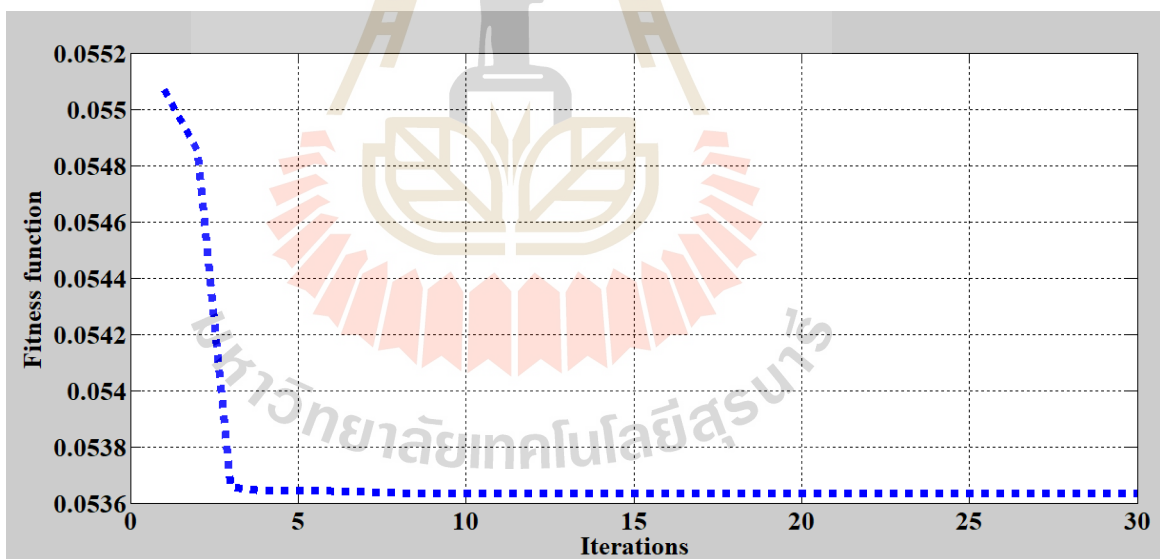


Figure 4. 17 Fitness curve by multiple RDGs (Injecting both P and Q)

4.5.3 Integration of RDGs in IEEE 69-nodes system.

RDGs introduced in RDN based on the ranking of VSI. The impacts that optimal RDG produces on real and reactive power losses, voltage profile, and

voltage stability index of the distribution system is studied (Base case with results tabulated in Table 4.12. The power loss reduction and maximization of VSI calculated for the system without considering RDG as shown in Table 4.12 and Table 4.14.

4.6 Existing IEEE 34-nodes radial feeder model

The IEEE Distribution Analysis Subcommittee (Kersting, 2001) has data for numerous test cases and hence the data for IEEE 34-nodes chosen for the radial distribution feeder. The original system is 60Hz, 24.9kV, 12 MVA with various fixed loads and distributed loads connected to a primary utility substation as shown in Figure 4.18. The node data and branch data of IEEE 34 nodes including its radial network are shown in a publication of (Mmary & Marungsri) in 2018.

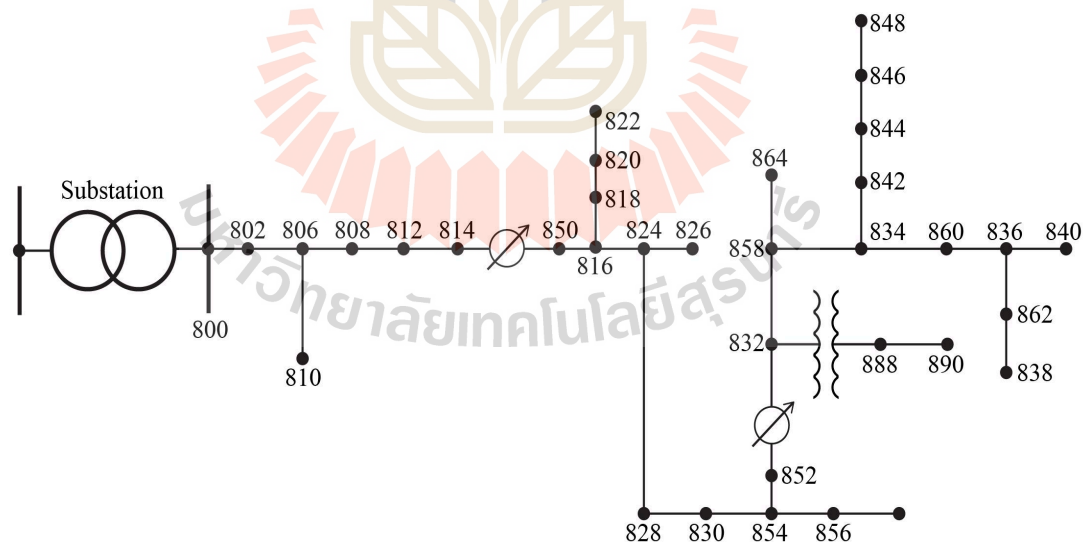


Figure 4. 18 Existing IEEE 34-nodes system (Silva et al., 2007)

The IEEE's Distribution System Analysis Subcommittee has published data for four different radial distribution test feeders. Although these feeders cannot be

considered typical, these feeders represent real-world systems located at four locations of the North American Grid. To validate these test feeders, complete data set about the power flow information are available, making them a useful benchmark. Figure 4.14 shows the one-line diagram of the test feeder. The characteristics of this test feeder are as follows:

- a. The nominal voltage of the test feeder is 24.9 kV
- b. Multiple single and three-phase laterals
- c. Long and lightly loaded
- d. Two in-line voltage regulators to regulate the voltage
- e. Unbalanced loading with “spot” and “distributed” load
- f. Shunt capacitors to improve the power factor

4.6.1 Load model

Spot loads are connected at a node. Distributed loads are modeled when the load is uniformly distributed along the length of the feeder and is hence connected to the middle of the line segment. The loads are three-phase, two-phase or single-phase and connected in star or delta.

Table 4. 12 Load model of IEEE 34-nodes

Code	Connection	Model
Y-PQ	Star (Wye)	Constant P and Q
Y-I	Star (Wye)	Constant current
Y-Z	Star (Wye)	Constant Impedance
D-PQ	Delta	Constant P and Q

D-I	Delta	Constant current
D-Z	Delta	Constant Impedance

The loads are modeled as constant complex power (PQ), constant current (I) and constant impedance (Z). Table 4.15 lists the codes used to describe the various loads. In case of constant current and constant impedance loads, kW and kVar is converted by assuming the rated voltage in p.u

4.6.2 Shunt capacitor bank

Two three-phase capacitor banks are connected in star. They have been modeled as constant susceptance.

4.6.3 Transformers

A three-phase step-down transformer, connected to star-delta, is used to step down the voltage from 24.9kV to 4.16kV for a small section of the feeder.

4.7 Real system of 34-nodes system

The proposed method have applied to solve the problem of placement and sizing RDG in real distribution system of 34-nodes. However, the distribution network under study is shown in Figure .4.19 adapted from Tanzania. System interconnected at slack bus number 5290 (Kiyungi 33kV). The network parameters and related data found in Appendix D.

VSI used for the placement of the RDGs. The first four nodes considered as an optimum place for RDG. The node numbers chosen as per VSI are 838, 848, 856 and

864. The outcome leads to two locations for placement of RDG, which are nodes 838, 848, 856 respectively with optimal size depicted in Table 4.16.

The adaption of IEEE 34-nodes network into the distribution network of Tanzania, made some changes such as voltage level from 24.9kV to 33kV. In another side, as voltage regulators are not so standard in Tanzania. For practical results, it seems better to omit voltage regulators between node number 814-850 and also node number 832-852 as modeled in a schematic network shown in Figure. 4.18. The control variable and its optimal values tabulated in Table 4.16 with four decision variables. The total load of the networks is 5.91MW and 3.07MVar. Also, the minimum voltage is 0.902 p.u bearing at node number 828 of the RDN. Thus, the system has a weak voltage profile at node 828, 834, and 838 due to the system hugely loaded.

Table 4. 16 Control variable limits and optimal values in 34-nodes

S/N	Control variable	Limit range		Optimal Value	
		Min	Max	GA	ABC
1	V_{838}	0.9	1.1	0.9967	0.9978
2	V_{848}	0.9	1.1	1.0051	1.0013
3	V_{856}	0.9	1.1	0.9861	0.9987
4	T	0.9	1.1	0.9914	0.9957

4.7.1 Simulation of real distribution system

The simulation results without RDG at are depicted in Table 4.17. From the minimum voltage of 0.9036p.u bearing at node number 838 of the RDN, also, the system has a weak voltage profile at node 838, 848, 856 due hugely loaded to the system.

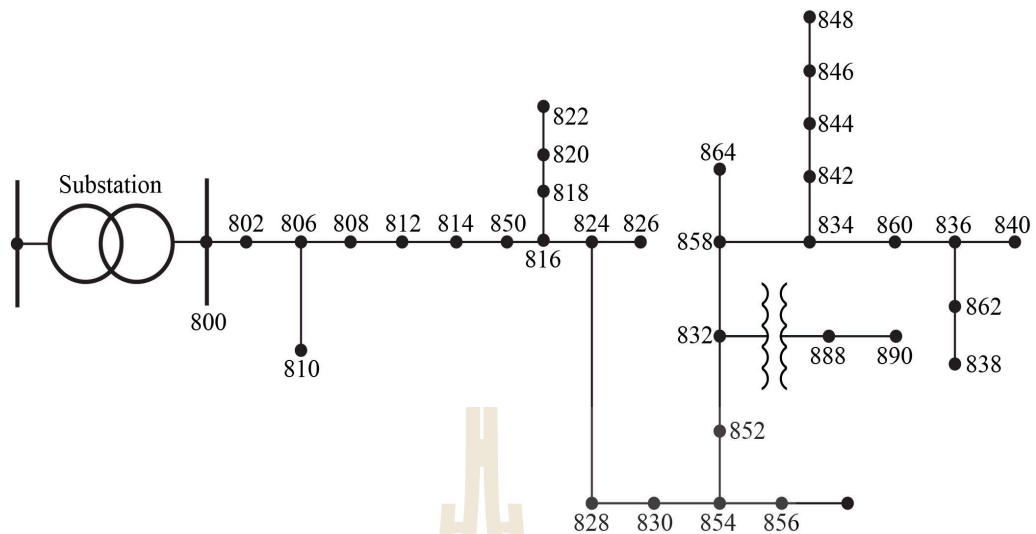


Figure 4. 19 Real system with 34-nodes system (Juanuwattanakul & Masoum, 2012)

Table 4. 17 Results of real system without RDG

S/N	Parameters	Value
1	Total reactive demand	3.007MVA _r
2	Total real demand	5.325MW
3	Min Voltage (node number)	0.9036 (838)
4	Max Voltage (node number)	0.9546 (1)
5	VSI min (node number)	0.6586 (838,848,864)
6	VSI max (node number)	0.8323 (1)
7	Total power losses	2732kW

4.7.2 Simulation result for case 1: Minimization of power loss.

The optimal solution that minimizes the objective function was found to be at nodes 838, 848, and 856, with the size of the RDG being 0.50MW, 0.43MW, and

0.50MW respectively. Here, total real power losses reduced to 1606kW from 2732kW. VSI and Power loss obtained by considering one objective function are demonstrated in Table 4.18.

Table 4. 18 Multiple RDG considering one objective function (power loss only)

Ploss (MW)	Location	Size of RDGs (MW)	VSImin	VSImax
1.606	838, 848, 856	0.5, 0.43, 0.5	0.618	0.695

4.7.3 Simulation results of case 2: Multi-objective Optimization

The placement and sizing of multiple RDGs have been investigated by considering MOOP. That means, simultaneously of power loss reduction and maximization of VSI. In a given mathematical code in Matlab, setup of iterations was given in interval of 0.01 which gives 100 times for evaluating the optimal weight factor. The obtained weight factor was 0.55 in power loss and 0.45 in VSI.

Scenario 1: Optimization with single RDG (Injecting both P and Q)

As depicted in Table 4.19, with the integration of RDG which inject both P and Q give a significant reduction of losses compared with RDG which inject only active power. Table 4.20 gives the comparison of scenario 2 in the case 2 with single RDG in the RDN with optimally located at node 848 and sized using ABC. The VSI improves from 0.741 to 0.845 at node 848. Moreover, summary of results of real system integrated with RDGs demonstrated in Table 4.20.

Table 4. 19 Optimization with single RDG (Injecting both P and Q)

Ploss (MW)	Location	RDGs (MW)	VSImin	VSImax
1.44	848	4.120	0.815	0.845

Scenario 2: Optimization with Multiple RDGs (Injecting both P and Q)

For the case of multiple RDG, power losses reduced to 1.235MW compared to 1.445MW as shown in Table 4.21 while Figure 4.20 illustrate about integration of multiple RDGs at position number 836,848 and 864 in real system of 34 node. However, simulated values of VSI in a real system without and with RDGs are revealed in Table 4.23 and Table 4.24 respectively.

Table 4. 20 Results of real system with RDGs

S/N	Parameters	Value
1	Total reactive demand	3.007MVar
2	Total real demand	5.325MW
3	Min Voltage (node number)	0.9546 (838,848,856)
4	VSI min (node number)	0.947 (838,848,856)
5	VSI max (node number)	0.964 (800)
6	Total power loss (kW)	84.01
7	Size of hybrid RDGs in (MW)	1.84, 1.120, 1.57
8	The output of Solar PV Module (Watts)	97.18
9	Number of PV module in the array	8
10	Number of the array in solar PV panels	5
11	The average output of WT (Table 2.1)	1.2

12	Number of WT	3
----	--------------	---

Table 4. 21 Optimization with Multiple RDGs (Injecting both P and Q)

Ploss (MW)	Location	RDGs (MW)	VSImin	VSImax
1.235	838, 848, 856	1.84, 1.120, 1.57	0.947	0.964

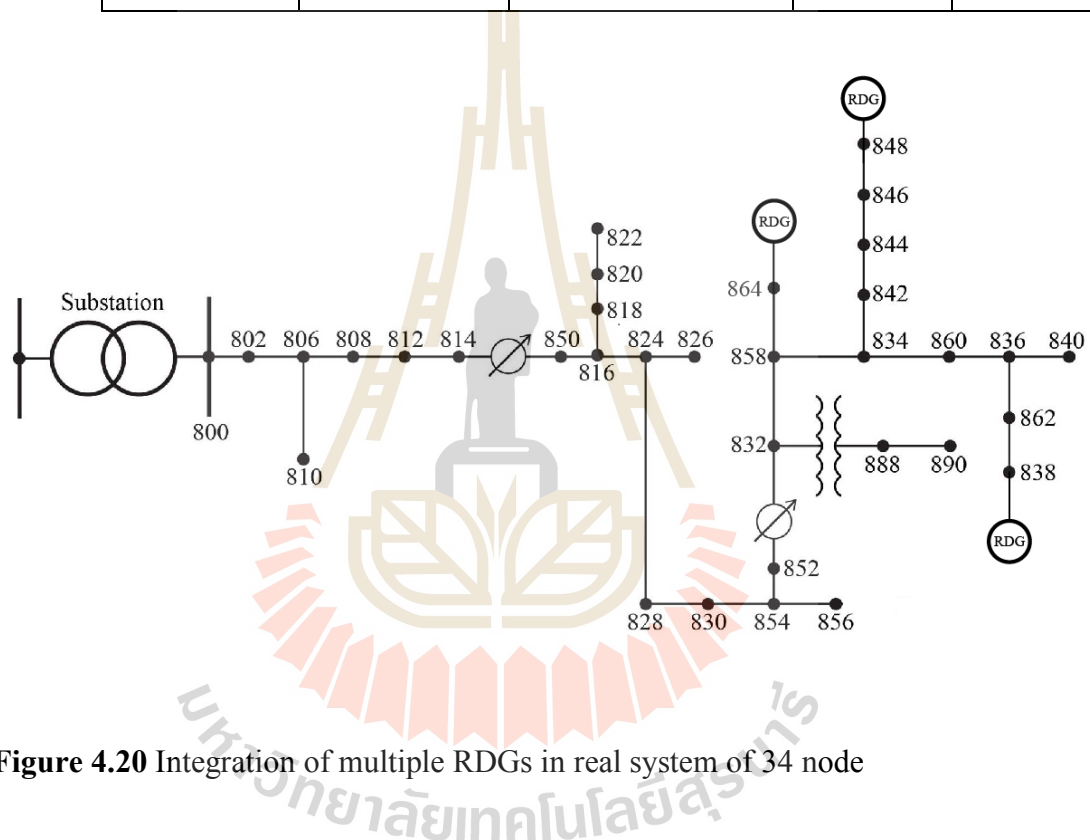


Figure 4.20 Integration of multiple RDGs in real system of 34 node

4.7.4 Sizing of BES in real system of 34-nodes

According to Reddy et al., (2010), the size of BES depends on average load supplied with hybrid RDG, energy storage technology (in MWh), which relate with an available source of RES. Since installed BES used for voltage support during adverse weather condition and at peak load only. Location of BES proposed to be in parallel (same location of RDG) with installed hybrid RDG to suit the requirement of

stable power from hybrid RDG. From the optimal values of hybrid RDG depicted in Table 4.22, the size of RDGs is 1.84MW. Thus, capacity calculated as shown in (4.1).

$$BES = \left[\frac{P_{RDG}}{V_{DC_rated} \times 0.6} \times \text{Number of bad hours} \right] \quad (4.1)$$

The obtained capacity of BES shown in equation (4.1) rated in Ampere-hour (AH). The number 0.6 used to maintain a reserve of 40% of the BES after a deep discharge.

Hence, from the given data of RDGs (1.84MW) and bad hours of weather condition assumed to be 4hrs, the optimal size of BES become 25140kAH. Finally, the proposed operation of hybrid system (charging of the BES) demonstrated in Figure 4.21 which combine power from solar PV, wind turbine and BES.

Table 4. 22 Proposed capacity of BES

RDG (MW)	1.840	1.112	1.570
BES(kAH)	12.27	7.41	10.47

The Efficient Energy Storage System gives the following advantage in power system:

- a) More efficient use of renewable energy generation.
- b) Maximization of renewable generation contribution to the utility grid.
- c) Better supply to the consumer with stable power supply
- d) Reduction of greenhouse gases emission and power losses
- e) Improving the reliability of the power system and use of power system in more efficient way.

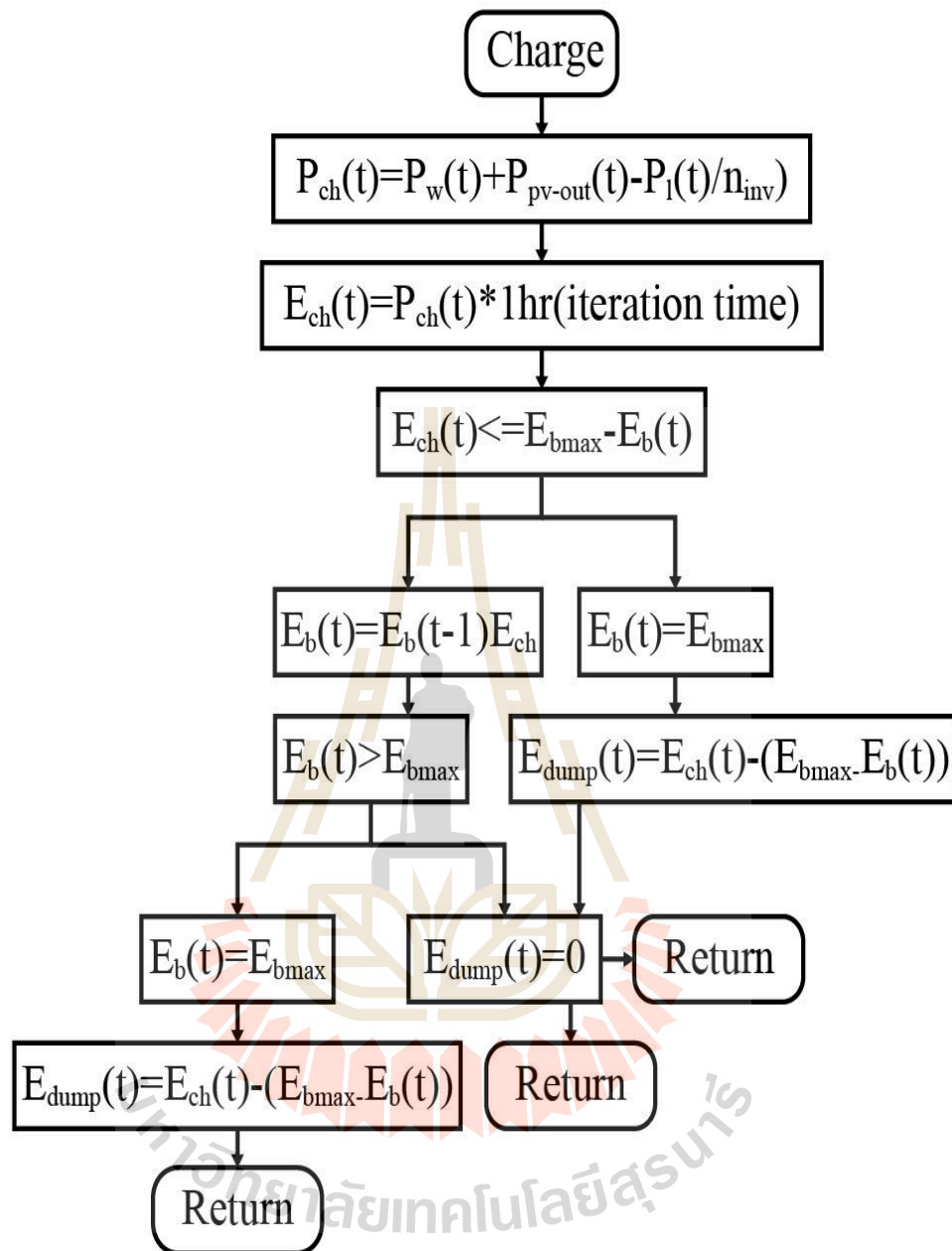


Figure 4.21 Proposed operation of hybrid system

Table 4. 23 Results of VSI in real system of 34-Nodes without RDG

Node Number	Node Number	VSI	Node Number	Node Number	VSI
800	1	1.00	834	25	0.849
802	2	0.901	842	26	0.896
806	3	0.905	844	27	0.701
808	4	0.893	846	28	0.812
810	5	0.861	848	29	0.654
812	6	0.872	860	30	0.522
814	7	0.845	836	31	0.883
850	8	0.884	840	32	0.872
816	9	0.873	862	33	0.851
818	10	0.881	838	34	0.755
820	11	0.873			
822	12	0.838			
824	13	0.856			
826	14	0.832			
828	15	0.875			
830	16	0.831			
854	17	0.885			
856	18	0.857			
852	19	0.856			
832	20	0.881			
888	21	0.855			
890	22	0.863			
858	23	0.868			
864	24	0.859			

Table 4. 24 Results of VSI into real system of 34-nodes with RDG (solar PV)

Nodes Number	Node No.	VSI	Nodes Number	Node No.	VSI
800	1	1.00	848	29	0.904
802	2	0.941	860	30	0.852
806	3	0.901	836	31	0.913
808	4	0.931	840	32	0.881
810	5	0.912	862	33	0.884
812	6	0.921	838	34	0.848
814	7	0.923	844	27	0.851
850	8	0.902	842	26	0.914
816	9	0.901			
818	10	0.921			
820	11	0.933			
822	12	0.914			
824	13	0.931			
826	14	0.912			
828	15	0.905			
830	16	0.901			
854	17	0.905			
856	18	0.917			
852	19	0.916			
832	20	0.911			
888	21	0.925			
890	22	0.933			
858	23	0.913			
864	24	0.941			
834	25	0.931			

The results for both cases of integrating RDGs analyzed in Table 4.24 and Table 4.25 as well. However, results with WT and Solar PV shows how the system may become stable by introducing active and reactive power into the RDN. In Table 4.25 performance of RDN measured by VSI enhanced compared to results found in Table 4.24.



Table 4. 25 Results of VSI into real system of 34-nodes with RDG (WT and PV)

Nodes Number	Node No.	VSI	Nodes Number	Node No.	VSI
800	1	1.00	848	29	0.914
802	2	0.991	860	30	0.872
806	3	0.995	836	31	0.943
808	4	0.993	840	32	0.882
810	5	0.991	862	33	0.894
812	6	0.992	838	34	0.898
814	7	0.985	844	27	0.881
850	8	0.994	842	26	0.936
816	9	0.993			
818	10	0.981			
820	11	0.973			
822	12	0.918			
824	13	0.976			
826	14	0.932			
828	15	0.975			
830	16	0.901			
854	17	0.925			
856	18	0.917			
852	19	0.936			
832	20	0.941			
888	21	0.955			
890	22	0.963			
858	23	0.968			
864	24	0.949			
834	25	0.949			

4.8 Chapter Summary

This research work provides insight into how the weight sum method works and has explored the significance of the weight with respect to Pareto optimal set and objective function values. The solutions influenced by multiple factors such as magnitude of the objective functions and articulation of preference on weight factor.

The results from ABC considering two types of RDGs were obtained using both the IEEE 33-nodes, IEEE 69-nodes and real system of 34-nodes network. The solution for RDG units placement and sizing has been developed in terms of selected parameter to obtain the maximum reduction of power loss and maximization of voltage stability. Results show the efficiency and robustness of the proposed ABC algorithm to finding optimal location and sizing of the RDG units for enhancing the performance of radial distribution system. The issue of penetration was analyzed concerning size and location of RDG while monitoring the power losses and improvement of VSI. For the conclusion of results, the next chapter finalizes about the conclusion and future work.

CHAPTER 5

CONCLUSION AND FUTURE WORK

5.1 Conclusion

The power loss in RDN is one of the crucial issues need to be considered by the utility, especially to the operational planning division. Improper planning of RDG into the power system, especially distribution system gives negative impacts such as high power losses and unstable voltage condition.

To solve the multi-objective Power Optimization problem; Artificial Bee Colony algorithm has been proposed, developed and efficiently applied in this research. Here the multi-objective optimization problem has been considered as a constrained single objective optimization problem by a linear combination of two objective functions as power loss and VSI. The efficiency of the proposed method was tested in solving optimization problems and successfully gives better solutions compared to the other meta-heuristic methods.

In this thesis, a combination of voltage stability and power loss reduction by proposed and implemented through proper integration of optimal hybrid RDG and BES. However, simultaneous optimization of power loss and voltage stability depicts better performance of RDN compared to separate analysis. It can be concluded that the introduction of optimal hybrid RDG with the help of ABC has improved the system performance, notably reduction of power loss and stability of the RDN which are essential for planning division.

5.2 Benefits of research work

- a) The Multi-objective function improved by taking into consideration power system parameters like stability issues.
- b) Research work will help the VSPP and utility companies in reducing both real and reactive power losses in their networks. This reduction in losses will enable them to avoid some of the penalties and compensations they incur and hence result in an improvement in their profit margins.
- c) The research work will enable the distribution companies to avoid the costs incurred during compensation of spoilt customer equipment due to voltage deviations outside the acceptable limits. As a result, this makes the companies more economical and reliable in operation.

5.3 Future work

The considerations for the future works should include the following,

- a) By combining RDG, capacitor, and BES simultaneously. By performing this approach, higher power loss reduction can be obtained.
- b) Towards more practical analysis, different types of loads should be considered instead of constant power/steady state value as in this thesis.
- c) The multi-objective function should be implemented in the optimization process, including techno-economic benefits of RDG.
- d) Smart protection system should be considered in active RDN

REFERENCES

- Abido, M. (2011). Multiobjective particle swarm optimization for optimal power flow problem. **In Handbook of swarm intelligence** (pp. 241-268): Springer.
- Abu-Mouti, F. S., & El-Hawary, M. (2011). Optimal distributed generation allocation and sizing in distribution systems via artificial bee colony algorithm. **IEEE transactions on power delivery**, 26(4), 2090-2101.
- Adaryani, M. R., & Karami, A. (2013). Artificial bee colony algorithm for solving multi-objective optimal power flow problem. **International Journal of Electrical Power & Energy Systems**, 53, 219-230.
- Aghatehrani, R., & Golnas, A. (2012). Reactive power control of photovoltaic systems based on the voltage sensitivity analysis. **Paper presented at the Power and Energy Society General Meeting**, 2012 IEEE.
- Alfayo, R., & Uiso, C. (2002). Global solar radiation distribution and available solar energy potential in Tanzania. **Physica Scripta**, 2002(T97), 91.
- Aman, M., Jasmon, G., Bakar, A., & Mokhlis, H. (2013). A new approach for optimum DG placement and sizing based on voltage stability maximization and minimization of power losses. **Energy Conversion and Management**, 70, 202-210.
- Aman, M., Jasmon, G., Mokhlis, H., & Bakar, A. (2012). Optimal placement and sizing of a DG based on a new power stability index and line losses. **International Journal of Electrical Power & Energy Systems**, 43(1), 1296-1304.
- Ayodele, T., & Ogunjuyigbe, A. (2015). Mitigation of wind power intermittency: Storage

- technology approach. **Renewable and sustainable energy reviews**, 44, 447-456.
- Baghaee, H., Jannati, M., Vahidi, B., Hosseinian, S., & Rastegar, H. (2008). Improvement of voltage stability and reduce power system losses by optimal GA-based allocation of multi-type FACTS devices. **Paper presented at the Optimization of Electrical and Electronic Equipment**, 2008. OPTIM 2008. 11th International Conference on.
- Bahmani-Firouzi, B., & Azizipanah-Abarghooee, R. (2014). Optimal sizing of battery energy storage for micro-grid operation management using a new improved bat algorithm. **International Journal of Electrical Power & Energy Systems**, 56, 42-54.
- Basso, T., & DeBlasio, R. (2011). IEEE smart grid series of standards IEEE 2030 (interoperability) and IEEE 1547 (interconnection) status. **Grid-Interop**, 2030, 5-8.
- Beaudin, M., Zareipour, H., Schellenberg, A., & Rosehart, W. (2014). Energy Storage for Mitigating the Variability of Renewable Electricity Sources. **Energy Storage for Smart Grids: Planning and Operation for Renewable and Variable Energy Resources (VERs)**, 1.
- Berrada, A., & Loudiyi, K. (2016). Operation, sizing, and economic evaluation of storage for solar and wind power plants. **Renewable and sustainable energy reviews**, 59, 1117-1129.
- Bilal, B. O., Sambou, V., Ndiaye, P., Kébé, C., & Ndong, M. (2010). Optimal design of a hybrid solar–wind-battery system using the minimization of the annualized

- cost system and the minimization of the loss of power supply probability (LPSP). **Renewable Energy**, 35(10), 2388-2390.
- Bouktir, T., & Guerriche, T. (2015). Optimal allocation and sizing of distributed generation with particle swarm optimization algorithm for loss reduction. **Science and technology**, 6(1), 59-69.
- Brown, P. D., Lopes, J. P., & Matos, M. A. (2008). Optimization of pumped storage capacity in an isolated power system with large renewable penetration. **IEEE Transactions on Power systems**, 23(2), 523-531.
- Celli, G., Ghiani, E., Mocci, S., & Pilo, F. (2005). A multiobjective evolutionary algorithm for the sizing and siting of distributed generation. **IEEE Transactions on Power systems**, 20(2), 750-757.
- Chaouachi, A., Kamel, R. M., Andoulsi, R., & Nagasaka, K. (2013). Multiobjective intelligent energy management for a microgrid. **IEEE Transactions on industrial electronics**, 60(4), 1688-1699.
- Connolly, D., Lund, H., Mathiesen, B. V., Pican, E., & Leahy, M. (2012). The technical and economic implications of integrating fluctuating renewable energy using energy storage. **Renewable Energy**, 43, 47-60.
- Devi, S., & Geethanjali, M. (2014). Application of modified bacterial foraging optimization algorithm for optimal placement and sizing of distributed generation. **Expert Systems with Applications**, 41(6), 2772-2781.
- Dufo-López, R., Bernal-Agustín, J. L., Yusta-Loyo, J. M., Domínguez-Navarro, J. A., Ramírez-Rosado, I. J., Lujano, J., & Aso, I. (2011). Multi-objective optimization minimizing cost and life cycle emissions of stand-alone PV-wind-diesel systems with batteries storage. **Applied Energy**, 88(11), 4033-4041.

- Dunn, B., Kamath, H., & Tarascon, J.-M. (2011). Electrical energy storage for the grid: a battery of choices. **Science**, *334*(6058), 928-935.
- Etinski, M., & Schülke, A. (2013). Optimal hybrid energy storage for wind energy integration. **Paper presented at the Industrial Technology (ICIT), 2013 IEEE International Conference on.**
- Fadaee, M., & Radzi, M. (2012). Multi-objective optimization of a stand-alone hybrid renewable energy system by using evolutionary algorithms: a review. **Renewable and sustainable energy reviews**, *16*(5), 3364-3369.
- Fetanat, A., & Khorasaninejad, E. (2015). Size optimization for hybrid photovoltaic–wind energy system using ant colony optimization for continuous domains based integer programming. **Applied Soft Computing**, *31*, 196-209.
- Girard, R., Bossavy, A., & Kariniotakis, G. (2011). Forecasting ramps of wind power production at different time scales. **Paper presented at the Annual EWEA 2011 Conference.**
- Grisales-Noreña, L. F., Gonzalez Montoya, D., & Ramos-Paja, C. A. (2018). Optimal Sizing and Location of Distributed Generators Based on PBIL and PSO Techniques. **Energies** (*19961073*), *11*(4).
- Hosenuzzaman, M., Rahim, N., Selvaraj, J., Hasanuzzaman, M., Malek, A., & Nahar, A. (2015). Global prospects, progress, policies, and environmental impact of solar photovoltaic power generation. **Renewable and sustainable energy reviews**, *41*, 284-297.
- Hung, D. Q., Mithulananthan, N., & Bansal, R. (2013). Analytical strategies for renewable distributed generation integration considering energy loss minimization. **Applied Energy**, *105*, 75-85.

- Jamian, J., Mustafa, M., Mokhlis, H., & Baharudin, M. (2014). Simulation study on optimal placement and sizing of Battery Switching Station units using Artificial Bee Colony algorithm. **International Journal of Electrical Power & Energy Systems**, 55, 592-601.
- Jones, L. E., & Olsson, G. (2017). Solar Photovoltaic and Wind Energy Providing Water. **Global Challenges**.
- Juanuwattanakul, P., & Masoum, M. (2012). Increasing distributed generation penetration in multiphase distribution networks considering grid losses, maximum loading factor and bus voltage limits. **IET generation, transmission & distribution**, 6(12), 1262-1271.
- Karaboga, D., & Basturk, B. (2007). A powerful and efficient algorithm for numerical function optimization: artificial bee colony (ABC) algorithm. **Journal of global optimization**, 39(3), 459-471.
- Kersting, W. H. (2001). Radial distribution test feeders. Paper presented at the **Power Engineering Society Winter Meeting**, 2001. IEEE.
- Kharrich, M., Akherraz, M., & Sayouti, Y. (2017). Optimal sizing and cost of a Microgrid based in PV, WIND and BESS for a School of Engineering. Paper presented at the Wireless Technologies, **Embedded and Intelligent Systems (WITS)**, 2017 International Conference on.
- Kong, J., & Jeyasurya, B. (2009). Multiobjective Power System Optimization Including Security Constraints. Paper presented at the **Intelligent System Applications to Power Systems**, 2009. ISAP'09. 15th International Conference on.

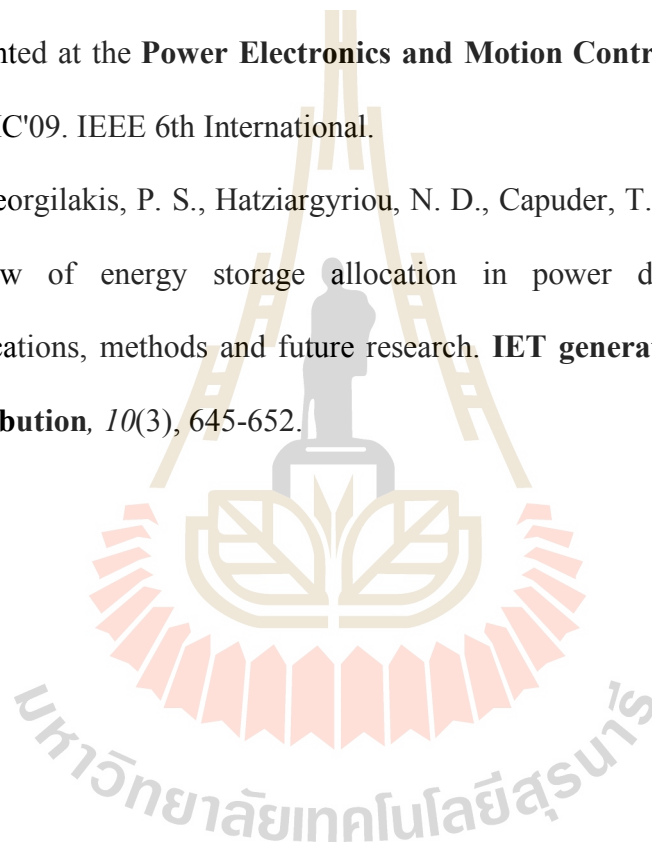
- Kothari, D. P. (2012). Power system optimization. Paper presented at the **Computational Intelligence and Signal Processing (CISP)**, 2012 2nd National Conference on.
- Liu, W., Xu, H., Niu, S., & Xie, J. (2016). Optimal Distributed Generator Allocation Method Considering Voltage Control Cost. **Sustainability**, 8(2), 193.
- Mamandur, K., & Chenoweth, R. (1981). Optimal control of reactive power flow for improvements in voltage profiles and for real power loss minimization. **IEEE Transactions on Power Apparatus and Systems** (7), 3185-3194.
- Mmary, E. R., & Marungsri, B. Multiobjective Optimization of Renewable Distributed Generation and Shunt Capacitor for Techno-Economic Analysis using Hybrid Invasive Weeds Optimization. **GMSARN International Journal** 12 (2018) 24 - 33. 24
- Mohamed, M. A., Eltamaly, A. M., & Alolah, A. I. (2016). PSO-based smart grid application for sizing and optimization of hybrid renewable energy systems. **PloS one**, 11(8), e0159702.
- Mohandas, N., Balamurugan, R., & Lakshminarasimman, L. (2015). Optimal location and sizing of real power DG units to improve the voltage stability in the distribution system using ABC algorithm united with chaos. **International Journal of Electrical Power & Energy Systems**, 66, 41-52.
- Murty, V., & Kumar, A. (2015). Optimal placement of DG in radial distribution systems based on new voltage stability index under load growth. **International Journal of Electrical Power & Energy Systems**, 69, 246-256.

- Mwakabuta, N., & Sekar, A. (2007). Comparative study of the IEEE 34 node test feeder under practical simplifications. Paper presented at the **Power Symposium, 2007. NAPS'07. 39th North American.**
- Naik, S. G., Khatod, D., & Sharma, M. (2013). Optimal allocation of combined DG and capacitor for real power loss minimization in distribution networks. **International Journal of Electrical Power & Energy Systems, 53**, 967-973.
- Niknam, T., Narimani, M., Aghaei, J., & Azizipanah-Abarghooee, R. (2012). Improved particle swarm optimisation for multi-objective optimal power flow considering the cost, loss, emission and voltage stability index. **IET generation, transmission & distribution, 6(6)**, 515-527.
- Ochoa, L. F., Padilha-Feltrin, A., & Harrison, G. P. (2005). Evaluation of a multiobjective performance index for distribution systems with distributed generation. Paper presented at the Electricity Distribution, 2005. CIRED 2005. **18th International Conference and Exhibition on.**
- Pan, H., Hu, Y.-S., & Chen, L. (2013). Room-temperature stationary sodium-ion batteries for large-scale electric energy storage. **Energy & Environmental Science, 6(8)**, 2338-2360.
- Paska, J., Biczal, P., & Klos, M. (2009). Technical and economic aspects of electricity storage systems co-operating with renewable energy sources. Paper presented at the **Electrical Power Quality and Utilisation, 2009. EPQU 2009. 10th International Conference on.**
- Passey, R., Spooner, T., MacGill, I., Watt, M., & Syngellakis, K. (2011). The potential impacts of grid-connected distributed generation and how to address them: A

- review of technical and non-technical factors. **Energy Policy**, 39(10), 6280-6290.
- Payasi, R., Singh, A. K., Singh, D., & Singh, N. K. (2015). Multi-objective optimization of distributed generation with voltage step constraint. **International Journal of Engineering, Science and Technology**, 7(3), 33-41.
- Reddy, P. D. P., Reddy, V. V., & Manohar, T. G. (2016). Application of flower pollination algorithm for optimal placement and sizing of distributed generation in distribution systems. **Journal of Electrical Systems and Information Technology**, 3(1), 14-22.
- Sadwick, L. P. (2016). Power Quality Enhancement. In: **Google Patents**.
- Saint, B. (2011). Update on IEEE 1547 series of standards for distributed resources interconnection. Paper presented at the **Power and Energy Society General Meeting**, 2011 IEEE.
- Senjyu, T., Sakamoto, R., Urasaki, N., Funabashi, T., Fujita, H., & Sekine, H. (2006). Output power leveling of wind turbine generator for all operating regions by pitch angle control. **IEEE Transactions on Energy Conversion**, 21(2), 467-475.
- Sharma, M., & Vittal, K. (2010). A heuristic approach to distributed generation source allocation for electrical power distribution systems. **Iranian Journal of Electrical and Electronic Engineering**, 6(4), 224-231.
- Shukla, T., Singh, S., & Naik, K. (2010). Allocation of optimal distributed generation using GA for minimum system losses in radial distribution networks. **International Journal of Engineering, Science and Technology**, 2(3), 94-106.

- Shukla, T., Singh, S., Srinivasarao, V., & Naik, K. (2010). Optimal sizing of distributed generation placed on radial distribution systems. **Electric power components and systems**, 38(3), 260-274.
- Silva, J. A., Funmilayo, H. B., & Bulter-Purry, K. L. (2007). Impact of distributed generation on the IEEE 34 node radial test feeder with overcurrent protection. Paper presented at the **Power Symposium**, 2007. NAPS'07. 39th North American.
- Singh, D., & Verma, K. (2009). Multiobjective optimization for DG planning with load models. **IEEE Transactions on Power systems**, 24(1), 427-436.
- Sortomme, E., & El-Sharkawi, M. (2009). Optimal power flow for a system of microgrids with controllable loads and battery storage. Paper presented at the **Power Systems Conference and Exposition**, 2009. PSCE'09. IEEE/PES.
- Varadarajan, M., & Swarup, K. (2008). Differential evolutionary algorithm for optimal reactive power dispatch. **International Journal of Electrical Power & Energy Systems**, 30(8), 435-441.
- Vrettos, E. I., & Papathanassiou, S. A. (2011). Operating policy and optimal sizing of a high penetration RES-BESS system for small isolated grids. **IEEE Transactions on Energy Conversion**, 26(3), 744-756.
- Weitemeyer, S., Kleinhans, D., Vogt, T., & Agert, C. (2015). Integration of Renewable Energy Sources in future power systems: The role of storage. **Renewable Energy**, 75, 14-20.
- Yan, R., & Saha, T. K. (2012). Voltage variation sensitivity analysis for unbalanced distribution networks due to photovoltaic power fluctuations. **IEEE Transactions on Power systems**, 27(2), 1078-1089.

- Yang, C.-F., Lai, G. G., Lee, C.-H., Su, C.-T., & Chang, G. W. (2012). Optimal setting of reactive compensation devices with an improved voltage stability index for voltage stability enhancement. **International Journal of Electrical Power & Energy Systems**, 37(1), 50-57.
- Zhao, J., Li, X., Hao, J., Zhang, C., & Lu, J. (2009). Wind farm reactive power output optimization for loss reduction and voltage profile improvements. Paper presented at the **Power Electronics and Motion Control Conference**, 2009. IPEMC'09. IEEE 6th International.
- Zidar, M., Georgilakis, P. S., Hatziargyriou, N. D., Capuder, T., & Škrlec, D. (2016). Review of energy storage allocation in power distribution networks: applications, methods and future research. **IET generation, transmission & distribution**, 10(3), 645-652.



APPENDIX A

Research Publication

Mmary, E. R., & Marungsri, B., (2018), Multiobjective Optimization of Renewable Distributed Generation and Shunt Capacitor for Techno-Economic Analysis using Hybrid Invasive Weeds Optimization. **GMSARN International Journal**, Vol 12, pp 24 – 33.

Mmary, E. R., & Marungsri, B., (2018), Optimal Hybrid Renewable Generaor for techno-economic benefits in smart distribution network. **The 6th International Electrical Engineering Congres**, 7-9 March 2018, Krabi, Thailand.

Mmary, E. R., et al., & Marungsri, B., (2017), Optimal Hybrid Renewable Energy in Unbalance Distribution Network using DIgSILET Power Factory software and Genetic Algorithm. **Presented in 2017 IEEJ PE&S IEEE PES Thailand Joint Symposium on Advanced Technology in Power System**, 7-8 March 20187, Bangkok, Thailand.

Mmary, E. R., et al., & Marungsri, B., (2017), Optimal Hybrid Renewable Energy for Power Factory Problems in Distribution System. **Presented in 2017 IEEJ PE&S IEEE PES Thailand Joint Symposium on Advanced Technology in Power System**, 7-8 March 20187, Bangkok, Thailand.



Multiobjective Optimization of Renewable Distributed Generation and Shunt Capacitor for Techno-Economic Analysis using Hybrid Invasive Weeds Optimization

Elifuraha Reuben Mmary* and Boonruang Marungsri

Abstract— The techno-economic benefits of smart distribution grid enhanced through the integration of voltage control device and Renewable DG (RDG). In this research paper, a new optimization method called hybrid Invasive Weeds optimization proposed to solve the multiobjective optimization problem of minimizing power loss, cost of energy, and voltage deviation. Invasive Weeds optimization (IWO) and Artificial Bee Colony (ABC) are the new nature-inspired algorithms used to solve constrained optimization problems in distribution networks integrated with capacitor and RDG for both reactive and real power compensation. The optimum location of RDG and capacitor determined by using ABC algorithm and performance indices while the optimum size of RDG and capacitor found out by hybrid invasive weeds optimization. The results depict that the optimal RDG and capacitor reduce power losses by 14.4%, and cost by 22.4%. The effectiveness of proposed hybrid approach implemented in MATLAB and tested on IEEE 34-nodes and IEEE 37-nodes test feeder. The obtained results prove indetails the efficiency of the proposed approach to solve MOP problems.

Keywords— Invasive weeds optimization, renewable DG, ABC algorithm, HIWO, optimal power flow.

1. INTRODUCTION

The needs of acceptable power quality, stability, and reliability in affordable create a climate for the penetration of renewable distributed generation in power distribution system of Thailand to enhance the desired performance. Usually, the power distribution networks are radial experiencing low X/R ratio, unidirectional of power flow, high power loss, voltage deviation, and voltage instability. Recently the cost of RDG has been reduced drastically due to the advanced technology [1]. Optimization techniques can use for deregulation of the power industry, by using the best allocation of multiple RDG units [2]. The advancement of RDG technology and the demand of the customers for reliable, affordable, and stable power supply has led to an increasing interest in RDG in power distribution networks [3]. However, issues related to reliability, stability, and variability have hindered the penetration of RDG units in power distribution grids [4]. Since RDG placement in on-grid critically affects the operation of the power distribution network.

To achieve improvement of voltage profile, power quality and reduction of power loss (enhanced performance) of radial power distribution network suitable sitting and size of RDG with shunt capacitor need to be provided. Since the integration of non-optimal size of RDG lead to complex operational situations in the

power distribution network [5].

Under the current standard IEEE 1547, most of the RDG designed to operate at unity power factor [3], [6]. Conventional devices [7] such as switchable capacitors, voltage regulators and tap changers employed by different researchers for solving voltage regulation problem, but they are not fast enough to compensate for transient events [8]. Other technologies such as permanent magnet synchronous machines used in biomass power plants, gas power plant, and wind farm employed for controlling both real and reactive power [9]. However, sustainable energy supply such as solar PV farm and wind turbine farm is the most promising technologies for supply power at sub-transmission and distribution networks for techno-economic benefits. However, the drawbacks of using one type of RES are intermittent and variability which may not match with the load demand [10]. A hybrid approach of combining solar PV and wind turbine system, can efficiently complementary characteristics of each RES to improve reliability, power quality, and stability in the radial distribution system. Hence, the goal of this paper is optimal for hybrid RDG system for increasing techno-economic benefits.

Placement and sizing of DG were the best the best research topics for the past of three decades. The placement of RDG as single objective optimization carried out in various optimization techniques for finding MOO of DG in-line with minimizing power loss, operation cost, and maximization of profit. These methods include Improved Bat Algorithm [11-12], Particle Swarm Optimization (PSO) [13], Artificial Bee Colony (ABC) [14], Genetic Algorithm (GA) [15], and Analytical expression (AE) based heuristics [16-17]. The limitation of AE based heuristics is the inability to handle multiple objectives and multiple RDGs. In [15], GA introduced to address the optimal sizing and location

Elifuraha Reuben is a Master Degree Candidate with School of Electrical Engineering, Institute of Engineering, Suranaree University of Technology (SUT), Thailand.

Boonruang Marungsri is Assistant Professor with school of Electrical Engineering, Suranaree University of Technology-Thailand.

*Corresponding author: Elifuraha Reuben; Email: reubsonmmmary@gmail.com.

of DG for voltage stability enhancement, and power loss reduction. Authors in [13] applied the PSO with improved differential evolution algorithm for the optimal siting of DG in power distribution networks. The objective was a reduction of real power loss with the optimal real power of DG in RDS. From [14], results of optimal sizing and location using ABC and PSO were compared.

Researchers found in [16] present a method for multiple DG siting using an analytical method for loss reduction as an objective function. They compare the optimal size of four types of DG. The effectiveness of IA method compared to loss sensitivity factor using 33-node and 69-node RDSs. MOPSO algorithm presented by authors in [19] used to optimize sizing, and siting of multiple DGs in RDS. The proposed algorithm tested in IEEE 34-node and 69-node RDNs to improve the voltage magnitude, stability, reduced power losses, and enhanced the supply reliability. The drawbacks of these algorithms are declared insecure convergence properties, the complexity of algorithmic for a big network, and long execution time. Besides, the solution trapped into local minima. To overcome the drawback of these methods, researchers have successfully applied meta-heuristic algorithms such as ABC [20], FPA [22], IWO [23], [37] and HIWOPSO [27]. It is reported that meta-heuristic algorithms are more efficient than classical algorithms for solving the MOO problem.

The ABC algorithm [20] gave better results in term of iteration, quality of the solution, and convergence. However, IWO for power loss reduction in radial power system subjected to both voltage constraints and power transfer for the optimum siting of DG performed in [23]. Authors in [24] present DE algorithm to determine optimal size and location of DG and shunt capacitor in power distribution system for minimum power loss and voltage profile improvement. The results analyzed in electricity benchmark of the 12-nodes power distribution network. However, results of inappropriate siting and sizing of DG and capacitor shows a reduction of techno-economic benefits of the entire system operation.

In this study, an attempt of combine solar PV, a shunt capacitor, and permanent magnet synchronous wind turbine in distribution made as multiple RDG units in radial distribution network using Hybrid Invasive Weeds Optimization (HIWO). The RDGs that are capable of supplying both active and reactive power is the most effective for power loss reduction. Power loss minimization investigated by integrating multiple DGs and shunt capacitor. The problem of RDG placement to minimize energy losses has been solved by ABC algorithm [20] for two different load scenarios. Multiple RDG placements have been obtained by FPA [21], [25] to achieve an extreme reduction in annual energy losses in the radial distribution system. Distribution test networks such as IEEE 34-nodes and IEEE 37-nodes have been used to validate the effectiveness of proposed method.

This paper presents Hybrid Invasive Weeds Optimization (HIWO) and voltage stability index (VSI) for finding both optimal location and size of shunt capacitor and RDG in power distribution network.

Hybrid technique of IWO and ABC adopted in this paper, has been proposed in [28], [29], while voltage stability index (VSI) adopted from [30]. IWO and ABC as new optimization algorithm used to diminish the problem of optimization considering reduction of total active power losses, the total operation cost, cost of energy loss, lower cost of electricity and voltage deviation in the rural community of Thailand. HIWO proposed to suit multi-objective problems due to its fast convergence performance and robustness. The results show that HIWO has better performance than the other algorithms in most of the functions. The obtained results analyzed and compared with recently published papers such as FPA [21], PSO [13], and GA [15] to confirm its notability

In Section 2, depicts modeling of renewable DG for optimal power flow. Deterministic power flow as a nonlinear multiobjective optimization problem with equality and inequality constraints analyzed in section 3 including problem formulation. In section 4 described ABC algorithm method while IWO as an intelligent optimization algorithm described in section 5 and section 6 shows the simulation results of the study. Finally, the main contributions of this paper summarized in Section 7.

2. MODELING OF RDG FOR OPTIMAL POWER FLOW

Wind turbine

In this research work, proposed wind turbine adapted from [21] and [31]. The parameters used are as follows: $P_{nom}=600$ kW, $V_{ci}=4$ m/s, $V_{nom}=16$ m/s $V_{co}=20$ m/s. Fig. 1 shows the wind speed data used to calculate the power generated by the wind turbine generator in the deterministic OPF algorithm.

The power output of wind turbine in (1) and (2) considers two main factors, the wind speed and the power curve of the wind turbine. According to [20] the power curve of a wind turbine can be modeled using a function split into three different parts:

$$P_{wt} = \begin{cases} 0 & V \leq V_{ci} \\ Y P_{nom} & V_{ci} \leq V \leq V_{co} \\ 0 & V > V_{co} \end{cases} \quad (1)$$

$$Y = \frac{V^2 - V_{ci}^2}{V_{nom}^2 - V_{ci}^2} \quad (4)$$

where P_{nom} , V_{nom} , V_{ci} , and V_{co} are nominal active power, nominal speed of the wind turbine, cut-in wind speed turbine, and cut-out wind speed of the wind turbine, respectively. P_{wt} and V denoted power output of the wind turbine and wind speed respectively.

Solar PV

The power output of the SPV shown in (3) dependent on the solar irradiance and ambient temperature of the site shown in (4) as well as the features of the module itself

[23]. The following equation used to determine the power output of the photovoltaic module PV [31]:

$$P_{pv} = \frac{P_{STC} T_s [1 + \mu(T_c - 25)]}{1000} \quad (3)$$

where P_{STC} is photovoltaic module maximum power at Standard Test Condition (STC) in Watts, T_s is solar irradiance in (W/m²), μ is the coefficient ($^{\circ}C^{-1}$), of solar PV, T_c is temperature ($^{\circ}C$) of the photovoltaic cell determined as a function of solar irradiance and ambient temperature.

$$T_c = T_a + \frac{I_s(T_{NOCT} - 20)}{800} \quad (4)$$

where T_a is ambient temperature ($^{\circ}C$), T_{NOCT} is operating cell temperature ($^{\circ}C$) of the Solar PV. Their performance characteristics are $P_{STC} = 250$ W, $\mu = 00450C^{-1}$, $T_{NOCT} = 460C$.

Hydropower

The mathematical formula depicted in (5) determine the power output of hydropower by Hernandez et al. 2012 [24] and Fuchs et al. 2010 [32] as follows:

$$P_h = \rho g H Q(t) \quad (5)$$

where P_h is hydraulic power produced at the shaft in MW, ρ is the density of water, g gravity due to gravity, $Q(t)$ is the rate of water flow in meter cubic per second, H the sufficient head of water across the turbine.

Cost Analysis

Purchased actual power cost from the grid:

Purchase effective power cost from grid including losses is evaluated using (6) [33].

$$T_c = \sum_{t=1}^t PW^t E_d P_d T \quad (6)$$

where PW is the present worth, and it is expressed by (7), t is a planning period for five years, E_p is the electricity market price, T indicates time in hours and yr shows the year, P_d is the total real power demand, and it is a combination of total active power load (Pload) and real power loss (Ploss) of a network. It may be expressed using (7).

$$PW = \frac{1 + \text{inf } R}{1 + \text{int } R} \quad (7)$$

Installation cost of Capacitor and RDG

Installation cost of shunt capacitor is a combination of capacitor purchase cost and fixed cost, and it can be evaluated using (8) while for DG expressed in (9). The

possible standard sizes and individual purchase cost (\$/kVAr) of shunt capacitor and \$/MW of RDG are available in [33].

$$C_{inst} = \sum_{i=1}^{ncap} K_c^{inst} Q_{c,i} + K_c^f \quad (8)$$

$$RDG_{inst} = \sum_{i=1}^{NDG} RDG_{c,i} * K_{RDG}^{inst} \quad (9)$$

O&M cost of RDG and Capacitor

RDG O&M cost depends upon the real power supply by RDG to a system, and it can be calculated using (11).

$$RDG_{OM} = \sum_{T=1}^{YR} \sum_{i=1}^{NDG} PW^t * P_{DG_i} * T * K_{RDG}^{OM} \quad (11)$$

Total annual cost saving

The total annual cost saving of a network is a difference between total annual cost before and after incorporation of RDG and shunt capacitor. It is evaluated using (12).

$$\%NS = \frac{T_c^{before} - (T_c^{after} + C_{Int} + I_{cost} + O_{cost})}{T_c^{before}} \quad (12)$$

where NS is Net Saving, T_c_{bef} and T_c_{aft} represent the purchase actual power cost from transmission grid before and after placement respectively, I_{cost} is Installation cost of RDG, and $Cost$ is Operation cost of RDG.

3. DETERMINISTIC OPTIMAL POWER FLOW

The MOPF problem can be formulated as follows [16]:

$$\min F(x, u) \quad (13)$$

subjected to

$$\begin{cases} g(x, u) = 0 \\ h(x, u) \leq 0 \end{cases} \quad (14)$$

where F is the MOPF, x and u are vectors of state and control variables, respectively.

For distribution networks, the vector of dependent variables (x) shown in (15) consisting of:

- The active power of the electric grid P_{gr}
- Load node voltages,
- The reactive power DG units which are as PV nodes Q_{DG} ;
- Branch flows S .

Therefore, x expressed:

$$x = [P_{gr}, V_L, S_i, Q]^T \quad (15)$$

where N_L , are number of PQ nodes and N_{PV} , are number of PV nodes.

Also, Vector of control variables (u) shown in (16) consists the following;

- The P of the DG units with nonrenewable energy sources PDG ;
- Node voltage;
- Voltages at PV nodes V_{PV} ;
- Tap settings of Transformer t ;
- Shunt VAR compensators Q_C .

Therefore, the vector of control variables expressed as:

$$u = [V_{PV}, P_{DG}, Q_C, T]^T \tag{16}$$

where N_{NR} , N_{PV} , N_T , and N_C are a number of the non-renewable DG units, number of PV nodes (RDG units modeled as PV nodes), number of regulating transformers, and number of VAR compensators, respectively.

Multi-objective OPF

The multiobjective function of this work is to find the optimal size and location of RDG. The equation shown in (17) depicts the general objective of this paper as MOF which of the cost of energy loss, power losses and voltage deviation at load nodes:

$$F = W_C C_{EL} + W_V \sum_{i=1}^{NL} |1 - V_i| + W_P \sum_{i=1}^N P_L \tag{17}$$

where

$$W_C + W_V + W_P = 1$$

W_C Weight factor for the cost of energy loss

W_V Weight factor for voltage deviation

W_P Weight factor for power loss

Cost of energy losses (CEL) [34]

The mathematical equation shown in (18) was used to compute the annual cost of energy losses.

$$CEL = P_L * (K_p + K_e L_f * 8760) \$ \tag{18}$$

where

K_p Annual cost of power loss = 57.6923\$/kW

K_e Cost of energy loss = 0.009615\$/kWh

L_f Loss factor = 0.47

Real power loss

The total active losses of the system shown in (19) can be computed as follows

$$P_L = \sum_{k=1}^N G_k [V_i^2 + V_j^2 + 2|V_j||V_i| \cos(\delta_i - \delta_j)] \tag{19}$$

where N is the total number of lines in the system; G_k is the conductance of the line 'k', V_i and V_j are the

magnitudes of the sending end and receiving end voltages of tie line; are angles of the end voltages.

Economical Saving

By using the proposed method, net savings given by (20) and (21) were used to analyze economic saving in addition to its technical advantage

$$Netsaving = (C_e * P_{Loss}^{Cap} * T) + (C_e * P_{Loss}^{RDG} * T) - (Cd * Ni) - (C_c * T_c) - (C_{RDG} * T_{RDG}) \tag{20}$$

$$NS = EC / yr - (Cost_{inst} + Cost_{pur}) - (Cost_{Op/year}) \tag{21}$$

where;

N_s Net saving

E_C Cost of total energy produced per year.

N_n The number of compensated nodes in the system

T_C The total capacity of the capacitor

T_{RDG} The total capacity of RDG

P_{Loss}^{RDG} The total power loss with RDG

P_{Loss}^C The total power loss with capacitor

Table 1: The parameter used for net savings [35]

S/N	Parameters	Value
1	Energy rate (Ce)	\$0.06/kWh
2	Installation cost (Ccl)	\$1000/each
3	Purchase cost (Cp)	\$3.0/kVAr
4	Time (T)	8760

Table 1 depicts parameters used for analyzing economic benefits of the proposed research.

Voltage Stability Index (VSI)

Fig. 1 depicts the electrical equivalent of the radial power distribution system. The voltage Stability Index (SI) shown in (21) is one of the most significant indices that contribute to the security of the network. Fixing of the RDG units in the power distribution system have a tremendous positive impact on the voltage stability index. Chakraborty M. et al. in [20] have proposed a new VSI for determining the most sensitive node to voltage collapse. The value of VSI is given by (21).

$$VSI = |V_i|^4 - 4[P_r X_{ij} - Q_r R_{ij}]^2 - 4[P_r R_{ij} + Q_r X_{ij}] |V_j|^2 \tag{21}$$

The node at which VSI has the lowest value is prone to collapse. Therefore, to evade the possibility of voltage collapse, the VSI of all nodes determined at the base case and after placement of both shunt capacitor and RDG.

System Limitations

The MOPF subjected to the following constraints:

Equality constraints

The equality constraints (2) represent power balance and power flow equations. The power balance equation in a distribution network with DG units with renewable and nonrenewable energy sources expressed as follows:

The equality constraints represent the power flow equations, which are given below for i th nodes:

$$\begin{cases} P_G + P_{RDG} - P_D = \sum_{k=1}^N G_k [V_i^2 + V_j^2 - 2|V_j||V_i|\cos(\delta_i - \delta_j)] \\ Q_G + Q_{RDG} + Q_C - Q_D = \sum_{k=1}^N B_k [V_i^2 + V_j^2 - 2|V_j||V_i|\sin(\delta_i - \delta_j)] \end{cases} \quad (22)$$

Inequality constraints

Inequality expression in (23) is functional which comprise: voltage magnitude of nodes, reactive power capabilities of RDG and power flow limits in the branch. However, these constraints may describe the practicability region of the problem control variables such as RDG unit active power output limits, magnitude limits of PV node voltage, transformer tap setting limits and shunt VAR compensator.

PV nodes constraints (Generator):

Voltage and reactive power of i th node of generator lie between their upper and lower limits as given below:

$$V_G^{\min} \leq V_G \leq V_G^{\max} \quad (23)$$

$$Q_G^{\min} \leq Q_G \leq Q_G^{\max} \quad (24)$$

where in (28) depicts minimum and a maximum voltage of i th generating units and in (29) present minimum and maximum reactive power of i th generating units.

PQ nodes constraints:

The voltage magnitude for all load nodes expressed as:

$$V_{Li}^{\min} \leq V_{Li} \leq V_{Li}^{\max} \quad (24)$$

where expression (22) depicts are the minimum and maximum load voltage of i th unit.

Tap Setting of Transformer:

Tap settings of Transformer between upper and lower limit as given below:

$$T^{\min} \leq T \leq T^{\max} \quad (25)$$

Shunt compensator constraints:

Shunt compensation is restricted by their limits as follows:

$$Q_{Ci}^{\min} \leq Q_{Ci} \leq Q_{Ci}^{\max} \quad (26)$$

where an expression (26) depicts the min and max VAR injection limits of i th shunt capacitor.

Constraints of RDG:

$$\begin{cases} 1.5MW \leq P_{DG} \leq 5.0MW \\ 0.5MVar \leq Q_{DG} \leq 2.0MVar \end{cases} \quad (27)$$

Reactive power (Q) of RDG supplementary to the OF as a quadratic penalty term [16]. The new expanded OF becomes:

$$F_p = F + \lambda_V \sum_{i=1}^N (V_i - 1)^2 + \lambda_{Q_{DG}} \sum_{i=1}^{NPV} (Q_{DG_i} - Q_{DG_i}^{\lim})^2 + \lambda_S \sum_{i=1}^N (S - S_i^{\lim})^2 \quad (28)$$

where λ_V , $\lambda_{Q_{DG}}$ and λ_S defined as penalty factors, x_{lim} is the limit value of the dependent variable x and given as [21]:

$$\begin{cases} x^{\lim} = x^{\min} & \text{if } \dots x < x^{\min} \\ x^{\lim} = x^{\max} & \text{if } \dots x > x^{\max} \end{cases} \quad (29)$$

4. METHODOLOGY

IWO Algorithm

IWO is the optimization algorithm developed by Mehrabian and Lucas in 2006. IWO is a novel ecologically inspired algorithm that mimics the process of weeds colonization and distribution [37]. Despite its recent development, it has shown successful results in some practical applications like optimization of optimal reactive power by using hybrid IWOPSO [36]. Each invading weed takes the unused resources in the field and grows to the flowering weed and produces new weed independently, as shown in Fig 1.

Steps of Invasive Weeds Optimization Algorithm:

Step 1: Initialization: As search space is taken, and a certain number of weeds are initialized randomly in the entire search space.

Step 2: Reproduction
The seeds produced by weeds increase linearly starting with worth fitness and ending with the best fitness.

$$s(i) = s_{\max} - abc \left(\text{floor} \left(\frac{s_{\max} * \mathcal{E}_{best}}{\mathcal{E}_{best} - \mathcal{E}_{worst}} \right) \right) \quad (30)$$

Step 3: Spatial dispersion
This step ensures the probability of dropping a seed in the remote area decreases nonlinearly.

Step 4: Competitive Exclusion

□

Fitter plants produce more seeds than fewer desirable plants, which tends to improve the convergence of the algorithm.

Step 5: Randomly initialized of the RDG and capacitor values (weeds values). The weeds with the highest fitness produce the maximum number of seeds and those with the lowest fitness produce minimal seeds. Seeds produced by the weed calculated by using (30)

Step 6: Now the generated seeds are added to the solution set, and the fitness value calculated for the combined set of weeds and seeds

Step 7: The population sorted in descending order of their fitness. Step 4-6 repeated until a maximum number of iteration reached.

Table 2: Controlled parameters for IWO

Parameters	Value
Max. Number of weeds	10
Total weeds in the population	100
Initial standard deviation	2
Final standard deviation	1e-3
Nonlinear modulation index	5

Artificial Bee Colony Algorithm

Artificial Bee Colony (ABC) algorithm, proposed by Karaboga for optimizing mathematical problems. ABC algorithm new swarm method that introduced by Karaboga in Turkey in 2005 [14], [20].

The ABC algorithm imitates the behaviors of bees in finding food sources and sharing the information with other bees. Since ABC is simple in easy to implement and has fewer control parameters. ABC algorithm is a combination of three types of honey bees namely employed bee, onlooker bee, and scout bee, where onlooker and scout bee considered as an unemployed bee. The employed bees' searches and exploits a food location while the onlooker bees wait in the hive. Then employed bee, share information with the onlooker bees regarding a food location.

Three control parameters used in the ABC based algorithm; the number of the food source which is equal to the number of onlooker bees, the value of limit and the MCN. In ABC, if a position cannot be improved further through a predetermined number of cycles, then that food font is assumed to be abandoned. The value of the predetermined number of cycles is an important control parameter of the ABC algorithm; this termed the limit for abandonment.

An optimization algorithm for ABC

Step-1: Initialize the food-source locations X_i (solutions population), The X_i form is as follows:

$$X_{ij} = X_{min,j} + rand(0,1)(X_{max,j} - X_{min,j}) \quad (31)$$

Step-2: Calculate the nectar amount of the population

using their fitness values using

$$Fitness = \frac{1}{1 + Objective_function} \quad (32)$$

Total Losses = Active Power Losses + Reactive Power Loss

Step-3: Produce neighbor solutions for the employed bees by using (39).

$$V_{ij} = x_{ij} + f_{ij}(x_{ij} - x_{kj}) \quad (33)$$

Step-4: Apply the acquisitive selection process between X_{ij} and V_{ij} . If all onlooker bees distributed, go to *Step 9*. Otherwise, go to next step.

Step-5: Determine the probability values $P_{(x_{ij})}$ for the solutions X_{ij} using (40)

$$P(X_{ij}) = \frac{F(X_i)}{\sum_{i=1}^n F(X_i)} \quad (34)$$

Step-6: Produce the new solutions V_i for the onlookers from the solutions x_i , depending on P_i apply the greedy selection process between X_{ij} and V_{ij} .

Step-7: Determine the abandoned solution for the scout bees, if it exists, and replace it with an entirely new solution using equation and evaluate them as indicated in *Step 2*.

$$X_{i,j}^{max} = x_{min,j} + rand(0,1)(x_{max,j} - x_{min,j}) \quad (35)$$

Step-8: If cycle = MCN, stop and print result. Otherwise, follow Step 3 as shown in Fig 2.

Table 2: Parameters of ABC in IEE 34 [20]

S/N	Parameters	Value
1	Limit	35
2	MCN	100
4	Food source	40

The Hybrid IWO and ABC Algorithm

From the two previous sections, it can be concluded that IWO and ABC have two different approaches for optimization. IWO offers good exploration and diversity, while ABC is an algorithm with reasonably deliberate and to the point movements in each iteration. In this section, we combine two algorithms and present a hybrid algorithm. In hybrid IWO/ABC algorithm, colonization is beginning in the same way as IWO. However, the weeds are located like the equations in ABC for flying bees. It means that after reproducing the weeds, the velocity updated and temporary position of weeds is estimated. Finally, these weeds distributed randomly

same as the process used in IWO to construct the next population.

HIWO algorithm for solving MOO Problem

1. Generate random population of N0 solutions,
2. For *iter* = 1 to the maximum number of generations;
 - a. Calculate fitness for each iteration;
 - b. Set *Pg* as the best position of all individuals
3. Set *Pi* as the best position of the individual in comparison with its predecessors;
4. Computation of weeds, corresponding to its fitness,
5. For each weed *S*;
 - a. Calculate the velocity;
 - b. Update the position;
6. Randomly generated weeds over the search space with a normal distribution around the parent plant
7. Add the generated weeds to the solution set, *W*
8. Sort the population in ascending order of their fitness;
9. Truncate population of weeds with smaller fitness until $N = Pmax$ and then to Next iteration

The HIWO used to solve the optimal capacity and location problem by considering the following cases:

- Case #1: allocation of a single RDG.
- Case #2: allocation of single RDG and capacitor
- Case #3: allocation of multiple RDGs only
- Case #4: allocation of multiple RDGs and capacitors

Table 3: Weighted factors value Control variable

Scenario	Wp	Wv	Wc
1	1	0	0
2	0.8	0.1	0.1
3	0.6	0.2	0.2
4	0.4	0.2	0.4
5	0.2	0.4	0.4
6	0.1	0.4	0.5

Table 4. Control Variables

Parameters	34-Nodes	37-Nodes
V	0.95 - 105	0.95-1.05
Qc (MVar)	1.5 - 8	1.5 - 8
P _{RDG} (MW)	1 - 5	1 - 5
Q _{RDG} (MVar)	0.5 - 2	0.5 - 2
T	0.95 – 1.05	0.95 – 1.05

5. SIMULATION RESULTS AND DISCUSSION

IEEE-34-Nodes System Results

The IEEE 34 node test feeder shown in Fig. 6 is an actual feeder located in Arizona and characterized by long, lightly loaded, multiple three and single-phase laterals and unbalanced distribution feeder with operating voltages of 24.9 kV. The line data and node data for this system is given in [24]. The total real power of RDS is a 4636.5kW and reactive power of is 2873.5 kVAr. The real and reactive power losses of RDN at the base case is 220.8 kW and 63.9 kVAr respectively. The cumulative voltage deviation of the base case is 1.16. Table 4 shows control variable used in this research study.

In Table 5 depicts performance analysis of IEEE 34 nodes with power losses reduced to 14.4%. In contrast, the voltage magnitude seems to be within the range of 0.95 to 1.0 in scenario number 4 shown in Table 3. Fig.3 and Fig.4 depict convergence characteristics of IWO and ABC respectively on solving MOO problem.

Table.5: Performance Analysis of IEEE-34-Nodes

Parameter	Case 3	Case 4
P _{RDG} (MW) (node)	2.2 (28)	1.61 (18) 1.82 (30) 1.58 (10)
Capacitor MVar (node)	-	1.28(26) 1.02(21)
Ploss (kW)	493.68	167.27
Qloss (kVAR)	270.00	46.49
Vmin in p.u	0.93	0.95
Vmax in p.u	0.99	1.00
VSI	0.178	0.04
CVD	0.968	0.22
% Ploss reduction	9	14.4
CEL (\$/Year)	716,830.24	337,614.18

Results using different Methods in IEEE-34-Node

The simulated results in Table 9 compared with GA [14], particle swarm optimization (PSO) [15] and Flower Pollination Algorithm [11], and GA method [17].

Table 6. Simulation Results of 34-Nodes

Parameters	GA [14]	PSO [15]	FPA[11]	HIWO
Vmin	0.947	0.951	0.932	0.951
Vmax	0.994	0.997	1.010	1.020
VSI.min	0.861	0.801	-	0.882
VSI.max	0.979	0.980	-	0.994
Ploss(MW)	0.169	0.168	0.173	0.167
Qloss(MVar)	0.051	0.049	0.055	0.046
Net saving %	17.891	15.57	-	38.84

From the given Case 1 to Case 4, only two cases considered for comparison which good results based on techno-economic benefits as shown in Table 5 for IEEE 34 nodes and Table 8. However, based on scenarios shown in Table 3, only scenario number 4 shows promising results in both test system, i.e. that is the IEEE 34-nodes and IEEE 37-nodes system.

IEEE-37-Nodes System Results

The problem of placement and sizing of the shunt capacitors and RDG has been solved for the unbalanced IEEE 37-nodes. However, the distribution network under study in modified IEEE-37 nodes system shown in Fig. 5 adapted from Tanzania. System interconnected at slack bus number 5290 (Kiyungi 33kV). The network parameters and related data found in [11]. VSI used for the placement of the RDGs and shunt capacitor. The first three nodes considered as an optimum place for RDG. The node numbers chosen as per VSI are 35, 26, 29, 37, 18, & 11. The outcome leads to two locations for RDG and two locations for capacitor placement, which are nodes 35 & 268 and 34 & 31 respectively with maximum capacitor ratings depicted in Table 8 with scenario number four shown in Table 3.

Performance of the system before and after installation of RDG are shown in Table 7 and Table 8.

Table.7: Performance of scenario one in IEEE-34-Nodes

Parameters	Without RDG	With RDG
P_{RDG} (MW) (Node)	-	1.61 (18) 1.82 (30) 1.58 (10)
Power loss (kW)	290.31	199.89
CEL (\$)/year	964,145.52	508,655
Δ VD	0.15	0.01
% loss reduction	-	14.4
Shunt capacitor kVAr (node)	-	1.08 (26) 1.02 (21)

Table.8: Performance analysis of IEEE-37-Nodes in scenario one, case four

Parameters	Without RDG	With RDG
P_{RDG} (MW) (Node)	-	1.24(28) 1.52 (35)
Power loss (kW)	367.89	170.89
CEL (\$)	4534.78	1049.41
Δ VD	0.27	0.03
% loss reduction	-	26.92
Shunt capacitor kVAr (node)	-	1104(34) 1010(31)

The Optimal sitting and sizing of single RDG in RDs network using proposed method revealed that the best location of the RDG and capacitor in the network depend on network configuration, load, and technology of renewable energy source to be used. The power loss reduced to 0.167MW as against the initial value of 290.3kW with a reduction also in voltage deviation to 0.004 from 0.155 depicted in Table 8.

The variation of voltage drop for the base case is shown in Fig.7 and Fig 8 for given 34-nodes and 37-nodes distribution networks respectively. Different scenarios were considered to obtain the optimal site and size of both capacitor and RDG. Additional to that, voltage, transformer tap changer, and power from RDG considered as constraints. Evaluation of case 1 to case 4 with consideration of scenarios of 34-nodes is shown in Fig. 9 while for 37-nodes is shown in Fig 10 respectively. It shows that simultaneously optimization of power loss, voltage deviation and energy losses gives better results on both sizes of RDG and location.

Economical Saving

By using the proposed method in addition to its technical advantages, an economic saving or benefit obtained after 15 years. The worth of the saving of reduction purchased energy for IEEE 34-nodes, and 37-node systems are \$14,096,064 and \$21,203,100, respectively. Also, ultimate benefit including the total costs of energy losses for a 34 and a 37 nodes systems are \$337,614.18 and \$, 1,049.41 respectively as shown in Table 5 and Table 7. The total combination of wind turbine and solar PV Generator brings to the total net present cost (TNPC) value of \$891,995 that is lower than the TNPC of \$2,578,224 for the hybrid renewable system consisting of hydropower generator, solar PV generator, wind turbine generator, converter and battery storage.

6. CONCLUSION

In this paper, the IWO and ABC algorithm has been implemented into presented case studies considering the IEEE-34-nodes and IEEE-37-nodes distribution system. Both VSI and ABC have been used to identify the potential nodes for sitting RDG and shunt capacitor. HIWO used to solve MOO problem considering both voltage and power constraints. The results show that the proposed method achieved better in power loss reduction, saving of cost of energy loss, and less voltage deviation when compared with other existing techniques. Hence, the proposed method can able to implement for any distribution system to enhance voltage profile and conclude that the proposed method of sizing and sitting of RDG and capacitor is suitable for techno-economic benefits. The obtained results via the proposed HIWO method is preferable regarding the excellence of the solution and the computational efficacy.

ACKNOWLEDGMENT

Authors would like to express our sincere gratitude to the management of the Suranaree University of Technology-Thailand for providing excellent infrastructure facilities

and encouragement which have made this research possible.

NOMENCLATURE

RES	Renewable Energy source
RDG	Renewable distributed generation
Qc	Capacitor reactive power
Qdg	Reactive power from DG
VSI	Voltage stability index
Qi	Reactive power flow from ith node
Pi	Active power flow from ith node
ABC	Artificial bee colony
IWO	Invasive weeds optimization
FPA	Flower pollination algorithm
DG	Distributed generation
Vi	Voltage at ith node
Tc	Total purchase power from the grid
V_i^{\max}	maximum voltage of ith node (p.u)
V_i^{\min}	minimum voltage of ith node (p.u)
Ps	Active Power from the substation
Qs	Reactive power from the substation
Vj	Voltage at jth node
V_L	Voltage at load node
Ep	Electricity market price
Ta	Ambient temperature
P_w	Present worth
C_{EL}	Cost of energy loss
L_{COE}	Levelised cost of energy
T_{NPC}	Total Net Present Cost
MOPF	Multiobjective Power Flow
PV	Photovoltaic

REFERENCES

- [1] Roy P.K., Ghoshal S.P and Thakur S.S., 2012. Optimal Control for Improvements in Voltage Profiles and RPL minimization using Biogeography Based Optimization", *Electrical Power and Energy Systems*, Vol. 34, No.1, pp. 830–838.
- [2] Abbas R, Maziar V, and Mostafa P, 2012. Optimal Reactive Power Dispatch for Improving Voltage Stability Margin Using a Local Voltage Stability Index," *Energy Conversion and Management*, Vol. 59, pp. 66-73.
- [3] IEEE Standard for Interconnecting Distributed Resources with Electric Power Systems, *IEEE Std* 1547, Aug. 2003.
- [4] Yeh H.G, Gayme D.F., and Low S.H., 2012. Adaptive VAR control for distribution circuits with photovoltaic generators," *IEEE Trans. Power Syst.*, vol. 27, no. 3, pp. 1656-1663.
- [5] Kursat A.U, 2012. Artificial Bee Colony Algorithm Solution for Optimal Reactive Power Flow," *Applied Soft Computing*, Vol.12, No. 5, pp. 1477–1482.
- [6] Thomson M. and Infield D. G, 2007. Network power-flow analysis for high penetration of distributed generation," *IEEE Trans. Power Syst.*, vol. 22, no. 3, pp. 1157-1162
- [7] Varadarajan M., and Swarup K.S., 2008. DE Algorithm for Optimal Reactive Power Dispatch, *Electrical Power & Energy Systems*, Vol. 30, No. 8, pp. 435–441.
- [8] Amit S, and Ashish S 2012. Multi-Objective Optimal Reactive Power Dispatch Considering Voltage Stability in Power Systems using HFMOEA," *Engineering Applications of Artificial Intelligence*, Available online.
- [9] Altaf Q.H, and Junghare A.S, 2012. Reactive Power Control Using Dynamic Particle Swarm Optimization for Real Power Loss Minimization," *Electrical Power & Energy Systems*, Vol. 41, No. 1, pp. 133–136.
- [10] Reza S, Azah M, and Hussain S, 2012. Optimal Allocation of Shunt Var Compensators in Power Systems Using a Novel Global Harmony Search Algorithm," *Electrical Power & Energy Systems*, Vol. 43, No.1, pp. 562–572.
- [11] Serhat D, Yusuf S, and Nuran Y, 2012. Optimal Power Flow Using Gravitational Search Algorithm," *Energy Conversion and Management*, Vol. 59, pp.86–95.
- [12] Verma H. K, and Yogesh M, 2012. Big Bang Big Crunch Optimization for Determination of Worst Case Loading Margin," *International Journal of Engineering Research and Applications*, Vol. 2, No. 4, pp. 421-426.
- [13] Hsiao Y.T, and Chiang H.D, 2000. Applying Network Window Scheme and a Simulated Annealing Technique to Optimal VAR Planning in Large-Scale Power Systems", *Electric Power Systems Research*, Vol. 2, No. 1, pp.1–8.
- [14] Xin-She Y, 2012. Flower pollination algorithm for global optimization." *International Conference on Unconventional Computing and Natural Computation*. Springer Berlin Heidelberg.
- [15] Abido M.A, and Bakhshwain J.M, 2005. Optimal Reactive Power Dispatch Using a Multi Objective Evolutionary Algorithm, *Electric Power, and Energy Systems*, Vol.17, No. 1, pp.13–20.
- [16] Kumari, M.S and Maheswarapu S, 2010. GA based Computation Technique for Multi-objective Optimal Power Flow Solution, *International Journal of Electrical Power and Energy Systems*, Vol. 23, No. 6, pp. 736 – 742.
- [17] Cai J, Mab X, and Peng H, 2010. A Multi-Objective Chaotic Ant Swarm Optimization for Economic Dispatch," *Electric Power & Energy Systems*, Vol.23, No.5, pp. 337– 344.
- [18] Shaheen H.I, Rashed G.I, Cheng SJ, 2011. "Optimal Location and Setting of UPFC for Enhancing Power System Security based on Differential Evolution Algorithm," *Electric Power & Energy Systems*, Vol. 23, No.1, pp. 94–105.
- [19] Lee JC, Lin WM, Liao GC, and Tsao TP, 2011. Quantum GA for Dynamic Economic Dispatch with Valve-Point Effects and Including Wind Power System," *Electric Power & Energy Systems*, Vol. 33, No. 2, pp. 189–197.
- [20] Jordan R, 2015. Optimal Power Flow for Distribution Networks with Distributed Generation,"

- Serbian Journal of Electrical Engineering* Vol. 12, No. 2, pp 145-170.
- [21] Technical specification of renewable energy resources, [Online document], 2017, Available http://www.windturbines.ca/vestas_v44.htm. [Accessed: Nov 24, 2017].
- [22] Atwa, M. and Salama M, 2011. Adequacy Evaluation of Distribution System Including Wind and Solar DG During Different Modes of Operation, *IEEE Transaction on Power Systems*, Vol. 16, No. 4.
- [23] Rama P.D, and Jayabarathi T., 2016. Optimal placement and sizing of multiple distributed generating units in distribution networks by invasive weed optimization algorithm," *Ain Shams Engineering Journal*, 7, 683-694.
- [24] Chien-Feng Y, Gordon G. L, Chia-Hau L, Ching-Tzong Su, and Gary W, 2012. Optimal Size of Reactive Compensation Devices with an Improved Voltage Stability Index (IVSI) for Voltage Stability Enhancement," *Electric Power & Energy Systems*, Vol. 38, No.1, pp. 50-57.
- [25] Granada M., Marcos J. R, Mantovani J.R, and Shahidehpour M, 2012. A Decentralized Approach for Optimal Reactive Power Dispatch Using a Lagrangian Decomposition Method", *Electric Power Systems Research*, Vol. 78, pp. 148-156.
- [26] Verma H. K., and Yogesh M, 2012. Big Bang Big Crunch Optimization for Determination of Worst Case Loading Margin," *International Journal of Engineering Research and Applications*, Vol. 4, No. 4, pp. 421-426.
- [27] Babu M. and Jaisiva S, 2017. Optimal Reactive Power Flow by Flower Pollination Algorithm," *Asian Journal of Applied Science and Technology (AJAST)*, Volume 2, Issue 3, pp 137-141
- [28] Rao S. R, Ravindra K, Satish K, 2012. Power loss minimization in distribution system using network reconfiguration in the presence of DG," *IEEE Trans Power System*.
- [29] Mallanchettiar J, Subathra V, 2017. Minimization of Cost by Simultaneous Placement of Multi-DGs and shunt Capacitors in Distribution System Using Hybrid Optimization," *International Journal of Advances in Computer and Electronics Engineering*, Vol. 2, No. 6, pp. 8-14.
- [30] Ulinuha A. et al., 2014. Enhancement of Electrical Distribution System Operation Using Intelligent Optimization Techniques Considering Unbalanced Condition," *Applied Mechanics and Materials*, Vol. 660, pp. 846-850.
- [31] Murthy, K. A, 2013. "Comparison of optimal DG allocation methods in radial distribution systems based on sensitivity approaches. *International Journal of Electrical Power & Energy Systems*, 53, 450-467
- [32] Madivada H., and Rao C. 2012. "An invasive weed optimization (IWO) approach for multi-objective job shop scheduling problems (JSSPs)." *International Journal of Mechanical Engineering and Technology (IJMET)*, vol. 3, no. 3, pp. 627-637
- [33] Devabalajia K.R, Mohamed I., Yuvaraja T, Ravia K, 2015. Power Loss Minimization in Radial Distribution System," *International Conference on Alternative Energy in Developing Countries and Emerging Economies*, vol. 79, pp. 917 - 923.
- [34] Chis M, Salama M, and Jayaram S, 1997. Capacitor placement in distribution system using heuristic search strategies. *IEEGener. Transm. Distrib.*, pp 225-230.
- [35] Prakash K, and Sydulu M, 2007. Particle swarm optimization based capacitor placement on the radial distribution system. *IEEE PES Gen. Meet.* pp 1-5.
- [36] Suresh M and Belvin E, 2017. Optimal placement of distributed generation in the distribution system by using a shuffled frog leaping algorithm (SFLA)," *Journal of Engineering and Applied Sciences*, V 12
- [37] Mehrabian, A.R, Lucas C., 2006. A novel Numerical Optimization Algorithm Inspired by Weed Colonization, *Ecological Informatics*, vol 1, pp-355-366.

CONFERENCE PAPERS

The 6th International Electrical Engineering Congress, 7-9 March 2018, Krabi, Thailand. (iEECON2018)

Optimal Hybrid Renewable Generator for Techno-Economic Benefits in Smart Distribution Network

Elifuraha Reuben Mmary and Boonruang Marungsri
School of Electrical Engineering
Suranaree University of Technology
Nakhon Ratchasima, Thailand

Email address: reubsonmmarv@gmail.com and bmslhvee@sut.ac.th

Abstract—Increasing penetration of Hybrid Renewable Generator in recent year's present new challenges for planning and optimal operation of the Smart Distribution Network. For this purpose, performance indices introduced for determine suitable position of HRGs together with shunt-capacitors. However, the hosting capacities of HRG determined by use of Artificial Bee Colony (ABC) algorithm. The performance of the proposed methods validated on standards IEEE 34-nodes and IEEE 37-nodes radial distribution networks (RDN). The results have shown improvement of voltage level from 0.902p.u to 1.001p.u, reduction of power loss from 1.12MW to 0.64MW and diminished reactive power loss from 0.72MVAR to 0.34MVAR by integrating of HRG to RDN. Results suggest that the proposed methods are reliable and can apply to the real radial distribution networks.

Keywords—Hybrid Renewable Generators, Distribution network, Improved Analytical Expression, Voltage stability.

I. INTRODUCTION

Nowadays, conventional power systems operate closer to their stability limits due to the growth in the load demand. Technical, environmental and Economic considerations are the reasons for distribution and transmission networks lines to be constructed. HRG is usually well-defined as the generating power plants that providing support of power to a RDN, connected to the grid at low voltage level [1, 2]. The objective is to provide models to the decision makers of distribution systems to address the uncertainty of renewable resources and hence resulting in optimal performance. This research paper introduces a framework based on optimization methods to study the effect of intermittency aspect of renewable generation on distribution systems' operation. The primary focus dedicated towards better inclusion of the random behavior of renewable energy resources in modeling the operations of SDN economically to suit technical requirements.

Various AI techniques applied with different researchers [3] for solving optimization problem of RG and shunt capacitor. In [4], an Evolutionary Programming approach introduced for the research of minimizing power loss through integration of renewable generator (RG) units. Authors in

[5], introduced an optimal DGs in a RDN using ABC algorithm. In [6], authors formulate a multi-objective (MO) function such as power loss and cost savings by incorporate multiple DG units and ABC algorithm. In [7], authors employ Genetic Algorithm (GA) for solving optimization problem of shunt-capacitors under load uncertainty.

The HRG technology categorized as dispatchable and non-dispatchable technology. The dispatchable renewable generator are hydropower plant, geothermal and natural gas-turbine, while non-dispatchable renewable generator including solar PV and Wind turbine. The problem of HRG planning has recently received much attention by power system researchers to gather maximum benefit from optimal HRG allocation in SDNs. Uncertainty and intermittent of RES can cause voltage violation since overvoltage profile may occur during the condition of high power output from RES and low condition of the load.

To overcome the problem above, many researchers tried to optimally regulate voltage profile, loss reduction, and stability by considering the uncertainties of RG and load through HRG. Authors in [8] present method of controlling dispatchable DG by considering probabilistic load flow. In [9], control voltage regulators, LTC, Capacitor bank and dispatchable RG were considered to satisfy voltage profile and loss reduction. All of them use the normal distribution to evaluate uncertainty problem. Researchers in [10-11] develop an analytical method for allocation of a single RG in RDN but fail to operate successfully due to its intermittent and uncertainty. In [12] an ABC Technique proposed to find the optimal locations of multiple HDG units and its optimal hosting capacity.

Improved analytical expressions, Cost-Benefit Factor (CBF) and performance index applied to achieve both maximum loss reduction, voltage stability enhancement at possible lowest cost. This research paper structured as follows: In section II, present about improved analytical expression, and voltage stability index. Section III depicts methodology and algorithm of HRG placement and sizing. Economic analysis for HRG placement discussed in section IV. Section V show in details simulation results and discussion. To test the effectiveness of proposed technique; results compared with the genetic algorithm based method.

II. IMPROVED ANALYTICAL EXPRESSIONS

A. Total Power Losses

The total real power losses in radial distribution networks represented by exact loss formula [19, 20].

$$P_L = \sum_{i=1}^N \sum_{j=1}^N (\alpha_{ij}(P_i P_j + Q_i Q_j) + \beta_{ij}(Q_i P_j - P_i Q_j)) \quad (1)$$

$$\begin{cases} \alpha_{ij} = \frac{r_{ij}}{V_i V_j} \cos(\delta_i - \delta_j) \\ \beta_{ij} = \frac{r_{ij}}{V_i V_j} \sin(\delta_i - \delta_j) \end{cases} \quad (2)$$

Where

V_i is voltage at node i ; P_i, P_j Active power injection at node i and j respectively; Q_i, Q_j Reactive power injection at node i and j respectively; N Number of nodes

The exact loss formula (1) is differentiated concerning the injected power at node i and equalizing to zero for obtaining the hosting capacity of HRG placed at node i for achieving maximum loss reduction.

$$\frac{\partial P_L}{\partial P_i} = 2 \sum_{j=1}^N (\alpha_{ij} P_j - \beta_{ij} Q_j) = 0 \quad (3)$$

$$P_i = P_{HRG} - P_{Di} \quad (4)$$

Where

P_{HRG} Power injection from HRG placed at node i ; P_{Di} the load demand at node i

Improved Analytical Expression used to obtain the capacity of HRG unit that will achieve maximum loss reduction and voltage stability in SDN become as follows:

$$P_{HRGi} = (\alpha_{ii}(P_{Di} + \lambda Q_{Di}) - \sum_{j=1}^n (\alpha_{ij} P_j - \beta_{ij} Q_j)) \quad (5)$$

$$-\lambda \left(\sum_{j=1}^n (\alpha_{ij} Q_j + \beta_{ij} P_j) \right) (\lambda^2 \alpha_{ii} + \alpha_{ii})^{-1} \quad (6)$$

$$Q_{HRGi} = \lambda P_{HRGi} \quad (6)$$

$$\lambda = \pm \tan(\cos^{-1}(p, f)) \quad (7)$$

B. Fast Voltage Stability Index(FVSI)

The problem facing the RDN operator is how to quantify the impact of RG on the voltage magnitude before the actual connection is permitted. The uncontrolled and unpredicted power injections of these units cause changes in current flows leading to variations in voltage drops across the lines and, hence, affect the quality of the supply voltage [7]. V. Murty and A. Kumar, [12] proposed a new Fast Voltage Stability Index (FVSI) used to identify potential nodes in a large power system. Fast voltage stability indicator $FVSI$ at

load node can be calculated using (8) and to maintain secure condition, $FVSI$ index must be less than.

$$FVSI_{ij} = \frac{4Z^2 Q_j}{V_i^2 X_{ij}} \quad (8)$$

Where

Z = Line impedance; Q_j = Reactive power at receiving node

V_i = Voltage at sending node; X_{ij} =Line reactance

C. Power loss Index (PLI)

Developed index [10] used to identify potential nodes for allocating RG and shunt-capacitor. It shrink the search space during optimization procedure.

$$\frac{\partial P_j}{\partial Q_j} = \frac{2Q_j P_k}{V_j} \quad (9)$$

III. ECONOMIC ANALYSIS OF HRG IN RDS

The intermittency of RES affects the economic efficiency of local distribution companies. Any unpredictable changes in the power produced by the solar or wind resources result in unbalance and consequently affect the financial capability of the distribution company. It measured through Cost Benefit Factor. CBF proposed to rate the profit of HRG placement in SDN presented in (12). The installation of HRG unit is profitable if the CBF is more significant than one;

$$CBF = \frac{\text{cost}(\Delta_power\text{loss}) + \text{cost}(\Delta P_{slack})}{\text{cost}(\text{added_HRG})} \quad (10)$$

A. Total cost of saved Energy

$$\begin{cases} \Delta p_{loss} = P_{losses_withoutHRG} - P_{Losses_withHRG} \\ \text{Cost}(\Delta p_{loss}) = \Delta p_{loss} * 8760 * \text{tariff_rate} \end{cases} \quad (12)$$

Also,

$$\begin{cases} \Delta p_{generated@slack} = P_{slack_withoutHRG} - P_{slack_withHRG} \\ \text{Cost}(\Delta p_{slack}) = 8760 * \Delta p_{slack} * \text{tariff} \end{cases} \quad (13)$$

B. Total cost of added HRG units

The cost of HRG unit's categories into the investment cost, fixed cost, operating and maintenance cost. The investment cost annualized into a stream of equal annual payments over a specified (T) time at a specific interest rate (d) by using the capital recovery factor (CRF) [12].

$$CRF(d, T) = \frac{d(1+d)^T}{(1+d)^T - 1} \quad (14)$$

Net annual cost of HRG = AFC + AC_{O&M}

$$\begin{cases} AFC = FC_{capital} * P_{HRG} * CRF(d, T) \\ AC_{O\&M} = (O \& M)_{cost} * P_{HRG} \end{cases} \quad (15)$$

Where

AFC = annual fixed cost

$AC_{O\&M}$ = annualized operation and maintenance cost

HRG placement shall satisfy the three criteria such as maximizing loss reduction, voltage stability and economy of modified IEEE 34 nodes & IEEE 37 nodes test system.

C. Installation cost of Shunt-Capacitor

Installation cost of SC is include purchase cost and fixed cost of SC which evaluated using (16) as per details from [8].

$$C_{cost} = \sum_{i=1}^{ncap} K_c^{inst} Q_{Ci} + K_c^f \quad (16)$$

IV. METHODOLOGY FOR OPTIMIZE HRG

Finding of Hosting capacity of HRG through ABC Algorithm shown in Fig.1. adopted from [7]. The constraints for ABC Algorithm in [8] considered during simulation.

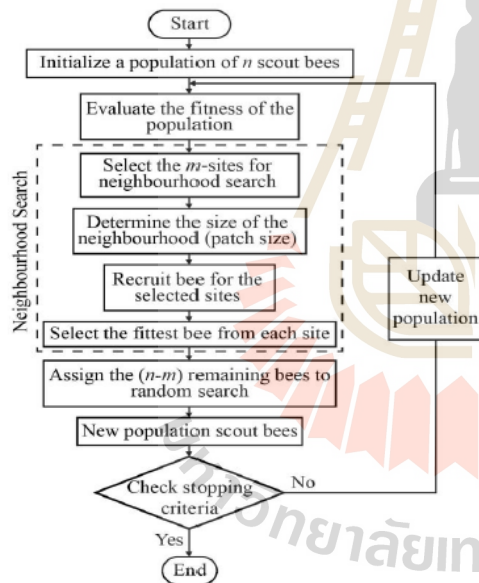


Fig. 1. Flow chart of ABC Algorithm

V. SIMULATION RESULTS AND DISCUSSION

The effectiveness of the $FVSI$, ABC and IA Expression made in IEEE 34-nodes [7] and IEEE 37 nodes [8] test system with a total load of 8.8MW +j5.3MVAR. System voltage under test was 22.5kV, 11kV, and total power loss of 1.22MW + j0.72MVAR examined and tabulated in Table I.

TABLE I. COST DATA FOR DIFFERENT RG UNITS TYPES [25]

Cost Data of Solar PV		Cost data of Wind	
Fixed capital cost	3000\$/MW	Fixed capital cost	1600\$/MW
O & M Cost	30\$/kW/year	O & M Cost	60\$/kW/year
Solar PV lifetime, T	=25years	Wind Turbine lifetime, T	=25
Tariff	0.05\$/kWh	Tariff	0.05\$/kWh

Case 1: Placement of (2.1 +j1.1) MVA single Renewable Generator (RG) unit operates at optimum location (node #19) achieve power loss reduction of 0.18 +j0.11 with the stability of 0.152. However, placing two and three HRG increasing the loss reduction to 35.4%, 58.1%, and 69.9% respectively. The stability indicator ($FVSI$) reduced to 0.152, 0.142 and 0.122 respectively.

Case 2: Placement of (2.6 +j1.2) MVA two RG (HRG) units operates at optimum location (node 25) achieve power loss reduction of 0.11 +j0.036 with the stability of 0.452.

Case 3: In this case, the loss reduction for placing single, two, and three HRG units is 18.3%, 23.7%, and 34.2% respectively. Placement of (3.8 +j1.4) MVA single HRG units operates at optimum location (node # 25) achieve power loss reduction of 0.21+j0.16 with the stability index of 0.692 as depicted in table II and Table III.

TABLE II. ENHANCEMENT OF $FVSI$ AND LOSS REDUCTION AT MINIMUM COST

RG	Power Losses %	$FVSI$	CBF
-	0	0.514	
1 RG	35.4	0.452	1.85
2 RG	58.1	0.131	1.57
3 RG	34.2	0.692	3.98

The number of RG limited to two units (as shown in Table II) to enhance the voltage stability and improve reduction of power loss. The CBF increases from 1.85 to 3.98 when it is three RG units, but it decreased to 1.57 during placement of two RG units. So, it is economical to place only two RG units (HRG) to enhance the voltage stability and maximizing power loss reduction

The 6th International Electrical Engineering Congress, 7-9 March 2018, Krabi, Thailand. (iEECON2018)

As depicted in Table III, results of utilizing HRG in case two, achieves higher improvement for both power loss reduction and improvement of VSI. Fig 1 show cost of electricity for given HRG into system in 12hrs of a day.

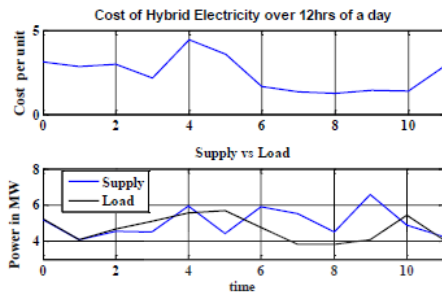


Fig. 2. Cost of electricity for given hybrid system in 12hrs of a day

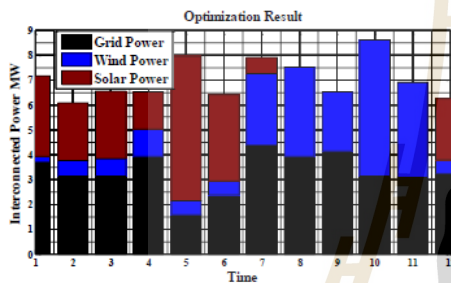


Fig. 3. Electricity generated for given hybrid system in 12hrs of a day

TABLE III. HRG PLACEMENT FOR MAXIMUM LOSS REDUCTION

	Optimum Size of HRG	Losses	FVSI
Case 1	2.1 +j1.1 (@ node 19)	0.18 +j0.11	0.452
Case 2	2.6 +j1.2 (@ node 25)	0.11 +j0.036	0.131
Case 3	3.8 +j1.4 (@ node 27)	0.21 +j0.16	0.692

ACKNOWLEDGMENT

The authors appreciatively acknowledge the support from Suranaree University of Technology, Thailand.

CONCLUSION

In this research paper, the ABC algorithm and FVSI implemented for minimize the active power loss of the RDN through the simultaneous placement of HRG and shunt-capacitor. The validation of the proposed method demonstrated on standard IEEE 34-nodes and applied to modified IEEE 37-nodes RDN. In both scenarios, case two demonstrate better results than the other cases. It noted that

the reduction of energy loss of 56.98% and cost saving of 14.85% depicts better compared to the base case for modified IEEE 37-nodes radial system. The advantages of the developed method lie in its simplicity, saving time because the power flow in this method is precise in achieving results.

REFERENCE

- [1] V. Murthy and A. Kumar, "Comparison of optimal DG allocation methods in radial distribution systems based on sensitivity approach," *International Journal of Electrical Power & Energy Systems*, vol. 53, pp. 450-467, 2013.
- [2] S. Kamalasan, D. Thukaram, and A. Srivastava, "A new intelligent algorithm for online voltage stability assessment and monitoring," *International Journal of Electrical Power & Energy Systems*, vol. 31, no. 2, pp. 100-110, 2009.
- [3] A. A. El Ela, M. Abido, and S. Spea, "Differential evolution algorithm for optimal reactive power dispatch," *Electric Power Systems Research*, vol. 81, no. 2, pp. 458-464, 2011.
- [4] N. Mohandas, R. Balamurugan, and L. Lakshminarasimman, "Optimal location and sizing of real power DG units to improve the voltage stability in the distribution system using ABC algorithm united with chaos," *International Journal of Electrical Power & Energy Systems*, vol. 66, pp. 41-52, 2015.
- [5] D. Karaboga and B. Bastuk, "A powerful and efficient algorithm for numerical function optimization: artificial bee colony (ABC) algorithm," *Journal of global optimization*, vol. 39, no. 3, pp. 459-471, 2007.
- [5] T. Shukla, S. Singh, and K. Naik, "Allocation of optimally distributed generation using GA for minimum system losses in radial distribution networks," *International Journal of Engineering, Science and Technology*, vol. 2, no. 3, pp. 94-106, 2010.
- [6] B. O. Bilal, V. Sambou, P. Ndiaye, C. Kébé, and M. Ndong, "Optimal design of a hybrid solar-wind-battery system using the minimization of the annualized cost system and the minimization of the loss of power supply probability (LPSP)," *Renewable Energy*, vol. 35, no. 10, pp. 2388-2390, 2010.
- [7] L. Yu, D. Czarkowski, and F. De León, "Optimal distributed voltage regulation for secondary networks with DGs," *IEEE Transactions on Smart Grid*, vol. 3, no. 2, pp. 959-967, 2012.
- [8] S. Kansal, V. Kumar, and B. Tyagi, "Hybrid Approach for Placement of Type-III Multiple DGs in Distribution Network," *J Electr Electron Syst*, vol. 3, no. 130, pp. 2332-0796.1000130, 2014.
- [9] S. Paul and W. Jewell, "Optimal capacitor placement and sizes for power loss reduction using combined power loss index-loss sensitivity factor and genetic algorithm," in *Power and Energy Society General Meeting, 2012 IEEE*, 2012, pp. 1-8: IEEE.
- [10] D. Q. Hung and N. Mithulananthan, "Multiple distributed generator placement in primary distribution networks for loss reduction," *IEEE Transactions on industrial electronics*, vol. 60, no. 4, pp. 1700-1708, 2013.
- [11] T. Niknam, M. Narimani, J. Aghaei, and R. Azizpanah-Abarghoee, "Improved particle swarm optimisation for multi-objective optimal power flow considering the cost, loss, emission and voltage stability index," *IET generation, transmission & distribution*, vol. 6, no. 6, pp. 515-527, 2012.
- [12] V. Murthy and A. Kumar, "Optimal placement of DG in radial distribution systems based on new voltage stability index under load growth," *International Journal of Electrical Power & Energy Systems*, vol. 69, pp. 246-256, 2015.

Optimal Hybrid Renewable Energy in Unbalance Distribution Networks Using DIgSILENT Power Factory Software and Genetic Algorithm

Elifuraha Reuben Mmary, Kelvin Melckzedek Minja, Pius Victor Chombo, Narupon Promvichai, Hussein Swalehe, Tassanai Supanarapan, Novatus Kimenyuka and Boonruang Marungsri

School of Electrical Engineering, Institute of Engineering, Suranaree University of Technology
111 University Avenue, Nakhon Ratchasima 30000, Thailand, Tel. 06661129-4190, Email: reubsonmmmary@gmail.com

* Corresponding Author Tel. 089717-7065-, Email: bmsvhee@sut.ac.th

Abstract — Distributed generation (DG) technologies such as Wind, Solar PV, Biomass, Hydropower, and Geothermal in distribution networks they have benefits in the improvement of distribution networks performance as it provides electricity power near the point of consumption by omitting the incremental cost. This paper focuses on systems optimization strategies to systematically dispatch of HRESs, location, and size for the sake of line loss minimization and cost reduction in a particular distribution network. The optimization problem is solved by the combination of DIgSILENT Power Factory Software and Genetic Algorithm (GA) with the aim of evaluating impacts of RES as DG in given radial distribution networks. Proposed algorithm was implemented in MATLAB for simulation and tested on the standard IEEE 34 and IEEE 13 bus test system for verification of the results. The results were presented to exhibit the efficiency of the proposed system. In other words, results show that any change of each parameter in the objective function of the GA and the matrix coefficients leads to the meaningful change in location and capacity of DG, in particular unbalance distribution network.

Keywords: Genetic Algorithm, DIgSILENT, Cost Reduction, DG, Hybrid Renewable Energy System.

I. INTRODUCTION

With the growing of Hybrid Renewable Energy Resources (HRES), the primary structure of power systems is changing from large centralized generation plants connected to the bulk transmission networks into decentralized systems with small generating systems connected directly to the distribution systems near load buses. HRES are intended mainly to attend the customers in a reliable and good quality manner reducing both investment & operation costs, improvement in the voltage profile and reducing total power losses.

Power distribution systems have been facing new challenges on their planning and operation procedures due to the widespread penetration of Hybrid renewable energy sources (HRES) units [1]. Also, DG can also have negative impacts on distribution networks. These effects include frequency deviation, voltage deviation, increased power loss, the cost of maintenance & operation of power generated and harmonics on the system. The increase of power losses is another effect that may occur. Thus careful considerations need to be taken when sizing and locating DGs in distribution

networks. Consequently, changes in the voltage profile can become a problem affecting the distribution network power quality [2]. The primary objective of any DGs in the distribution system does not only increase the market value of service by providing the right amount of reliability but also lower the cost of operation, maintenance, and construction as to provide service at lower rates. In [3], optimal location and capacity of DRES play a pivotal role in maximizing the benefits gained from HRES. On the other side, non-optimal placement or sizing of DGs may cause undesirable effects. In [4], the distribution capital investment credit received by independent power plant depend on incremental system reliability improvement rendered by the DG solution. In other words, the size, location, capacity dispatch and security of DG will be able on comparable incremental safety provided by the distribution solution under consideration.

IEEE 1547 Standard for Interconnecting DGs has an amendment to the voltage regulation by controlling DG active and reactive powers [7]. The new IEEE 1547 interconnection standard is expected to help reduce the costs and other barriers to grid interconnection by offering a cost-reduction and reliability-enhancing opportunity to DG's owners and operators. The optimal dispatch of a DG system is the least-cost solution to the supply of a site's energy demand by utility purchase, DG, or a combination of the two [8]. In [9] proposed the use of new coding in PSO which included both active and reactive powers of DGs to achieve better profile improvement by optimizing the size and location of the DGs. In their proposed method, four set of weighting factors is chosen based on the importance and criticality of the different loads. Their results showed that the weighting factor had a considerable effect on voltage profile improvement. Particle Swarm Optimization on a multi-load level used to minimize the cost of active losses, investment and operation cost of DG and emission cost [10]. The application of more advanced artificial intelligence method was proposed as a solution to overcome the problem [8]. Their challenge was to develop efficient algorithms for dealing with problems with a large number of DGs to be sited.

A suitable placement of large-scale distributed generator has proven to provide significant improvements in the reduction of transmission losses, both active and reactive

power flows, hence cost reduction in \$/h from generating units. Moreover, optimal dispatch of a DG installation at each time-step depends on current site loads, energy prices, and DG system availability, as well as the actual structure of tariffs and uncertain forecasts of these parameters at future time-steps. [11]. In order to size and allocate DG, many interesting algorithms and solutions have been developed. The solution may vary from one application to another. Optimization strategies have been presented in recent literature with objective functions aiming to power loss minimization, cost reduction, profit maximization and environmental emission reduction [12].

The optimization methods are classified into analytical, numerical and heuristic [13-14]. Optimal location is identified by calculating Voltage index at each node, and then variation technique is used to find the DG size [15]. The problem of optimal sizing and location is usually considered as a theoretical research problem. However, in [16], DG placement critically impacts the operation of the distribution network as inappropriate DG placement may result in increased system losses along with a rise in network capital and operating costs.

This paper presents Genetic algorithms (GA) and Digital Simulation & Electrical Network Calculation Program (DIGSILENT) for finding the optimal size, location and capacity dispatch of DGs connected to unbalanced distribution feeders for maximizing the profit of distribution companies that use DG in their networks for obtaining multiple benefits without violating the system constraints. Reduced loss cost evaluates the advantages in the presence of DG. The DG in the proposed algorithm is modeled as a voltage controlled (PV) node with the flexibility to be converted to constant power (PQ) node in case of reactive power limit violation. The proposed algorithm is implemented in MATLAB and tested on the IEEE 34-bus feeder and the IEEE 13-node test feeder. The results obtained are compared with published results for validation.

II. PROBLEM FORMULATION

Optimal power flow (OPF) in active distribution system aims to minimize system generation cost, power loss, voltage deviation and to maximize social welfare while considering power balances, production loading limits and line capacity constraints [17]. The problem is to determine allocation and size of the DGs which minimizes the distribution power losses and improve the voltage profile for a fixed total capacity of the DGs. The use of an algorithm that could efficiently analyze the influence of DG sizing and location on the system characteristics is necessary for the distribution network manner. The 'multi-objective performance index' (MOPI) calculation of the distribution networks for DG size and location planning model [18] considers all formerly mentioned indices by strategically giving a weight.

Three objectives are considered in the optimization model, which includes reducing system line losses, reducing voltage deviation and maximize actual power outputs of DG units in distribution power system [19].

The effect of increasing number of DG units is also presented.

The MOPI based on GA is given by

$$MOPI = \sigma_1 PLI + \sigma_2 QLI + \sigma_3 VPI + \sigma_4 CI \quad (1)$$

Subjected to following constraints:

$$\sum_{p=1}^4 \sigma_p = 1.0 \quad ,$$

$$\text{Where } \sigma_p \in [0,1]$$

TABLE I. INDICES WITH WEIGHTS [16]

Indices	σ_p
PLI	0.40
QLI	0.20
CI	0.25
VPI	0.15

Table 1 shows the values of weights used in the present work, considering normal operation analysis. However, as these values can be varied according to engineer's study, for this analysis, actual power losses received a significant weight of 0.40, and the current capacity index (CI) was received a second major of 0.25. Since it was given prominent figures regarding the level of flows through the network regarding the maximum size of conductors in distribution systems.

The 'multi objective function' is a cut down subject to various operational constraints to meet the electrical stipulations of the distribution network. These limitations are:

a) *Minimization of line loss*: The first objective is to minimize the system line loss after DG injection into the distribution network. This objective can be expressed as follows

$$\text{Min } F(x) = \sum_{ij \in B} g_{ij} (V_i^2 + V_j^2 - 2V_i V_j \cos \theta_{ij}) \quad (2)$$

Where B means branches,

V_{ij} is the voltage magnitude of nodes,

G_{ij} conductance

b) *Minimization of voltage deviation*: The second objective is to minimize the voltage difference between nodal voltage and specified voltage magnitude. The nodal voltage magnitude is an important indicator to evaluate the system security and power quality. The minimization of voltage deviation can help to guarantee the better voltage level in distribution power system

2017 IEEE PE&S – IEEE PES Thailand Symposium on Advanced Technology in Power System, Bangkok, Thailand, 7-8 March 2017

$$\min F_2(x) = \sum_{i=0}^n \left(\frac{V_i - V_i^{spec}}{V_i^{max} - V_i^{min}} \right)^2 \quad (3)$$

Where;

V_i^{spec} is specified voltage magnitude at the bus

$V_i^{max} V_i^{min}$ are the upper and lower voltage limits respectively

c) *Maximization active power output of DG units:*

The third objective is to maximize the active power outputs of DG units, which can be expressed as follows

$$\text{Max } F_3(x) = \sum_{i=1}^n P_{DG} \quad (4)$$

III. SYSTEM CONSTRAINTS

A. *Power Limits:*

The algebraic sum of all incoming and outgoing power including the line losses over the whole distribution network and electricity generated from DG unit should be equal to zero.

$$P_{gs} + \sum_{DG=1}^m P_{DG} = P_{load} + P_{loss} \quad (5)$$

B. *Distribution Line Capacity Limits:*

Power flow through any distribution feeder must comply with the thermal capability of the line.

$$S_{ij} \leq S_{ij}^{max} \quad (6)$$

C. *Voltage Drop Limits:* The voltage drop limits depend on the voltage regulation limits

$$|V_1 - V_j| \leq \Delta V_{max} \quad (7)$$

D. *Power factor constraints:* Power factor of overall system should exceed the minimum value and less than the maximum value as shown by the following equation

$$PF_{min} \leq PF_{sys} \leq PF_{max} \quad (8)$$

$$\sum_{b=1}^{CB} Q_C(b) \leq \sum_q^N Q_D(q) \quad (9)$$

E. *DG Technical Constraints:* As the energy resources inherently limit DG capacity at any given location, it is necessary to maintain capacity between the minimum and maximum level.

F. *Bus Voltage:*

$$V_{min} \leq V_{ibus} \leq V_{max} \quad (10)$$

G. *Power and Voltage Generated at Slack Bus:*

$$P_{Gmin} \leq P_G \leq P_{Gmax} \quad (11)$$

$$V_{Gmin} \leq V_{gs} \leq V_{Gmax} \quad (12)$$

TABLE II. VARIABLE USED FOR THE OPF DURING SIMULATION

VARIABLES	LIMITS	
	MIN	MAX
V1-V13(p.u)	0.9	1.1
V1-V34(p.u)	0.9	1.1
T1,T2 (p.u)	0.9	1.1
Q (MVAR)	0	50
PDG (MW)	1	8

IV. METHODOLOGY FOR OPTIMIZATION

A. *Implementation for DG location*

Various technical issues are to be addressed while considering the presence of distributed generator in Distribution Systems. It is necessary to compute several indices in order to describe the impacts on the 'distribution network' due to the presence of DG during maximum power generation [20].

1. *Real and Reactive Power Loss Indices (PLI and QLI)*

Power loss Index used to appoint the candidate buses for DG placement. Since bus with significant PLI will have the priority to be the candidate bus for installation of DG [14]

The real and reactive power loss indices are defined as

$$PLI = \frac{PL_{DG}}{PL} \quad (13)$$

$$QLI = \frac{QL_{DG}}{QL}$$

(14)

PL_{DG} and QL_{DG} are the total real and reactive power losses of the 'distribution system' after inclusion of DG, PL and QL are the total real and reactive system losses without DG in the Distribution System.

2. Voltage Profile Index (VPI)

One of the advantages of proper location and size of the DG is the improvement in voltage profile. This index penalizes the size location pair which gives higher voltage deviations from the nominal, in this way, the closer the index to zero better is the network performance [21].

The VPI can be defined as follows:

$$VPI = \max \left(\frac{V_1 - V_i}{V_1} \right) \quad (15)$$

Where V_1 is substation bus voltage and V_i is voltage at bus i

3. MVA Capacity Index (IC)

The index (IC) gives crucial data about the level of MVA flow/currents through the network regarding the maximum capacity of conductors. Values higher than unity (calculated MVA flow values greater than the MVA capacity) of the index provides the amount of capabilities violation regarding line flows, whereas the lower values indicate the size available

$$CI = \max \left(\frac{S_{ij}}{CS_{ij}} \right) \quad (16)$$

Where S_{ij} is MVA flow in branch i - j with DG in the system.
 CS_{ij} is MVA capacity of branch i - j without DG unit

B. Sizing of Solar PV and Wind Turbine System

The purpose of the sizing of the HRE system through HOMER is to calculate the number of solar modules and size of wind turbine needed to reliably meet the load requirement of a given area throughout the year. This methodology assesses the effects and optimizes the capacity and location of HRE on a distribution feeder and determines the maximum penetration level for HRE installations that will not violate changes to the feeder. The optimization methodology consists of several steps that narrow down the possible capacities of the HRE and locations on the distribution system using technical constraints [22]. The goal of the optimization methodology is to find the single point (size and location) of HRE operation that provides the lowest annual cost according to meteorological data.

C. Parameters Of Implemented GA

The GA was programmed using MATLAB with following essential features:

- ❖ Chromosome length codification: 16
- ❖ Population range size (Np) : 45
- ❖ Maximum number of generations: 900
- ❖ Elitism probability: 0.1
- ❖ Crossover probability: 0.72
- ❖ Mutation probability: 0.0052

- ❖ The selection method used was roulette wheel, based on the multi objective performance index (MOPI).

V. MATHEMATICAL MODELLING OF HRE

A. A mathematical model of Solar PV:

The output power of a solar PV panel at any time is a function of a solar radiation and atmospheric temperature

$$P_{sol}(t) = P_{rat} \cdot f_{loss} \frac{G_h}{G_s} \left[1 + \alpha_p (T_c - T_s) \right] \quad (17)$$

Where;

P_{rat} is the rated power output capacity of the PV panel,

f_{loss} loss factor of solar PV due to dirty,

G_h is hourly solar irradiation incident on the solar PV,

G_s is the standard solar radiation (1000W/m²), α_p is the

temperature coefficient of power, T_c is cell temperature of

PV, and T_s is cell temperature under standard test condition.

B. A mathematical model of Wind Turbine:

The wind turbine power output is proportional to the kinetic energy, air density, etc. Other parameters of wind turbine include cut in speed and rated wind speed.

$$P_{wind}(t) = 0.5\alpha\rho(t)Av(t)^3 \quad (18)$$

Where α is the Albert Betz constant, $\rho(t)$ is air density.

C. Utility Grid:

In HRES, if the power generated is more than load, then remaining power can be supplied to the grid.

$$P_{gs}(t) = P_{pV}(t)\eta_{mv} + P_{bg}(t) - P_L(t) \quad (19)$$

Power supplied by grid if RES not enough to meet the electricity demand.

$$P_{gs}(t) = P_L(t) - [P_{pV}(t)\eta_{mv} + P_{bg}(t)] \quad (20)$$

The capacity of solar and wind turbine is calculated from the average power estimated by irradiance and wind speed respectively. Table 1 shows the data of solar irradiation [16] over 24 hours and wind speed data [17]. Power generated is calculated for every irradiance level and wind speed by using (11) and (12).

TABLE III. SOLAR AND WIND DATA FOR 24 HOURS [18]

Time (Hours)	Solar Irradiance Data (W/m ²)	Wind speed data (m/sec).
1	0.5	3.0325
2	0.5	3.5412
3	0.5	4.9342
4	0.5	5.7786
5	4	6.5527
6	32.1779	6.3937
7	203.302	5.236
8	406.6817	3.632

9	575.9177	4.1387
10	872.7758	4.5565
11	737.8383	4.3235
12	733.1562	4.0157
13	815.881	2.7205
14	818.2873	2.6466
15	732.5891	3.9623
16	565.7632	3.4079
17	544.154	5.3587
18	455.1528	6.0713
19	139.9814	5.2234
20	37.669	4.8908
21	6	2.1175
22	0.5	1.7315
23	0.5	4.7083
24	0.5	4.9598

TABLE IV. MONTHLY AVERAGED INSOLATION INCIDENT ON A HORIZONTAL SURFACE (kWh/m²/day) [23]

Jan	Feb	Mar	Apr	May	Jun
0.67	1.33	2.31	3.65	4.90	4.99
Jul	Aug	Sep	Oct	Nov	Dec
4.86	4.01	2.78	1.56	0.81	0.50

TABLE V. MINIMUM AND MAXIMUM DIFFERENCE FROM MONTHLY AVERAGED INSOLATION (%) [23]

Jan	Feb	Mar	Apr	May	Jun
-16	-20	-17	-11	-14	-15
-17	-12	-16	-18	-32	-20
Jul	Aug	Sep	Oct	Nov	Dec
19	22	27	25	12	17
16	25	19	18	16	20

VI. SIMULATION RESULTS AND DISCUSSION

The proposed algorithm was tested using both IEEE 13 and 34 nodes radial system [7-8]. The base values are 100KVA and 23kV. The simulations were performed using MATLAB v.2009 software. Variable limits are given in Table II were used as system constraints. Voltage Profile Indices (VPI) are used to detect the most sensitive bus to voltage collapse and also the critical line in a power system network.

The proposed GA-based algorithm was to determine the optimal size and location of distributed generation unit

such that MOF given at (1) is minimized. The system line data and bus data are presented in [15]. It is shown that the optimal placement of DG units in the system caused a reduction in both power losses, cost deduction and maximized MVA capacity of the grid.

Results help to understand the impact of HRE on distribution network as sized through HOMER software based on TNPC. In this case study of 13 and 34 nodes, the results of HRE is observed to supplement the system. The effect on voltage and power losses are positive since the HRE operates successfully. In this case study, HRE is not allowed to inject more than 8MW. That means OLTC and capacitor bank have to serve to maintain the voltage within the ANSI C84.1 in the case of uncertainty.

The voltage profile of the modified IEEE 13 and 34 nodes are presented in figure 1 and figure 2 respectively. It can be seen from the graph that, most of the load bus have voltage range between 0.734 to 0.821p.u before optimization. In another language, we can say that power flow in the system exceeds the specified limits (thermal capacity limits) which tend to cause more power losses.

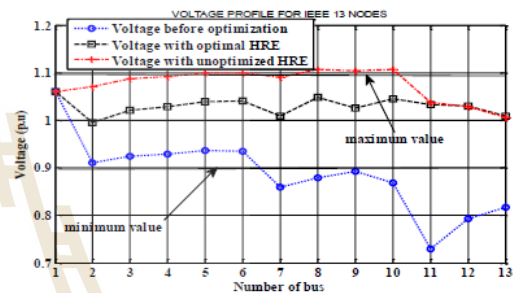


Fig. 1. Voltage profile for modified IEEE 13 nodes

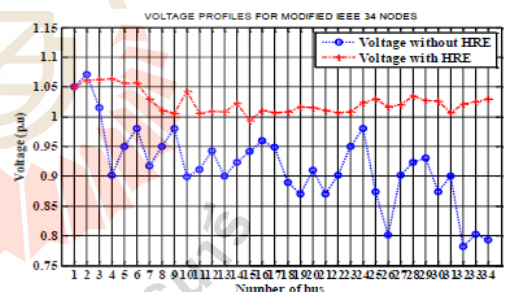


Fig. 2. Voltage profile for modified IEEE 34 nodes

Integration of HRE into the distributed system increases the minimum node voltage from 0.712 to 0.86 p.u although there were still below the standard as specified in [15]. In meanwhile, additional of DG up to 2.4MW at nodes 10, 8 and 11 raise the voltages to the range of 1.02 to 1.145 p.u.

2017 IEEE PE&S – IEEE PES Thailand Symposium on Advanced Technology in Power System, Bangkok, Thailand, 7-8 March 2017

As shown in Table VI, with the integration of 1.82MW on the distribution system at node 11 and 13, active and reactive losses dropped to 0.65MW from 1.2 MW. The effects of HRE on distribution system performance depends on several factors, including distribution structure, HRE placement, number or size of HRE and operational strategy. Well optimized HRE contributes positive impacts like voltage profile improvement, losses reduction, cost reduction and maximize the capacity of DGs.

CONCLUSION

Results show that installation of DG units mostly it has made improvement of voltage profile in the radial distribution network and loss reduction. The loss sensitivity factors and VPI were used to determine the candidate locations of the nodes where DG has been placed. Loss sensitivity factor application in DG allocation was efficient in finding DG location successfully. The total loss in the system is decreasing by determining optimal location and size of distributed generation unit in a radial distribution system. Thus, the objectives of the research work were achieved successfully. The implemented methods (GA-DIGSILENT) was proved to be a better method for optimizing the location and size of multi-type of DGs in different power networks with the aim of reducing both real and reactive power losses for improving system voltage profiles and consequently cost reduction as well.

ACKNOWLEDGMENT

The authors are satisfactory to thank Suranaree University of Technology, the school of electrical engineering (Institute of Engineering), and Provincial Electricity Authority of Thailand for their technical support.

REFERENCES

- [1] A. Keane and M. O'Malley, "Optimal allocation of embedded generation on distribution networks," *IEEE Trans. Power Syst.*, vol. 20, no. 3, pp. 1640–1646, Aug. 2005.
- [2] C. Yammani, M. Sydulu, S. Matam, "Optimal Placement of Mult DGs in Distribution System with consideration the DG Bus available limits "Energy and Power," *International Journal of Electric Power System Research*, February 2012, pp. 18-23
- [3] D. Karaboga and B. Bosturk, "A powerful and efficient algorithm for numerical function optimization: artificial bee colony optimization," *Journal of Global Optimization*, Vol. 39, pp. 459-471.
- [4] D.M. Stewart, S. V. MacPherson, D. Nakafuji, and T. Atukai, "Analysis of high-penetration levels of photovoltaics into the distribution grid on Oahu, Hawaii, detailed analysis of echo feeder wfl," NREL subcontract report NREL/SR-5500-54494, Tech. Rep
- [5] E. Dall'Anese, G. B. Giannakis, and B. F. Wollenberg, "Optimization of unbalanced power distribution networks via semidefinite relaxation," in *North American Power Symposium (NAPS)*, 2012. IEEE, 2012, pp. 1–6.
- [6] H. L. Willis, "Analytical methods and rules of thumb for modeling DG-distribution interaction," in *Proc. IEEE Power Eng. Soc. Summer Meeting*, Jul. 2000, pp. 1643–1644.
- [7] IEEE Std 1547TM (2003) Standard for Interconnecting Distributed Resources with Electric Power Systems
- [8] IEEE PES Distribution System Analysis Subcommittee's Distribution Test Feeder Working Group. Available at <http://ewh.ieee.org/soc/pes/dsacom/testfeeders>
- [9] J. Hazral and A. K. Sinha, "A Study on Real and Reactive Power Optimization using Particle Swarm Optimization," *International Conference on Industrial and Information Systems*, pp. 323328, 9-11 August 2007.
- [10] K. Turitsyn, P. Sulc, S. Backhaus, and M. Chertkov, "Distributed control of reactive power flow in a radial distribution circuit with high photovoltaic penetration," in *Proc. IEEE Power and Energy Soc. General Meeting*, Jul. 2010, pp. 1–6
- [11] M. H. Moradi, and M. Abedini, "Optimal load shedding approach in distribution systems for improved voltage stability," *4th International Power Engineering and Optimization Conference (PEOCO)*, 196-200, 2010.
- [12] M. M. Elnashar, R. El-Shatshat, and M. A. Salama, "Optimum Siting and Sizing of a Large Distributed Generators in a Mesh-Connected System," *International Journal of Electric Power System Research*, Vol. 80, June 2010, pp. 690-697.
- [13] MathWorks Inc., *Genetic Algorithms and Direct Search TOOLBOX*, CD-ROM Manual, 2004.
- [14] M.F. Akorede, H. Hizam, I. Aris and M.Z.A. Ab kadir, "A Review of Strategies for Optimal Placement of Distributed Generation in Power Distribution Systems," *Research Journal of Applied Sciences* 5(2): pp 137-145, 2011
- [15] O. Amanifar, "Optimal distributed generation placement and sizing for loss and the reduction and voltage profile improvement in distribution systems using particle swarm optimization and sensitivity analysis [abstract only]," in *Electrical Power Distribution Networks (EPDC)*, 2011 16th Conference on, April 2011, pp. 1–1.
- [16] R. K. Singh and S. K. Goswami, "Optimum Allocation of Distributed Generations Based on Nodal Pricing for Profit, Loss Reduction and Voltage Improvement Including Voltage Rise Issue," *International Journal of Electric Power and Energy Systems*, Vol. 32, No. 6, July 2010, pp. 637-644
- [17] S.Tarakalyani Kumaraswamy & B.Venkata Prasanth (2014). Optimal Location Of Distributed Generation On Radial Distribution System For Loss Reduction and Voltage Profile Improvement. *Afr J. of Comp & ICTs*. Vol 7, No. 5. Pp 29-36.
- [18] T. Gözel and M. H. Hocaoglu, "An analytical method for the sizing and siting of distributed generators in radial systems," *Elect. Power Syst. Res.*, vol. 79, no. 6, pp. 912–918, Jun. 2009.
- [19] T. Ramana, V. Ganesh, and S. Sivanagaraju, "Distributed generator placement and sizing in unbalanced radial distribution system" *Cogeneration & Distributed Generation Journal*, Vol. 25, Issue 1, pp. 52- 71, 2010.
- [20] U. Leeton, D. Uthitsunthorn, U. Kwannetr, N.Sinsuphun and T. Kulworawanichpong, "Lower Loss Minimization Using Optimal Power Flow Based on Particle Swarm Optimization," *ECTI Conference*, pp.469-473, 2010.
- [21] V. V. S. N. Murty and A. Kumar, "Optimal placement of Dg in radial distribution systems based on new voltage stability index under load growth," *Electrical Power and Energy Systems*, vol. 69, pp. 246-256, 2015.
- [22] W. El-Khattam, Y. G. Hegazy and M. M. A. Salama, "An Integrated Distributed Generation Optimization Model for Distribution System Planning," *IEEE Transactions on Power Systems*, Vol. 20, No. 2, May 2005, pp. 1158-1165
- [23] Surface meteorology data and solar energy, available at <https://eosweb.larc.nasa.gov/cgi-bin/sse/grid.cgi?&num>. Document generated on Thu Feb 9 09:35:36 EST 2017.

Optimal Hybrid Renewable Energy for Power Flow Problems in Distribution System.

Elifuraha Reuben Mmary, Kelvin Melckzedek Minja, Pius Victor Chombo, Narupon Promvichai, Hussein Swalehe, Tassanai Supanarapan, Novatus Kimenyuka and Boonruang Marungsri *

School of Electrical Engineering, Institute of Engineering, Suranaree University of Technology
111 University Avenue, Nakhon Ratchasima 30000, Thailand, Tel. 06661129-4190, Email: reubsonmmmary@gmail.com
* Corresponding Author Tel. 089717-7065, Email: bmslvtee@sut.ac.th

Abstract—The penetration of Hybrid Renewable Energy sources (HRES) in the distribution network change the characteristics of the decentralized network which has an impact on various technical parameter based on its size and location. In this paper, optimization problems are achieved by an acceptable value for an objective function subjected to limitations. The purpose is to minimize power losses and improve voltage profile of distribution system. Efficient and reliable techniques of optimization using Differential Evolution (DE), HOMER and Artificial Bee Colony algorithm (ABC) are presented for optimal sizing and location of HRES in decentralized networks. The real power losses and the voltage profile of distribution system are formulated as an objective function in the optimization of problems. The effectiveness of DE and ABC developed in MATLAB were tested in IEEE 13, and 34 nodes test feeder. Results of proposed method were compared with results of previous research.

Keywords —DE, ABC, Distributed Generation, Power loss, Voltage profile.

I. INTRODUCTION

The use of Distributed Generation (DG) is increasing day by day due to many factors including their environmentally friendly in nature, increased power demand and others related to growing of consumer's needs. In the traditional of the passive power system, the electrical power flows has one direction, from generation to customers/end-users [1]. The government of Thailand expects that the penetration of RES into the grid in 2025 will be 30% of the population, technology, and industry grow [2]. Adding of DG will change the old paradigm from unidirectional to bidirectional power flow in which performance, efficiency, and improvement of voltage profile will increase in the electrical grid [3].

The advent of new energy resources integrated to the distribution system significantly alters the voltage profile and the flow of power within the network. However, in [4] the main change in power grid nowadays is the addition of DGs which cause unidirectional of power from the end user to the grid. DGs can be developed using local renewable energy sources, such as micro hydro, wind power, biomass, etc. and selection of the type of renewables used for DG depends highly on the topology, location, and climate of the area where it is placed.

In 2005, installed of PV globally was 5.4GW, 2012 total capacity installed was exceeded 100GW worldwide [5]. As the number of HRES increases, it brings some concerns for the power system operation such as voltage profile during light load scenarios [6]. Based on a survey that we conducted to the distribution networks operators (PEA) we found that the urgent issues that need serious rectification were overvoltage, voltage unbalances and overloading caused by HRES. It is proven the fact that non-optimal positioning and sizing of HRES may affect the systems to the worst, resulting in increased losses and voltage variations [7], power quality issues, reverse power flows, overheating of feeders, switchgear, and costly grid reinforcement[8].

IEEE 1547 Standard for Interconnecting DGs has an amendment to the voltage regulation by controlling DG active and reactive powers [9]. The German standard VDE 4105 mentions that all the DGs connected to allow voltage system shall apply power factor adjustment to support the voltage regulation. The power factor adjustment varies based on the electrical source [5]. There are some approaches to overcome these problems such as allowing DGs to inject and absorb electrical power to keep the point of mutual coupling voltage within the desired level [10].

It is useful to determine the goals of optimal power flow problems. The primary goal of optimal power flow is to minimize the total losses hence voltage profile improvement of the entire system to serve the load demand for a particular power system while maintaining the security of the system operation. The permissible voltage violation limits for the system range between 1000V to 132Kv are $\pm 6\%$ of the nominal voltage [11]. Voltage control in distribution network was obtained using on-load tap changer at medium voltage substation and reactive power compensation [12]. On-load tap changer of transformer provides regulation range from -10% to +10% using 32 steps [13]. Additionally, the mechanical operation of OLTC may cause a certain delay on voltage regulation. Thus, in [14], penetration of DG in the networks play a significant role in the voltage regulation without violating voltage buses limits. However exceeding the number of DG in the networks may jeopardize the effectiveness of voltage regulation.

Several objectives have to be defined by inserting DG in the distribution system. In [15-16], the primary purpose for DG placement is to minimize the losses of power systems. However,

other targets such as voltage profile and reliability improvement, cost minimization and maximizing DG capacity and penetration level of DG have also been considered in different studies.

The rest of this paper aim to describe a new approach to maximizing MVA capacity, minimize total losses and to improve voltage profile in distribution system using DE Algorithms & HOMER Software without encountering voltage rise phenomenon in different buses. Hence, during normal system operating conditions, there is no violation on other system parameters like MVA flow of transmission lines, load bus voltage magnitude, generator MVAR. The proposed methods have been tested on IEEE 13, and 34 nodes test feeder power system.

II. MATHEMATICAL MODELLING OF HRES

DGs can be divided into two parts from the energy source viewpoint. These are renewable energy such as solar PV, the wind, biomass & geothermal and nonrenewable such as fuel cell, cogeneration, etc. The power generated from renewable sources is assumed to be constant in one-hour duration. Active power constraint for DG source is formulated as follows;

$$P_G^{\min} \leq P_G \leq P_G^{\max} \quad (1)$$

The reactive power output of DG units is also important and must be considered. Small and medium sized DG units mostly use Synchronous generators that are not capable of providing reactive power. The reactive power generation of DG units which use SG depends on reactive power control strategies such as constant Q, constant power factor mode, and Voltage regulated mode [17].

A. Specifications Solar photovoltaic panel

The output power of a solar PV panel at any time is a function of a solar radiation and atmospheric temperature [18].

$$P_{sol}(t) = P_{rat} f_{loss} \frac{G_h}{G_s} [1 + \alpha_p (T_c - T_s)] \quad (2)$$

Where; P_{rat} is the rated power output capacity of the PV panel; f_{loss} is the loss factor of solar PV due to dirty; G_h is hourly solar irradiation incident on the solar PV; G_s is the standard solar radiation (1000W/m²); α_p is the temperature coefficient of power; T_c is cell temperature of PV; T_s is cell temperature under standard test condition.

B. Power Inverter

The power inverter is used to convert DC generated by solar PV panel to AC at the desired frequency to serve the AC loads. The maximum power converted will depend upon size of inverter rating (P_{inv})

$$P_{inv}(t) = P_{PV}(t) \eta_{inv} \quad (3)$$

$$\text{Where: } P_{PV}(t) = P_{sol}(t) N_{sol} \quad (4)$$

$$P_{inv}^{\max}(t) = P_L^{\max}(t) + P_{gs}^{\max} \quad (5)$$

Where P_{sol} is the power generated by a single panel of PV, N_{sol} is the total number of solar PV panels.

C. Wind turbine

The power output of wind turbine is proportional to the kinetic energy, air density, etc. Other parameters of wind turbine include cut in speed and rated wind speed [19].

$$P_{wind}(t) = 0.5 \alpha \rho(t) A v(t)^3 \quad (6)$$

Where α is the Albert Betz constant, $\rho(t)$ is air density

D. Utility Grid

In HRES, if the power generated is more than load, then remaining power can be supplied to the grid.

$$P_{gs}(t) = P_{PV}(t) \eta_{inv} + P_{bg}(t) - P_L(t) \quad (7)$$

Power provided by the network if RES not enough to meet the electricity demand.

$$P_{gs}(t) = P_L(t) - [P_{PV}(t) \eta_{inv} + P_{bg}(t)] \quad (8)$$

III. METHODOLOGY

The proposed HRES is comprising of the wind turbine and Photovoltaic (PV) array system. The HOMER software was first used to optimize the placement and size of HRES in the distribution network. DE technique was then applied to the optimize voltage profile and line losses. The base values used are 100kVA and 22kV. A DG size obtained from HOMER was ranging 0.5MW to 2MW. DGs were operated in unspecified power factor unlike what was commonly used in the literature. The first bus in both radial systems was considered as a feeder of electrical energy from transmission network. The remaining buses of distribution system except the voltage controlled buses were seen for optimal size and placement of DGs. The Network was tested by using both IEEE 13 and 34 nodes with data given in [7-8].

A. Differential Evolution

Differential evolution (DE) is an improved version of the genetic algorithm for faster optimization. Among the DE's advantages are its simple structure, ease of use, speed, fewer control parameters and robustness [16-18]. The population consists of N_p individuals and dimension D that equals the number of design parameters. The initial population is randomly generated within the control parameter limits.

B. HOMER

HOMER is a micropower optimization model developed by the National Renewable Energy Laboratory to assist in the

2017 IEEE PE&S – IEEE PES Thailand Symposium on Advanced Technology in Power System, Bangkok, Thailand, 7-8 March 2017

design of the micro power system and facilitate the comparison of various types of Renewable-energy technology and component cost based on available meteorological data. The HOMER software perform optimization process for every selection of sensitivity variables. The sensitivity variables are such as the global solar and wind speed shown in Table 1. Then, the list of various configurations of hybrid renewable energy will be tabulated from the lowest to the highest TNPC. The optimal solution of the hybrid renewable energy system is referring to the most depressed TNPC.

IV. DG PLACEMENT AND SIZE OPTIMIZATION

Due to optimization of the HRES application in power distributed system, a unified techno-economic approach is considered as single optimization routine. This technique optimizes the capacity and location of HRES on distributed feeder and determines the maximum penetration level of these DGs that will not cause changes to the grid. The goal of the optimization is to find the single point (size and location) of HRES operation that provides the lowest annual cost.

The annualized cost of a component is equal to its annual operating cost plus its capital and replacement cost annualized over the project lifetime.

TABLE I. SOLAR AND WIND DATA FOR 24 HOURS

Time (Hours)	Solar Irradiance Data (W/m ²)	Wind speed data (m/sec).
1	0	3.0325
2	0	3.5412
3	0	4.9342
4	0	5.7786
5	4	6.5527
6	32.1779	6.3937
7	203.302	5.236
8	406.6817	3.632
9	575.9177	4.1387
10	872.7758	4.5565
11	737.8383	4.3235
12	733.1562	4.0157
13	815.881	2.7205
14	818.2873	2.6466
15	732.5891	3.9623
16	565.7632	3.4079
17	544.154	5.3587
18	455.1528	6.0713
19	139.9814	5.2234
20	37.669	4.8908
21	6	2.1175
22	0	1.7315
23	0	4.7083
24	0	4.9598

A. Case study for IEEE 34 BUS

Once a utility has determined which feeders are optimal for HRES, a more detailed analysis must be conducted. This section focuses on validating the optimization methodology that determines the amount and placement of HRES on a modified IEEE 34-bus test feeder. (Figure 1 [22]).

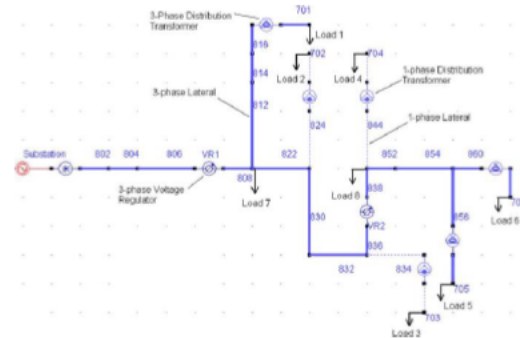


Fig. 1. Modified IEEE 34 Nodes System

This test feeder is based on the IEEE 34-bus test feeder [15]. The IEEE 34-bus test feeder is a publicly available feeder with full descriptions of system components. The feeder was developed by the IEEE Power Engineering Society Distribution System Analysis Subcommittee so that people would have a standard feeder for use in evaluating analysis techniques. Fig. 2 is the one-line diagram of the 34-bus test feeder. The feeder is a nominal 13.2-kV feeder with two VRs at locations VR1 and VR2. The major differences between this VR1 & VR2 are designed nominal voltages used to ensure that voltage stays within the ANSI C84.1 limits under full-load conditions.

B. Case study for IEEE 13 BUS

Test feeder is based on the IEEE 13-bus test feeder [7-8]. The IEEE 13-bus test feeder is a publicly available feeder with full descriptions of system components. The feeder was developed by the IEEE Power Engineering Society Distribution System Analysis Subcommittee so that people would have a standard feeder for use in evaluating analysis techniques.

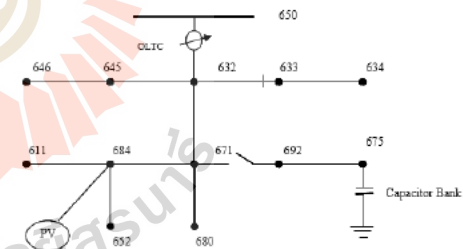


Fig. 2. Modified IEEE 13 Nodes System

C. Performance Index

The system performance index measures the deviation of system variables such as line flows, bus voltages, from its rated

□

2017 IEEE PE&S – IEEE PES Thailand Symposium on Advanced Technology in Power System, Bangkok, Thailand, 7-8 March 2017

value. It is used to evaluate candidate DGs in distribution networks without violating limitation of the control variable. Since an index for quantifying the extent of line overloads may be defined regarding MW performance index [26].

i) Real Power Loss Index(PLI)

$$PLI = \frac{P_{LWDG}}{P_{LWODG}} \times 100 \quad (9)$$

ii) Real Power Loss Index(PLI)

$$PLI = \frac{P_{LWDG}}{P_{LWODG}} \times 100 \quad (10)$$

The lower value of this index indicates better benefits regarding real power loss reduction occurred due to DG location and size.

iii) Reactive Power loss Index(QLI)

$$QLI = \frac{Q_{LWDG}}{Q_{LWODG}} \times 100 \quad (11)$$

iv) Voltage Profile Index (VPI)

One of the advantages of proper location and size of the DG is the improvement in the voltage profile. This index penalizes the size and location pair which gives higher voltage deviations from the nominal value (V_i). In this case, closer the index to zero, better is the network performance.

$$VPI = \frac{|V_i| - |V_i|}{|V_i|} \times 100 \quad (7)$$

In the calculation of PIV, the maximum and minimum voltage limits, generally a margin of $\pm 10\%$, i.e., 1.1 p.u. for maximum and 0.9 p.u. for the minimum [22] are required to be known.

V. OPTIMAL POWER FLOW

A. Problem Formulation

The To investigate the optimal location of HRES a standard IEEE 13 nodes and 34 nodes test feeder have been considered. The optimal power flow problem is to optimize the steady state performance of power system regarding one or more objectives functions while satisfying equality and inequality constraints. It consists of a nonlinear objective function defined with nonlinear constraints. The optimal power flow problem can be expressed as a constrained optimization problem as follows;

$$\text{Minimize } f(x)$$

Subjected to $a(x) = 0$, equality constraints

$b(x) \geq 0$, inequality constraints

By converting both equality and inequality constraints into penalty terms [15], function will be described as follows;

$$P(x) = f(x) + \Omega(x) \quad (12)$$

$$\text{But } \Omega(x) = \rho \left\{ g^2(x) + [\max(0, h(x))]^2 \right\} \quad (13)$$

Where $P(x)$ is the penalty function

$\Omega(x)$ is the penalty term

ρ is the penalty factor

B. Objective Function

The OPF is a static, nonlinear and non-convex optimization problem, which determines a set of optimal variables from the network state, load data, and system parameters. Optimal values are computed to achieve a particular goal such as minimum generation cost or transmission line power loss subjected to some equality and inequality constraints. The primary objective of this approach is to find the optimal capacity and the location of the DG units to produce the minimum active losses on the distribution system.

The following formula presents the total losses in the power network;

$$P_{loss} = \sum_{i=1}^{N_B} \sum_{j=1}^{N_B} [\alpha_{ij} (P_i P_j + Q_i Q_j) + \beta_{ij} (P_i Q_j - P_j Q_i)] \quad (14)$$

Where;

$$\alpha_{ij} = \frac{R_{ij} \cos(\delta_i - \delta_j)}{V_i V_j} \quad (15)$$

$$\beta_{ij} = \frac{R_{ij} \sin(\delta_i - \delta_j)}{V_i V_j} \quad (16)$$

- ✓ V_i, V_j is the bus voltage
- ✓ R_{ij} Resistance of the line
- ✓ P_{ij}, Q_{ij} are active and reactive power of the network
- ✓ N_B Number of buses
- ✓ δ is the load angle.

C. System Constraints

The Power flow equations in the network must be satisfied throughout the optimization process. In [24], authors describe optimization of power transmission line by controlling variable within their limits. These control variable are generator MW,

2017 IEEE PE&S – IEEE PES Thailand Symposium on Advanced Technology in Power System, Bangkok, Thailand, 7-8 March 2017

voltage magnitude, transformer tapping, injected reactive power and thermal limits. The equations can be mathematically expressed as follows:

1) Equality constraints

$$P_{Gi} - P_{Li} = \sum_{j=1}^{N_b} |V_i| |V_j| [G_{ij} \cos(\delta_i - \delta_j) + \beta_{ij} \sin(\delta_i - \delta_j)] \quad (17)$$

$$Q_{Gi} - Q_{Li} = \sum_{j=1}^{N_b} |V_i| |V_j| [G_{ij} \sin(\delta_i - \delta_j) - \beta_{ij} \cos(\delta_i - \delta_j)] \quad (18)$$

Where:

- P_{Gi} is the real power generation at bus i
- Q_{Gi} is the reactive power generation at bus i
- P_{Li} is the real power demand at bus i
- Q_{Li} is the reactive power demand at bus i
- NB is the total number of buses

2) Inequality constraints (Variable limitations)

$$V_i^{\min} \leq V_i \leq V_i^{\max} \quad (19)$$

$$T_i^{\min} \leq T_i \leq T_i^{\max} \quad (20)$$

$$Q_i^{\min} \leq Q_i \leq Q_i^{\max} \quad (21)$$

$$P_{Gi}^{\min} \leq P_{Gi} \leq P_{Gi}^{\max} \quad (22)$$

Where:

- V_i^{\min}, V_i^{\max} are the upper and lower limits of voltage magnitude at bus i
- T_i^{\min}, T_i^{\max} are upper and lower limits of tap changer
- Q_i^{\min}, Q_i^{\max} are upper and lower limits of reactive power source i
- $P_{Gi}^{\min}, P_{Gi}^{\max}$ are upper and lower limits of power generated by generator i

D. Types of DGs based on terminal Characteristics;

In [25], different types of the DG's can also be categorized by their terminal characteristics as follows;

Type 1: DG units capable of injecting active power only (P), such as fuel cells, photovoltaic cells, etc.

Type 2: DG units capable of injecting reactive power only (Q), such as synchronous compensator and capacitors

Type 3: DG units capable of injecting both active and reactive power (P and Q), such as Voltage Source Converter (VSC) based DG unit and synchronous machine based DGs are in this group.

Type 4: DG units capable of injecting active power (P) but consuming reactive power (Q), such as induction generators used in wind farms.

In this paper, type-1 and 4 of DG units are integrated into the distribution network for the aim of loss reduction and voltage profile improvement. From [24], the optimal DG sized at bus 'i' when it supply only active power (type 1), the necessary condition for minimal loss is given by;

$$P_{Gi} = P_{Di} - \frac{1}{A_{ij}} \sum_{j=2}^n (A_{ij})(P_i - B_{ij}Q_j) \quad (23)$$

VI. SIMULATION PROCEDURE

The simulation platform consists of two separate tools namely Differential Evolution and HOMER capable for modeling, simulating and analyzing the complex power system with options of various load types, generators and other critical power system parameters.

A. Simulation platform

The process of estimating optimal HRES involves

1. Estimate optimal size and location of DG in HOMER
 - Acquire meteorological data
2. Collect Power system data of distributed system to DE
 - Bus data and line data.
3. Perform DE algorithm
 - Get optimal voltage profile and losses

VI. RESULTS AND DISCUSSION

The Proposed DE based algorithm is applied to the 13 bus to determine the optimal size and location of DG units. In this step, line losses and voltage profile were evaluated in the distribution circuit (with and without DG) at the various locations. It should be noted that a node which is overloaded it has low voltage and hence higher power losses. Comparison of different sizes of DGs was made, but DG with 1.2MW recognized for the entire network. As a result of the placement of DG units in the system, the level of voltage variation and power losses tend to decrease where the maximum difference of 2.2% occurred. The total real power losses ranged from 2.57 to 4.256 MW. (Table II)

The Proposed DE based algorithm is applied to the 34 bus to determine the optimal size and location of DG units. Figure. 6 shows the voltage profile for with 20% of HRES total installed at bus number 3, 16 and 12.(Figure 4) As a result of inserting DG units in the system, the level of voltage profile improve for all studies with the optimized size of HRES. It is clear that for most of the lines the loading decreased while some of the lines it was kept the same or increased but still within the load limits.

The total real power losses ranged from 0.725 to 1.846MW

The MVA intake from the grid ranged from 40.5 to 44.8MVA. (Table III).

Fig. 4. Voltage profile for modified IEEE 34 Nodes

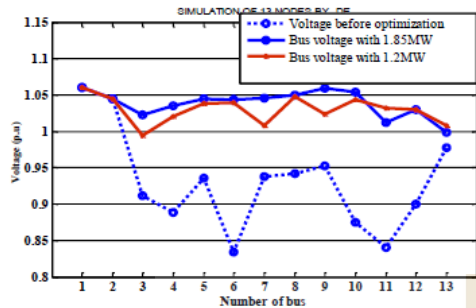


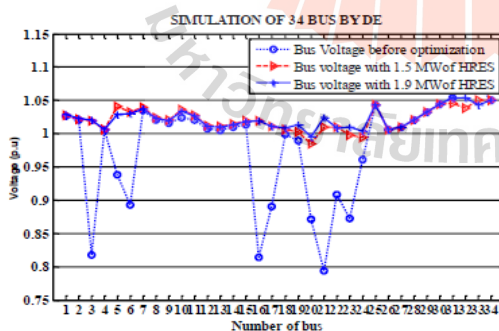
Fig. 3. Voltage profile for modified IEEE 13 Nodes

TABLE II. POWER LOSSES FOR 13 NODES

DG Penetration level	Bus Location	Losses (MW)
0%	-----	4.256
10%	6	2.033
15%	11	2.57
20%	6,11	1.42

TABLE III. POWER LOSSES FOR 34 BUS

DG Penetration level	Bus Location	Losses (MW)
0%	-----	1.846
10%	3,16	1.743
20%	21	1.448
25%	3,16,21	0.725



CONCLUSION

The optimization methodology described in this paper has been evaluated using realistic distribution feeders that were constructed based on the IEEE 34-bus test feeder and IEEE 13 bus test feeder. The results show that the integration of HRES is highly efficient in reducing power losses and improving the voltage profile in the radial distribution system. The voltage profile improvement is articulate from the analysis that heavily loaded bus voltage profile is augmented more than the lightly loaded bus. The results have been compared with those obtained using other techniques. Also, it provides a likely and preferable performance over other algorithms regarding active and reactive power losses. Applications of the network reconfiguration in distributed generation with the most recent optimization algorithm to enhance the voltage profile, cost reduction and reduce of both active and reactive losses are the future scopes of this work.

ACKNOWLEDGMENT

The authors are likely to thank the school of electrical engineering (Suranaree University of Technology) and Provincial Electricity Authority of Thailand for their technical support.

REFERENCES

- [1] A. A. Bayod-Ru'jula, "Future development of the electricity systems with distributed generation," *Energy*, vol. 34, pp.377-83, 2009.
- [2] C.LMaster, " Voltage rise the big issue when connecting embedded generation to long 11 kV overhead line. " *Power Eng J* 2002; 16: 5-12
- [3] C. Suthapamma , Peerapol Jirapongb , Phattamapom Bunchoo and Panida Thararak, "Reliability Assessment Tool for Radial and Loop Distribution Systems Using DIgSILENT PowerFactory," *IEEE Trans. On Power Delivery*, vol. 19, N 3 p.1360-1367, July 2004)
- [4] G. P. Harrison, and A.R. Wallace, "Maximizing distributed generation capacity in deregulated markets," in *Proc. 2003 IEEE Transmission and Distribution Conference and Exposition*, vol. 2, pp. 527-530.
- [5] G. Celli, E. Ghiani, M. Lodo, and F. Pilo, "Voltage Profile Optimization with Distributed Generation," *IEEE Russia Power Tech*, 2005.
- [6] H. L. Willis, "Analytical methods and rules of thumb for modeling DGdistribution interaction," *Power Engineering Society Summer Meeting, IEEE*, vol. 3, pp. 1643-1644, Seattle, Washington, USA, 16-20 July 2000.
- [7] IEEE Std 1547TM (2003) Standard for Interconnecting Distributed Resources with Electric Power Systems.
- [8] IEEE PES Distribution System Analysis Subcommittee's DistributionTest Feeder Working Group. Available at: <http://ewh.ieee.org/soc/pes/dsacom/testfeeders>.
- [9] I. Kim, Raeeey Regassa, and Ronald G. Harley, "The Modeling of Distribution Feeders Enhanced by Distributed Generation in DIgSILENT," *Photovoltaic Specialist Conference (PVSC)*, 2015 IEEE 42, 14-19 June 2015.
- [10] H.,Khan, Choudhry, M.A.: Implementation of distributed generation algorithm for performance enhancement of distribution feeder under

2017 IEEE PE&S – IEEE PES Thailand Symposium on Advanced Technology in Power System, Bangkok, Thailand, 7-8 March 2017

- extreme load growth. *International Journal of Electrical Power and Energy Systems* 32(9), 985–997 (2010).
- [11] I. Ziari, G Ledwich., Ghosh, A., Cornforth, D., Wishart, M.: Optimal allocation and sizing of DGs in distribution networks. In: *IEEE Power and Energy Society General Meeting*, pp.1–8 (2010)
- [12] IEEE Distribution System Analysis Subcommittee, 1991. Radial distribution test feeders, *IEEE Trans. on Power Systems*.
- [13] K.Gnanambal, S.Suriya "Optimal Sizing Of Distributed Generation For Voltage Profile Improvement Considering Maximum Loadability Limit," *ICIET*, vol. 3, pp. 304-309, March 2014.
- [14] J. Owuor, J. Munda, and A. Jimoh, "The IEEE 34 node radial test feeder as a simulation testbench for Distributed Generation," *IEEE AFRICON*, Victoria Falls, Livingstone, Zambia, Sept. 13-15, 20 11.
- [15] L. Weibing, L. Min, W. Xianjia, "An improved particle swarm optimization algorithm for optimal power flow," *IEEE 6 th International Power Electronics and Motion Control Conference 2009*, pp. 2448-2450, 17–20 May 2009.
- [16] M.R AlRashidi, M.E El-Hawary, "Hybrid Particle Swarm Optimization Approach for Solving the Discrete OPF Problem Considering the Valve Loading Effects," *IEEE Transactions on Power Systems*, vol. 22, no. 4, pp. 2030-2038, 2007.
- [17] M.H., Moradi, M. Abedinie and H.B. Tolabi, "Optimal multi-distributed generation location and capacity by Genetic Algorithm," *4th International Power Engineering and Optimization Conf. (PEOCO 2010)*, IEEE, pp. 440-444, Shah Alam, Selangor, Malaysia, 23-24 June 2010.
- [18] M. Gomez-Gonzalez, A. López, and F. Jurado, "Optimization of distributed generation systems using a new discrete PSO and OPF," *Electric Power Systems Research*, vol. 84, pp. 174-180, 2012.
- [19] M.H. Aliabadi, B. Behbahani, A. Jalilvand, "Combination of GA and OPF for allocation and active and reactive power optimization in distributed generation units," *2nd IEEE International Conference on Power and Energy (PECon 08)*, pp. 1541-1544, Johor Bahru, Malaysia, 1-3 December 2008.
- [20] N. Khalesi, N. Rezaei, M.R. Haghifam, "DG allocation with the application of dynamic programming for loss reduction and reliability improvement," *Electrical Power and Energy Systems*, vol. 33, no. 2, pp. 288-295, February 2011.
- [21] P. Kang, D. Birtwhistle, "Condition Assessment of Power Transformer On-Load Tap-Changers Using Wavelet Analysis," *IEEE Trans. Power Delivery*, 2011, pp. 394-400.
- [22] R. Caldon, M. Coppo, R. Turri, "Distributed voltage control strategy for LV networks with inverter-interfaced generators," *Electric Power Systems Research*, vol 107, 2014, pp. 85-92.
- [23] S.Sharma, Subhadeep Bhattacharjee, Aniruddha Bhattacharya, "Optimal Location and Sizing of DG to Minimize Loss of Distribution System Using SIMBO-Q Method," *International Conference on Control, Instrumentation, Energy & Communication*, vol. 16, pp. 340-344, November 2014.
- [24] U.Leeton, T.Kulworawanichpong "Combination of GA and OPF for allocation and active and reactive power optimization in distributed generation units," *2nd IEEE International Conference on Power and Energy (PECon 08)*, pp. 1541-1544, Malaysia, 1-3 December 2008.
- [25] V. Ferry, S.Ambra, D. Jaap, "Voltage control with on-load tap changer in medium voltage feeders in the presence of distributed generation," *Electric power system Res 2007*; pp 1314-22.
- [26] V.Jaiswal, A.K. Gaustam, S.P.Singh, "Optimal sizing & siting of DG with Load models using Genetic Algorithm under different loading condition," *ICETESES 2016* IEEE-16, pp. 139-146, 2016.
- [27] V. V. S. N. Murty and A. Kumar, "Optimal placement of Dg in radial distribution systems based on new voltage stability index under load growth," *Electrical Power and Energy Systems*, vol. 69, pp. 246-256, 2015.
- [28] C. T. Borges and D. M. Falcao, "Optimal distributed generation allocation for reliability, losses, and voltage improvement," *Int. J. Elect. Power Energy Syst.*, vol. 28, no. 6, pp. 413–420, Jul. 2006.

APPENDIX B

Branch data for IEEE 33-Nodes

S/N	From	To	R (ohms)	X (ohms)	From	To	R (ohms)	X (ohms)
1	1	2	0.0802	0.0443	25	6	26	0.1766
2	2	3	0.4289	0.2335	26	26	27	0.2471
3	3	4	0.3184	0.1734	27	27	28	0.9213
4	4	5	0.3315	0.1805	28	28	29	0.6996
5	5	6	0.7125	0.6575	29	29	30	0.4415
6	6	7	0.1628	0.5754	30	30	31	0.8477
7	7	8	1.488	0.8814	31	31	32	0.2701
8	8	9	0.8961	0.6882	32	32	33	0.2966
9	9	10	0.1710	0.0604	23	23	24	0.7812
10	10	11	0.1710	0.0604	24	24	25	0.7795
11	11	12	0.3257	0.1151	23	23	24	0.7812
12	12	13	1.2771	0.0741				
13	13	14	0.4711	0.6629				
14	14	15	0.5141	0.4891				
15	15	16	0.6496	0.5068				
16	16	17	1.1214	0.6105				
17	17	18	0.6368	0.5338				
18	2	19	0.1426	0.1455				
19	19	20	1.3056	1.2605				
20	20	21	0.3563	0.449				
21	21	22	0.6167	0.8716				
22	3	23	0.3915	0.2867				

APPENDIX C

Load data for IEEE 33-Nodes

Nodes	P (kW)	Q (kVar)	Nodes	P (kW)	Q (kVar)
1	0	0	25	840	400
2	200	120	26	120	50
3	180	80	27	120	50
4	240	160	28	120	40
5	120	60	29	240	140
6	120	40	30	400	120
7	400	200	31	300	140
8	400	200	32	420	200
9	120	40	33	120	80
10	120	40	24	840	400
11	90	60			
12	120	70			
13	120	70			
14	240	160			
15	120	30			
16	120	60			
17	120	40			
18	180	80			
19	180	80			
20	180	80			
21	180	80			
22	180	80			
23	180	100			

APPENDIX D

Branch data for real system of 34-Nodes

S/N	From	To	R (p.u)	X (p.u)	From	To	R (p.u)	X (p.u)
1	800	802	0.0421	0.0236	846	848	0.1066	0.0414
2	802	806	0.0429	0.0335	834	860	0.2471	0.1455
3	806	810	0.0784	0.0134	860	836	0.0913	0.2867
4	806	808	0.0315	0.0105	836	840	0.0996	0.5331
5	808	812	0.0125	0.0575	836	862	0.0415	0.0102
6	812	814	0.0628	0.0754	862	838	0.0477	0.0164
7	814	850	0.0188	0.0414	842	844	0.0795	0.0520
8	850	816	0.0961	0.0882				
9	816	818	0.1710	0.0604				
10	818	820	0.1710	0.0604				
11	820	822	0.0257	0.1151				
12	816	824	0.2771	0.0741				
13	824	828	0.0711	0.0629				
14	828	830	0.0141	0.0891				
15	830	854	0.0496	0.0168				
16	854	856	0.1014	0.0105				
17	854	852	0.0368	0.5338				
18	832	888	0.0126	0.1455				
19	888	890	0.0156	0.0605				
20	832	858	0.0563	0.0491				
21	858	864	0.0167	0.0716				
22	858	834	0.0915	0.2867				
23	834	842	0.0312	0.0594				

APPENDIX E

Load data for real system of 34-Nodes

Nodes	Nodes	P (MW)	Q (MVar)	Nodes	P (MW)	Q (MVar)
1	800	0	0	834	0.06	0.025
2	802	0.1	0.06	842	0.06	0.025
3	806	0.09	0.04	844	0.12	0.07
4	808	0.12	0.08	846	0.27	0.16
5	810	0.06	0.02	848	0.15	0.05
6	812	0.06	0.03	860	0.21	0.11
7	814	0.28	0.08	836	0.06	0.01
8	850	0.24	0.06	840	0.37	0.16
9	816	0.05	0.03	862	0.45	0.23
10	818	0.06	0.04	838	0.09	0.04
11	820	0.06	0.03	864	0.06	0.025
12	822	0.12	0.08			
13	824	0.06	0.01			
14	826	0.09	0.04			
15	828	0.09	0.04			
16	830	0.09	0.04			
17	854	0.09	0.04			
18	852	0.09	0.04			
19	856	0.09	0.05			
20	832	0.09	0.04			
21	888	0.42	0.2			
22	890	0.43	0.2			
23	858	0.06	0.025			

BIOGRAPHY

Mr. Elifuraha Reuben Mmary was born on June 14, 1984 in Kilimanjaro region, Tanzania. He received his Bachelor's Degree in Electrical Engineering from Dar es salaam Institute of Technology in 2014. After graduation, he has been employed under the position of Project Engineer with Power & Energy Solution Co., Ltd. He served in position of Tutorial Assistant in department of Electrical Engineering, Dar es salaam Institute of Technology. He continued with his graduate studies for the research of power system optimization with renewable energy in a school of Electrical Engineering, Institute of Engineering, Suranaree University of Technology.

